UTILIZING PHOSPHORUS BUDGETS AND ISOTOPIC TRACERS TO EVALUATE PHOSPHORUS FATE IN SOILS WITH LONG TERM POULTRY LITTER APPLICATION

by

Janae Bos

A Thesis

Submitted to the Faculty of Purdue University

In Partial Fulfillment of the Requirements for the degree of

Master of Science

Department of Agronomy

West Lafayette, Indiana

August 2020

THE PURDUE UNIVERSITY GRADUATE SCHOOL
STATEMENT OF COMMITTEE APPROVAL

Dr. Shalamar Armstrong, Chair

School of Agronomy

Dr. Mark Williams

School of Agricultural and Biological Engineering

Dr. Doug Smith

School of Agronomy

Approved by:

Dr. Richard Grant

Dedicated to

David, Tyler, and Caleb Bos

Dale and Carma Herbst

National Soil Erosion Research Laboratory, West Lafayette, IN

ACKNOWLEDGMENTS

Dr. Mark Williams for his expertise and continued guidance on the research component of this project. Dr. Doug Smith for encouraging me to further my education and giving me the opportunity to purse a master's degree. Brittany Kent for her laboratory assistance and attention to detail. My family and friends who extended help when necessary. All the Purdue Faculty who instructed courses that I took – I learned so much and felt privileged to learn from amazing professors.

This research was supported by the USDA Natural Resources Conservation Service Conservation Effects Assessment Project Watershed Assessment Studies and Agricultural Research Service National Program 211. Supplemental funding for this project was provided by the Texas State Soil and Water Conservation Board and the US Environmental Protection Agency through a Clean Water Act 319(h) grant. This research was a contribution from the Long-Term Agroecosystem Research (LTAR) network. LTAR is supported by the USDA.

TABLE OF CONTENTS

LIST OF TABLES

LIST OF FIGURES

ABSTRACT

Converting a nutrient management plan from commercial fertilizers to poultry litter helps effectively utilize waste from the nearly 10 billion broiler birds across the United States. Nine field scale watersheds from the USDA ARS Grassland, Soil and Water Research Laboratory near Riesel, TX were evaluated for P inputs and P outputs to determine phosphorus budgets for 15 years of annual application of poultry litter ranging from 75 – 219 kg P ha^{-1} yr^{-1} on cultivated and pasture/grazed fields. The cumulative net P continued to increase regardless of the application rate and had a positive relationship with soil level P (Mehlich-3 P) and flow weighted mean concentration (FWMC) for dissolved reactive P for both cultivated and pasture managed fields. We assessed hydrological connectivity within two nested watersheds by using the before-after-control-impact (BACI) design. Results showed hydrological connectivity during high rainfall years whereas low rainfall years had minimal connectivity compared to the controls. These results suggest the P contributions from upstream fields receiving poultry litter, even at high application rates, did not exhibit a treatment effect during the low rainfall years at downslope monitoring stations.

As nutrient source variability increases in nutrient management plans, improving our ability to differentiate P sources and their fate in soils is critical. We evaluated soils with unique P inputs: inorganic P, poultry litter, and cattle grazing for isotopic signatures by forming silver phosphate and determining the $\delta^{18}O_P$. Isotopic signatures of the oxygen molecules which are strongly bound to P, provided signatures of 17.09‰, 18.00‰, and 17.20‰ for fields receiving commercial fertilizer, poultry manure, and cattle grazed, respectively. Significant effort was made to determine critical steps in the method to successfully precipitate Ag_3PO_4 for analysis. Results show adding a cation removal step as well as monitoring and adjusting pH throughout the method increases probability of successful Ag_3PO_4 precipitation. Findings from this study provide a valuable framework for future analysis to confirm unique $\delta^{18}O_P$ signatures which can be used to differentiate the fate of different phosphorus sources in agricultural systems.

CHAPTER 1. INTRODUCTION

Over the last several decades much research has been done to better understand nutrient transport and its effect on surface water bodies. Although substantial efforts have been made to reduce agricultural non-point source pollution to waterways, elevated levels of phosphorus (P) and nitrogen (N) are still problematic in many areas. These elevated nutrient levels can cause harmful algal blooms (HABs) and hypoxia in surface water bodies such as Lake Erie and the Gulf of Mexico. One of the main challenges to mitigating non-point source pollution is identifying and differentiating among contributing nutrient sources. For example, the Ohio EPA Lake Erie Phosphorus Task Force Final Report (O. EPA, 2010) lists a variety of point and non-point sources contributing to Lake Erie; however, as many contributing sources converge in the lake, a single concentration of phosphate (PO_4) or total P (TP) is reported (mg/L), regardless of the original source. Management strategies could be improved if the contributing sources were able to be differentiated. For instance, the primary source of PO_4 entering a surface water body could be from agricultural fields (i.e., recently applied fertilizer or a previous year fertilizer application legacy P), from a wastewater treatment plant, or a combination of sources. If organic and inorganic fertilizer is concurrently applied to an agricultural field to meet nutrient uptake demands (Harmel, Smith, Haney, & Dozier, 2009), the fate and transport of the different sources of P within a field is also currently unknown. Using the phosphate stable oxygen isotope ($\delta^{18}O_P$) could potentially help identify separate sources of P in both water bodies and agricultural systems, and enable policy makers, researchers, and farmers to make management decisions that are both environmentally and economically beneficial.

To differentiate among potential sources of P, novel methods of analyzing P must be used. Traditional soil extractions such as water extractable P, Bray-P, and Mehlich-3 P are useful in determining the quantity and intensity of available P (Sims, 1998). Hedley, Stewart, and Chauhan (1982) developed a series of extractions to determine the organic and inorganic fractions of P within the soil; however, these extractions are unable to provide information on the source of P. Determining the $\delta^{18}O_P$ signature(s) in a soil sample can potentially isolate contributing sources. Biochemists in the 1960s and 1970s started measuring the excess $\delta^{18}O$ in PO_4 by investigating reaction rates of oxygen (O) with water and P (Boyer, 1978; Cohn, 1958). Researchers then showed that biological activity promoted the O exchange between water and PO_4 at typical earth

temperatures (Blake, O'Neil, & Surkov, 2005; Kok & Varner, 1967; Longinelli & Nuti, 1973). This research helped lay the groundwork enabling future researchers to analyze the $\delta^{18}O_P$ in soil and water samples. Recently, researchers have found that $\delta^{18}O_P$ signatures may be useful to differentiate between contributing P sources (Granger et al., 2017; Federica Tamburini, Pfahler, Sperber, Frossard, & Bernasconi, 2014; Young et al., 2009) and as a tracer of microbial P cycling within the soil profile (Alon Angert et al., 2011; Ford, Williams, Young, King, & Fischer, 2018; Larsen, Middelboe, & Johansen, 1989; Federica Tamburini et al., 2014; Zohar, Shaviv, Young, et al., 2010).

This research project will provide further insight into the reliability of using the $\delta^{18}O_P$ as a tool to differentiate between contributing P sources in agricultural systems. Soil samples collected over a 16-year study will be analyzed to determine changes in soil P pools over time and to provide insight into the long-term impacts of annually applied poultry litter at various rates. Phosphorus fractionation in conjunction with the $\delta^{18}O_P$ will also provide a framework for understanding the accumulating P over time, utilizing legacy P in agricultural systems, and identifying the contributing sources to legacy P pools within a field.

1.1 Literature Review

1.1.1 Harmful Algal Blooms, Eutrophication, and Hypoxia

The National Institute of Health examined the relationship between harmful algal blooms (HABs) and eutrophication (Anderson et al., 2008) and concluded that eutrophication and Paralytic Shellfish Poisoning (PSP) has a strong correlation where there are high nutrient inputs from sewage treatment plants, surface runoff, and groundwater sources. As a result, researchers are using paralytic shellfish poisoning (PSP), neurotoxic shellfish poisoning (NSP), amnesic shellfish poisoning (ASP), ciguatera fish poisoning (CFP), fish kills, reduction of submerged vegetation, aquatic mammal mortalities as indicators and trackers for monitoring HABs across the world (Anderson et al., 2008; Glibert et al., 2002). Figure 1.1 shows only 15 locations across the world in 1970 where PSP was an indicator of an HAB. In contrast, in 2015, over 120 locations were identified, according to the National Office for Harmful Algal Blooms at Woods Hole Oceanographic Institution (2018). This represents a 700% increase in HABs over the last 45 years.

The increase of HABs over the last several decades is directly correlated to the increased nutrient loading to waterbodies (Anderson et al., 2008). Although algal blooms occur in both saltwater bodies and freshwater bodies, excessive N is primarily responsible for HABs in saltwater bodies whereas P is primarily responsible for HABs in freshwater bodies (SSSA, 2018). Water quality impairment as the result of nutrient enrichment can be found across the U.S. (Figure 1.2). Over the past decade, Lake Erie, one the five Great Lakes in the U.S., has served as an example of the effects on nutrient enrichment on surface water quality. Located on the eastern border of Michigan and Ohio, environmental concerns in Lake Erie have continually risen over the past decade due to an increase in dissolved P loads in Lake Erie, resulting in more frequent algal blooms, many of them are classified as HABs. In 1974, a watershed monitoring program was initiated by the U.S. Army Corps of Engineers' called the Lake Erie Wastewater Management Study to monitor the lake. Since then, Heidelberg University in Ohio has been monitoring water quality parameters for Lake Erie and its contributing tributaries.

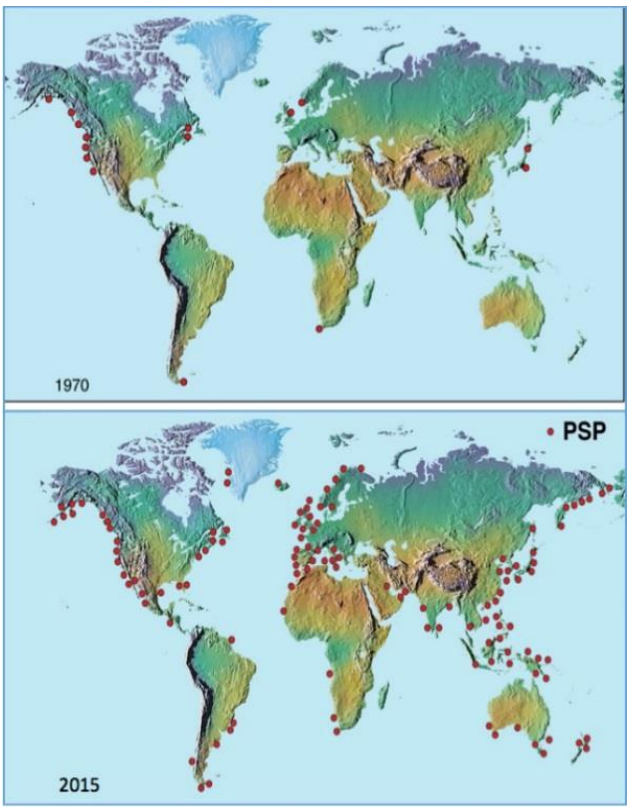

Figure 1.1. Increase of HABs (PSP) from 1970 – 2015

Source: (WHOI, 2018)

According to the "Experimental Lake Erie Harmful Algal Bloom Bulletin 35" (NOAA 2017) , seven out of fourteen years have carried a spring total bioavailable P load of greater than 100 metric tons. The increased P load contributes to the HABs in Lake Erie. This is not only a concern to the aquatic life, but also the local economy. Tourism along the coast of Lake Erie accounts for 28% of total tourism throughout Ohio (Association, 2015). The overall impact of the HABs in Lake Erie is a concern to farmers, residents, policy makers, tourists, etc., as researchers and project teams are continually working to improve the situation.

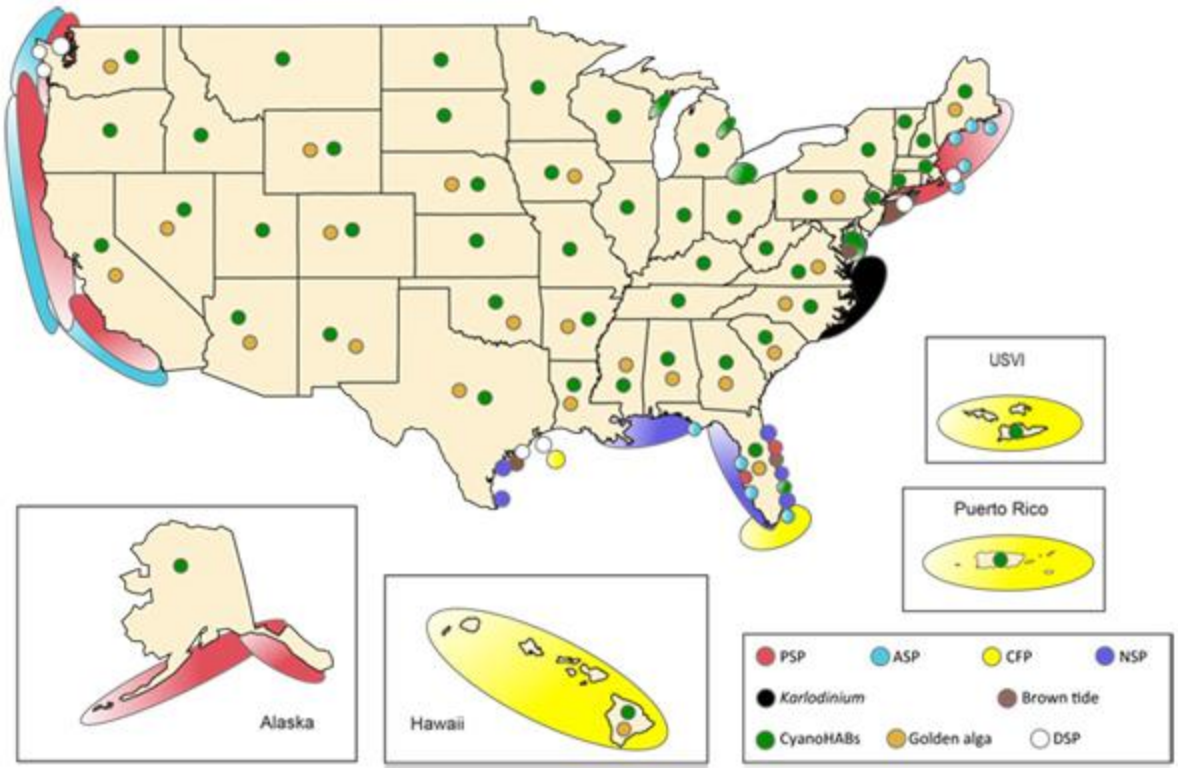

Figure 1.2. HAB poisonings in United States.

HAB poisoning in U.S. Ovals indicate regional phenomena whereas circles are localized. These include paralytic shellfish poisoning (PSP), neurotoxic shellfish poisoning (NSP), amnesic shellfish poisoning (ASP), ciguatera fish poisoning (CFP), brown tides (BT), cyanoHABs and a number of other HAB phenomena such as fish kills, loss of submerged vegetation, shellfish mortalities, and widespread marine mammal mortalities. *(WHOI, 2018)*

This coastal concern occurs reaches many coastal waters, including the Gulf of Mexico. The primary species responsible for HABs in the gulf region is ichthyotoxic dinoflagellate Karenia brevis (formerly Gymnodinium breve Ptychodiscus brevis), however, other species are present (Anderson et al., 2008). According to The Florida Fish and Wildlife Commission, the first documented red tide occurred in 1878 and the severity remained relatively consistent for the next hundred years. However, in late 1940s through the late 1950s a significant increase was documented with an even higher number of HABs beginning in 1995 to present (Commission, 2018). Most coastal regions are investing resources into investigating the environmental concerns associated with HABs and effective management strategies to mitigate contributing sources.

1.2 Contributing P Sources

Sources of P are typically divided into point and nonpoint sources. Nonpoint sources typically include contributions from either an urban/residential system or an agricultural system. Application of inorganic fertilizers, animal manure, or decomposing plant residue can be typical of an agricultural nonpoint source, whereas turf grass management or storm runoff from an urban or residential neighborhood represent urban nonpoint source pollution. Regardless of the P source, P is introduced into the system, accumulated and cycled, some of which becomes available to plants while some is transported downstream. The P cycle is a complex system where P is mineralized, immobilized, adsorbed or desorbed from mineral surfaces, dissolved or precipitated. Both point and nonpoint sources of P play a major role in exceeding acceptable P loads in a water body.

1.2.1 Point Sources

The Environmental Agency defines *point source* "as any discernible, confined and discrete conveyance, including but not limited to any pipe, ditch, channel, tunnel, conduit, well, discrete fissure, container, rolling stock, concentrated animal feeding operation, or vessel or other floating craft, from which pollutants are or may be discharged. This term does not include agricultural stormwater discharges and return flows from irrigated agriculture (EPA)." Point sources typically include Wastewater Treatment Plants (WWTP), home sewage systems, and industrial plants. Point source pollution continues to be problematic in many watersheds, especially in urban watersheds, but is largely regulated by the U.S. EPA by issuing National Pollutant Discharge Elimination System (NPDES) permits and routine monitoring of effluent or water quality entering the waterways. Since the Clean Water Act was passed in 1972, significant improvements have been made at reducing point source pollution.

1.2.2 Non-point sources

The general consensus in literature is nonpoint source nutrient loads are primarily responsible for the HABs in lakes and waterbodies around the world, especially in watersheds dominated by agricultural land use due to both organic and inorganic fertilizer applications (Carpenter, Caraco, Correl, Howarth, & Sharpley, 1998). Since nonpoint source pollution is a gradual accumulation of P from innumerable smaller sources, it continues to be extremely difficult

to quantify and manage. Regulatory agencies around the world are maintaining strict guidelines on point source pollutants and shifting their focus on how to manage and regulate the nonpoint sources.

Using Lake Erie as a case study, Maccoux, Dove, Backus, and Dolan (2016) found that the majority of P in Lake Erie comes from nonpoint source pollution (Table 1.1). Similar findings were also reported by Scavia et al. (2016), with 85% of the nutrient load in the Maumee River entering Lake Erie coming from synthetic fertilizers and manures. These findings not only highlight the importance of nonpoint source pollution to downstream water quality but also show the importance of mitigating nutrient loss from agricultural landscapes.

Table 1.1 Source pollution to Lake Erie.

	Nonpoint	Point	Atmospheric deposition	Upstream loads from the Great Lakes area
Total P loads	71%	19%	~5%	~5%
Soluble reactive P	49%	39%	6%	6%

Source: (Maccoux et al., 2016)

1.2.3 Point and nonpoint source identification

The Clean Water Act was initiated in 1948, and although major revisions occurred in 1972, 1977, and 1987, clarity as to what is classified as agricultural stormwater discharge still looms. There are many cases across the U.S. where lawsuits have been filed to distinguish point from nonpoint source contaminations and whether certain contributions are exempt because they are classified as "agricultural stormwater discharge" entering waterways (Echikson, 2014). Whether permits are required or not, farmers and landowners are typically making efforts to avoid excessive nutrient application to agricultural fields. For example, 56 – 80% of farmers in the Lake Erie region applied P at or below the current fertility recommendations (Smith et al., 2018).

Historically, water quality assessments of dissolved P and total P have primarily been used to estimate nonpoint and point source contributions to water bodies (Brooker, Longnecker, Kujawinski, Evert, & Mouser, 2018). Increased efforts to reduce nutrient loading is pushing research towards trying to delineate between contributing sources so further action can be

implemented to reduce overall loads. Using the unique signature from the phosphate stable oxygen isotope from soil and water samples is one way researchers have successfully been able to identify contributing sources (Ford et al., 2018; Gooddy et al., 2015; Granger et al., 2018; Pistocchi et al., 2017; Young et al., 2009). A different approach to distinguish between point and nonpoint source contributions is by analyzing for dissolved organic matter and dissolved organic phosphorus using ultrahigh resolution mass spectrometry (MS). Using this approach, Brooker et al. (2018) reported that samples collected 41 miles apart shared unique dissolved organic matter (DOM) and dissolved organic P (DOP) signatures that were 75% - 85% similar, suggesting that ultrahigh resolution MS is another potential approach to differentiating contributing sources.

1.2.4 Separating P from nonpoint sources: Recently applied P vs. legacy P

As population increases and the number of farms decrease, more demand is placed on the farmer's ability to maximize yields. Finding the balance between maximizing yield and minimizing inputs can be daunting, especially with continual and increasing awareness of the impacts of agriculture on environmental issues, such as water quality. Agricultural advancements have enabled farm managers to use precision agriculture to optimize fertilizer applications (N and P), however, excessive nutrient runoff continues to be problematic.

Management practices are implemented to maximize yield, which traditionally, include fertilizer application. As N and P are both essential nutrients to plant growth, the current standard recommendation is to apply fertilizer according to soil fertility results with little consideration for other impacts, such as the potential of contaminating water sources (Smith et al., 2018). While some of the applied fertilizer is indeed used for plant uptake, some N and P can accumulate in fields and watersheds over time, especially if application rates exceed crop requirements An in-depth study of three watersheds over 30 years (China, UK, and US) showed that two out of the three watersheds (UK and US) nutrient outputs exceeded the inputs, implying that the contributions to the elevated nutrient losses were from nutrient applications from previous years (Powers et al., 2016).

With the increasing impact and awareness of nonpoint transport of P to streams and rivers, more attention is being focused on the excessive application of fertilizers to agricultural systems. When fertilizer inputs exceed plant uptake, phosphorus accumulates over decades through manure and fertilizer applications and will continue to mobilize, even after inputs decline (Powers et al.,

2016). The mobilization of legacy P into waterways makes it difficult to assess the immediate impacts of current conservation measures compared to contributions from historical fertilizer applications. For 30 years, stream monitoring of DRP and TP loads in two Ohio streams determined that initially, implementation of conservation practices (50% no till and a 25% applied P reduction) resulted in significant decreases in DRP loading and TP loading (Baker & Richards, 2002); however, over time, DRP loads began to increase while TP loads continued to decrease (Richards, Baker, & Crumrine, 2009). The increased trend of DRP in the same watersheds was also confirmed by Jarvie et al. (2017) stating that even with extensive implementation of conservation practices, reduced application of P, and reduced sediment loss, increasing loads of DRP continued to enter the waterways. Further research is needed to clarify where the increased loads are coming from, whether it is from recently applied P or if it is bound legacy P becoming soluble and susceptible to runoff.

It is becoming apparent that the implementation of conservation practices and improved nutrient management strategies is having a slower impact on water quality than anticipated. The legacy P of historical management practices has created sinks and stores of P and is masking the immediate effects of current management strategies (A. Sharpley et al., 2013).

1.3 Soil P and P loss

Phosphorus introduced into an agricultural system can come from plant residue, organic fertilizer, inorganic fertilizer or atmospheric deposition. The phosphorus then becomes part of a complex system where it:

1. Converts into a soluble form of P which is readily available for plant uptake.
2. Is weakly bound to a soil particle that could be released and used for plant uptake.
3. Strongly binds with other elements in the soil such as Al, Mg, or Fe, which is unavailable for plant uptake.
4. Transported off the field, typically by surface or subsurface runoff.

The amount of P that is in soil solution is both time-specific as well as crop-specific which will be available for plant uptake during the growing season and the life cycle of the crop (Holford, 1997). Research has provided a sound understanding of the relationship between how much P is applied and how much is either used for plant uptake, weakly or strongly bound, or transported off the field. Since implementation of conservation practices is not having the immediate impact as

intended, the need to determine the original source of the DRP leaving the field is justifiable. Identifying contributing sources such as manure application, synthetic fertilizers, sewage, effluent, or atmospheric deposition will greatly impact management and conservation strategies to target specific contributing sources. The ability to look at the spectrum of inputs across an agricultural system allows a more focused approach to management decisions.

1.3.1 $\delta^{18}O_P$ as a tracer

Using the $\delta^{18}O_P$ as a tracer to differentiate P inputs in soil and water provides a tool to better target conservation management strategies for the more persistent and/or problematic sources. When an agricultural system receives a mixture of inorganic and organic fertilizers, the fate of the individual source and its contribution to the P cycle is unknown. Soil tests determine DRP, TP, or a fractionation of soil P among different pools; however, the traditional soil tests do not distinguish how each source contributes to each of those pools or losses from the field. The stable phosphate isotope has successfully been identified and used in agricultural soil and water samples (Ford et al., 2018; Granger et al., 2017) to further understand the fate of various contributing sources of P in an agricultural system. Identifying the unique $\delta^{18}O_P$ signature of each source enables conservation management practices to be targeted at a specific point and/or nonpoint source.

Phosphorus has 23 isotopes, but only one is stable (^{31}P) making source identification impossible. However, since P strongly binds to oxygen (O) (Young et al., 2009) and O has three stable isotopes (^{16}O, ^{17}O, and ^{18}O), analysis of the O atoms bound to PO_4 can be analyzed by stable isotope mass spectrometry (A. S. Colman, 2002; Kornexl, Gehre, Hofling, & Werner, 1999; McLaughlin, Paytan, Kendall, & Silva, 2006; McLaughlin, Silva, Kendall, Stuart-Williams, & Paytan, 2004). To determine the $\delta^{18}O_P$ signature, the ratio of $^{18}O/^{16}O$ on the phosphate molecule is analyzed and then compared to known source signatures as well as calculated equilibrium values (Granger et al., 2017; Federica Tamburini et al., 2012; Young et al., 2009).

Young et al. (2009) evaluated the isotopic signatures for different phosphate sources (e.g., inorganic vs. organic P fertilizers) and compiled their findings with data from other published $\delta^{18}O_P$ results (Ayliffe, Veeh, & Chivas, 1992; A. S. Colman, 2002; Gruau et al., 2005; McLaughlin, Paytan, et al., 2006). Federica Tamburini et al. (2014) expanded the compiled dataset of $\delta^{18}O_P$ results and looked at signatures within specific P pools. Collectively, all chemical fertilizers had a mean signature for $\delta^{18}O_P$ of +20.8‰ whereas animal waste (dog and goose) produced a signature

of +15.7‰ and +18.3‰, respectively. However, bulk animal waste has not been successfully characterized for P (Young et al., 2009) because the measured $\delta^{18}O_P$ can be altered due to exchange with reagent O (Liang & Blake, 2006a, 2006b).

Using the phosphate stable oxygen isotope as a tracer can benefit research at the process, soil, plant, and ecosystem levels (Federica Tamburini et al., 2014):

- Process level: $\delta^{18}O_P$ determination in P fractions induced by enzymes (specifically phytase) could clarify why plant structural P is enriched in ^{18}O;
- Soil level: $\delta^{18}O_P$ determination within different P pools in both organic and inorganic pools can be used to determine the process in which equilibrium is achieved;
- Plant level: factors that affect $\delta^{18}O_P$ determination in both metabolic P and structural P can be used to determine if the equilibrium equation can be applied to both plants and soil organisms; and
- Ecosystem level: $\delta^{18}O_P$ determination can be used to identify sinks or sources of P as well as insight on the biological process: when P is applied to a P-limited system, the $\delta^{18}O$-P could provide information on the biological process, but when P is applied to a P abundant system, $\delta^{18}O_P$ could be used to identify the sources of P.

As identified by Tamburini, et al., this research will provide further insight into many levels of the fate of P in soil by using $\delta^{18}O_P$ as a potential identifier of contributing sources of phosphorus to water bodies and agricultural systems. Ultimately, it will provide a mechanism to more fully understand how to more efficiently utilize applied P to fields and reduce P loss from agricultural fields.

1.3.2 Phosphorous oxygen bond

Although P can be bound to different elements in the soil (e.g., C & O in phosphonates, N in phosphazenes, H in phosphides, and other elements in phosphides), most of the P is bound to O forming PO_4 (Figure 1.3) and less plentiful in the other forms when found in a soil-plant system (Federica Tamburini et al., 2014).

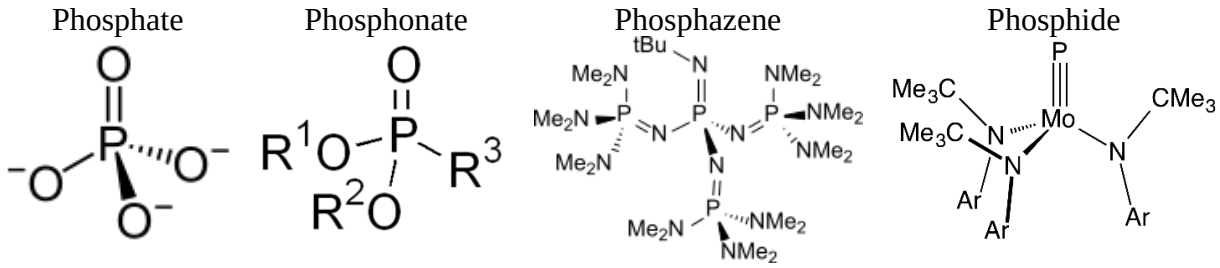

Figure 1.3. P molecules

(Source: Wikipedia on 7/20/2018)

Understanding the P-O bond has enabled the O isotopes in the P molecules to be used as an indicator or a signature of the P source. This is done by determining the ratio between the heaviest and lightest O isotopes, ^{18}O and ^{16}O (Federica Tamburini et al., 2014). The P sources can then be identified by determining the isotopic variability of the O isotopic composition in the PO_4 molecule (McLaughlin et al., 2004).

Although the chemistry is known of how the isotopic ratio is obtained, researchers are still teasing out factors that influence the exchange of the O molecule bound to PO_4. Because the bond is resistant to inorganic hydrolysis, biological processing is necessary to force the O to exchange with water (Blake, O'Neil, & Garcia, 1997; Longinelli, Bartelloni, & Cortecci, 1976). The biological cycle of P-compounds erases the source signature and will reflect equilibrium, if it is indeed in equilibrium, rather than source values (Blake et al., 2005; Colman, Blake, Karl, Fogel, & Turekian, 2005; McLaughlin, Chavez, Pennington, & Paytan, 2006; McLaughlin, Kendall, Silva, Young, & Paytan, 2006; Paytan, Kolodny, Neori, & Luz, 2002). This is done by breaking the P-O bonds and resetting the isotopic signature to a temperature-dependent value and by using the $\delta^{18}O_P$ as well as the amount of biological cycling that has occurred (McLaughlin & Paytan, 2007).

1.3.3 Soil P fractionation

Fractionation among soil P pools is a valuable tool when determining the transport of P through the soil profile. Researchers and chemists have developed methods to optimize the P fractionation method and have successfully quantitated various soil P pools over the last several decades (Amaizah et al., 2012; S. C. Chang & Jackson, 1957; Cross & Schlesinger, 1995; Hedley et al., 1982; Kashem, Akinremi, & Racz, 2004). The S. C. Chang and Jackson (1957) method was

used to distinguish soil P pools from commercial fertilizer which was applied over 40 years. Observations showed P pools increased except for Ca-P and TP and they suggested the migration P through the soil was due to the dominance of Al-P (Amaizah et al., 2012). The Hedley et al. (1982) fractionation method has been successfully used by several researchers and was confirmed to provide a general index of the different forms (both biological and geochemical) forms of P in the soil (Cross & Schlesinger, 1995). Fractioning P (using the Hedley method or an alternative) quantitates the targeted P, however, it does not allow for the source of that P to be identified. Fractioning usually consists of a water extractable-P, $NaHCO_3$-P, a weak NaOH-P, a strong NaOH-P, HCl-P, and a TP.

Although there are numerous methods to fractionate P, for the purpose of this project, obtaining quantifiable proportions of phosphorus (both organic and inorganic) would hopefully provide a long-term trend of changes in soil P pools over time. This is useful because as observed in the Western Lake Erie Basin (WLEB) there has been a steady increase in SRP since 2002, even though there has not been an increase in commercial fertilizer or applied manure within the watershed (Jarvie et al., 2017). This illustrates the potential for P to move from a non-labile to labile state and confirms the value in fractionating archived soil to delineate the long-term change in soil P pools. Investigating this spectrum of P pools within a soil will help develop a tool for successful watershed management and remediation (A. Sharpley et al., 2013), and fractioning these P pools through sequential extraction will clarify where applied P is being stored.

The research location for the proposed project has long history of poultry litter application (over 16 years), with the first 10 years having an average annual application of 1192 mg kg^{-1} of soluble reactive P applied with a standard deviation of 796 mg kg^{-1} (Waldrip et al., 2015). In addition, soil P pool fractions were determined and as expected, over 10 years, the cumulative P increased in all soils that had poultry litter applied, regardless of land use. Extracted P pools using a modified Hedley fractionation method resulted in the HCl-P>$NaHCO_3$-P>NaOH-P>H_2O-P with HCl-P comprising 59-76% of the total extractable P in the cultivated soils. When compared to the control cultivated field (Y6), the high rate poultry litter application increased the HCl-P by nearly 700 mg P kg^{-1} (Waldrip et al., 2015). It is suggested that some of this increase could be due to the supplemental diet of poultry with Ca^{2+} and P (Kebreab & Vitti, 2010) directly contributing to the calcium bound P released during the HCl-P extraction. $NaHCO_3$-P contributed a much smaller portion of P and had less variability whereas the H_2O-P had very little in the controls but increased

by 758% in the high rate poultry application rate after 10 years (Waldrip et al., 2015). Although fields with grazed cattle had higher P loss during storm flow (Harmel, Torbert, Haggard, Haney, & Dozier, 2004), the addition of manure from cattle grazing alone did not significantly contribute to the TP (Waldrip et al., 2015).

1.3.4 Soil P pool $\delta^{18}O_P$

One challenge in this research is determining which pool of P to target while identifying the isotopic signature. Federica Tamburini et al. (2014) compiled published results from different research identifying the range of $\delta^{18}O_P$ targeting P pools from HCl-P (n=4), NaOH-P (n=1), Acetic Acid-P (n=1), Bray-P (n=1), water extractable-P (n=1), Microbial P (n=1), HNO_3-P (n=2), Resin-P (n=4), NH_4F-P (n=1), and $NaHCO_3$-P (n=1) (A. Angert, Weiner, Mazeh, & Sternberg, 2012; Alon Angert et al., 2011; McLaughlin, Cade-Menun, & Paytan, 2006; McLaughlin, Paytan, et al., 2006; Federica Tamburini et al., 2012; Zohar, Shaviv, Young, et al., 2010). Results varied from as low as 5.6‰ $\delta^{18}O_P$ to as high as 23.7‰ $\delta^{18}O_P$, but as indicated by the data, a wide range of signatures can be determined even within a single extraction method due to potential P input sources. Method refinement is ongoing and further research is needed to clarify and improve the signature viability.

The most common approach for the $\delta^{18}O_P$ is using the Resin-P and HCl-P extracted pool. The HCl-P pool fraction is not readily available to plants and microorganisms, it is usually free of organic P and takes a long time for the P to become available for plant uptake (Negassa & Leinweber, 2009). Among published results, the HCl-P varied from 5.6‰ – 21.3‰ and Resin-P ranged from 12.7‰ – 22.8‰ (Federica Tamburini et al., 2014). Although published results are informative, further characterization is necessary on soils with historical management records to provide signatures to clearly differentiate contributing sources. The HCl-P pool is considered to be a good approximation of the inorganic P in Ca-P minerals such as apatite so it is the preferred pool to target for $\delta^{18}O_P$ analysis (F. Tamburini, Bernasconi, Angert, Weiner, & Frossard, 2010; F. Tamburini et al., 2012).

A long-term study (27y) investigated the application of N, P, and potassium (K) and analyzed $\delta^{18}O_P$ and then calculated the isotope equilibrium range within different phosphorus pools (Figure 1.4). Results show the control plot compared to N and K application did not show significant differences; however, the plots with P application varied significantly. Compared to the control, H_2O-P_i and NaOH-P_i had significant variability, whereas HCl-Pi and $NaHCO_3$ had consistent results among the different P treatments (Bi et al., 2018).

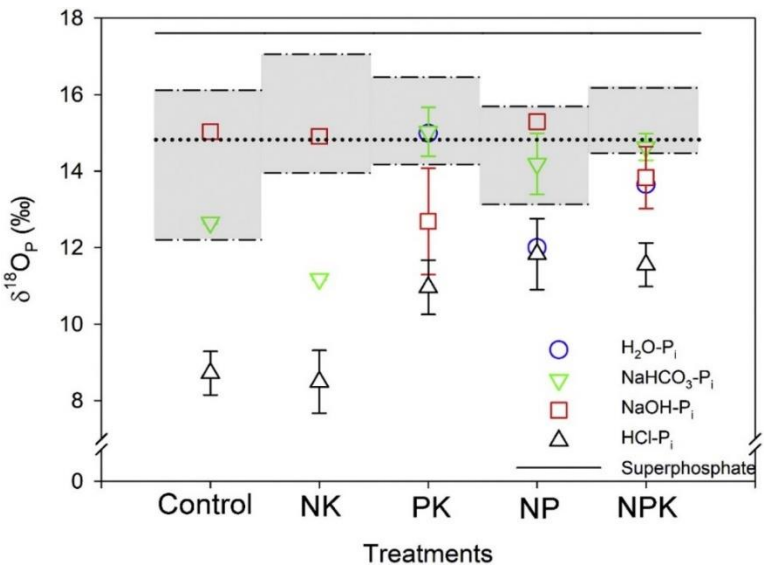

Figure 1.4. Oxygen isotope ratios and equilibriums in NPK treatment

Oxygen isotope ratios in phosphate of soil inorganic P pools and calculated equilibrium for different fertilizer treatments over 27y: nitrogen and Potassium (NK); Phosphorus and Potassium (PK); Nitrogen and Phosphorus (NP); Nitrogen, Phosphorus and Potassium (NPK) Source: (Bi et al., 2018)

1.3.5 Isotopic Equilibrium

Once $\delta^{18}O_P$ isotope values have been determined, the values are used to calculate equilibrium as well as percent P contribution to a system. To calculate equilibrium and percent P, a series of parameters are needed, including soil temperature, $\delta^{18}O$ signatures from discrete P pools for control samples, treated samples, and the isotope composition of the original source (Bi et al., 2018; Longinelli & Nuti, 1973).

The $\delta^{18}O_P$ equilibrium is calculated by using soil temperature and the isotopic signatures for both PO_4 and H_2O Equation 1-1) (Longinelli & Nuti, 1973), where T is the temperature and $\delta^{18}O_P$ *and* $\delta^{18}O_w$ is the oxygen isotope of dissolved phosphate and oxygen isotopic composition of the soil water, respectively.

$$T(°C) = 111.4 - 4.3(\delta^{18}O_P - \delta^{18}O_w)$$

Equation 1-1. Equilibrium equation for $\delta^{18}O_P$
(Longinelli & Nuti, 1973)

Although Equation 1-1 was originally used to calculate equilibrium for water samples, it can also be used to calculate equilibrium for soil samples. Hence, soil temperatures and datasets for water isotopes for the study area will need to be acquired. Soil temperature values can be estimated based on the NRCS website for the Riesel TX area or if available, pulled from archived data collected at Riesel research station. The water isotope data ($\delta^{18}O_w$) is available from the International Atomic Energy Association (IAEA) for precipitation across the globe. This is a potential resource to obtain this data; however, if data is unavailable for that area through IAEA, values can be obtained through other publications or estimated based on current rainfall events.

Another equilibrium equation was recently derived to calculate the equilibrium of microbial turnover of phosphate (S. J. Chang & Blake, 2015). Each approach is unique in its approach to calculate equilibrium, however, the reasoning behind which equation to use for this project needs further research. Hence, both equations are included for future reference and a determination of which approach to take will be made at a later stage of this research. Each equation can potentially produce unique equilibrium values with the Chang and Blake equation (Equation 1-2) producing slighter greater values (Tonderski et al., 2017).

$$\boldsymbol{\delta^{18}O_{PO4} = \left(\delta^{18}O_w + 10^3\right)e\left[\frac{14.43\frac{10^3}{T} - 26.54}{10^3}\right] - 10^3}$$

Equation 1-2. Equilibrium for microbial P turnover (S. J. Chang & Blake, 2015)

Isotopic mass balance is difficult to calculate because the rate and cycling of the microbial cycled P is still being investigated. If assumptions are made that no P is cycled from microbes and the sole source of P is from fertilizers, a mass balance can be estimated (Bi et al., 2018). With these assumptions, by using the isotope composition of P fertilizer as well as an average equilibrium in conjunction with the content from inorganic P pools, Bi et al. (2018) successfully calculated equilibrium (Equation 1-3).

$$equilbrium\ \delta^{18}O_{PO4} = (\delta^{18}O_{PO} *\ C_o + (C_t - C_o) * \delta^{18}O_{ps})/C_t$$

Equation 1-3. Isotopic Mass Balance

(Bi et al., 2018)

Lastly, calculating percentage of P contributed to a system through fertilizer application versus microbially cycled P is vital to effectively design management strategies to mitigate excessive P contamination. This approach requires a two source mass balance, where $\delta^{18}O_{Pt}$ in the Hedley Pi pool and the $\delta^{18}O_{Po}$ is the isotopic value for the control and the isotope composition for the fertilizer source is represented by $\delta^{18}O_{Ps}$ in Equation 1-4.

$$\%\ P\ fertilizer\ equilibrium = \frac{\delta^{18}O_{Pt} - \delta^{18}O_{Po}}{\delta^{18}O_{Ps} - \delta^{18}O_{Po}} \text{x}100\%$$

Equation 1-4. % P contributed

(Bi et al., 2018)

1.4 Spatial and temporal variability

1.4.1 Spatial variability/spatial analysis

Analysis of soil $\delta^{18}O_P$ in agricultural settings has been generally limited to plot scale studies, but to broaden the understanding of P source interactions in a field setting, the scope of the sampling area also needs to be investigated. Spatial variation of $\delta^{18}O_P$, environmental factors, and management practices (including the usage of organic or commercial fertilizer) are all intertwined in a complex system. Determining a sampling design/scheme can be a challenge and must be carefully considered.

A broad sampling grid of 210 m by Peukert et al. (2012) found that $\delta^{15}N$ and $\delta^{13}C$ and nutrient variability is not geospatially different in soils that are similar in management, climate, and soil class. They did determine, however, that 83 m was the minimum grid size if assessing spatial variability for bulk density or soil organic matter. Granger et al. (2017) confirmed no significant spatial variability for $\delta^{18}O_P$ at any of the 3 sampling grids (75 m, 25 m, and 10 m). Although there was a strong correlation between TP and HCl_{PO4}, the $\delta^{18}O_P$ did not have a strong spatial trend with any of the parameters. Using a kriging with external drift (KED) model, the strongest correlation was between $\delta^{18}O_P$ and HCl_{PO4} which had a weighted correlation of only 0.30. The lack of a strong correlation with any of the measured parameters reaffirms the need to expand

the potential parameters in which a relationship with $\delta^{18}O_P$ can be established. This parameter could serve as an indicator of potential available P and hot spots within an agricultural system.

Another watershed scale study was recently done by Ford et al. (2018), and reported that soil water extractable P was not in equilibrium with long-term water isotope values. Even though the field had not received poultry litter in 10 years, it is suggested the soils at the research site at least partially retained their original $\delta^{18}O_P$ signature of poultry litter from 10 years prior, providing a mode to identify P hot spots in an agricultural system. Using $\delta^{18}O_P$ from storm events on a watershed scale, the authors illustrated the ability to partition P from both shallow and deep subsurface sources as well as water extractable P bound to surface soils in water samples prior to an event. Using the $\delta^{18}O_P$ to identify different phosphorus sources in an agricultural system in conjunction with access to historical management data provides the knowledge needed to use the $\delta^{18}O_P$ as a tracer of applied P to determine the soil-plant-water interaction of different management systems.

Several physical, chemical or biological processes acting at a different spatial scale may influence the spatial variability of a given soil (Goovaerts, 1998) and this variability exists in agricultural systems as well as natural systems, regardless of the management (Goovaerts, 1998; Marriott et al., 1997). To be able to identify potential hot spots of legacy P in agricultural systems, further investigation needs to be done to determine if there is a relationship between $\delta^{18}O_P$ and other parameters. Stable isotopes of carbon and nitrogen have been successfully used for source identification in numerous studies (Kendall & McDonell, 1998) and investigating a potential correlation between $\delta^{13}C$ or $\delta^{15}N$ could provide further insight to understanding the long-term fate of P in an agricultural system and the contributing sources of P to surrounding water bodies.

1.4.2 Temporal variability

Limited research has been done investigating change in $\delta^{18}O_P$ isotopic signature over time. As of now, the majority of research has published discrete samples comparing treatments and/or P pools (A. Angert et al., 2012; Blake, Alt, & Martini, 2001; Elsbury et al., 2009; Ford et al., 2018; Granger et al., 2017; Federica Tamburini et al., 2012; Federica Tamburini et al., 2014; Young et al., 2009). Using archived soil samples from the last 16 years will be a unique approach compared to the discrete sample approach.

There are limited number of published results presenting temporal comparisons. One approach applied ^{18}O-labeled P_i to soils as a tracer to assess change over a growing season. Findings showed a rapid transformation of available P in soil into Ca-P at a rapid rate (Joshi, Li, & Jaisi, 2016). A separate approach was comparing change within one stormflow event, evaluating the transition of transport from an unsaturated to a saturated state. With this approach, isotopic results confirmed the potential to be used as tracers due to the observation of indicators of poultry litter that had been applied 10 years prior to the study (Ford et al., 2018). The $\delta^{18}O_P$ over 16 years will be useful to investigate the change over time in a complex system.

1.5 **Summary**

Recently, awareness of non-point source pollution to HABs has hastened the need to investigate ways to mitigate contributing P sources to lakes and streams. Investigating methods to differentiate point and non-point sources contributing to waterbodies is on-going and progress is being made. Groundwork for using the isotopic signatures of PO_4 started in the 1960s and has recently been applied to soil and water to identify unique isotopic signatures. This research has shown, chemical fertilizers, sewage treatment facilities, organic fertilizers, and other P sources to have a unique isotopic signature, providing a tool to target specific problematic sources which are contributing to waterways (Federica Tamburini et al., 2014; Young et al., 2009). Research has shown the $\delta^{18}O_P$ to be stable regardless of environmental factors and is gaining attention in the literature as a valued tool to further investigate P at the process, soil, plant, and ecosystem levels (Federica Tamburini et al., 2014).

Although successful attempts have been made to identify the stable isotopic signatures in both soil and water, confirmation of these signatures on a field scale with long term management records will be a valuable contribution to classify poultry litter compared to chemical fertilizers, specifically. Observing a quantifiable change in soil P pools over time (17 years) as well as assessing the uniformity of those P pools using a grid sampling scheme will be used to compare signatures from $\delta^{18}O_P$ as well as $\delta^{13}C$ and $\delta^{15}N$ for the sample set. Relationships will be assessed to determine if a correlation exists between $\delta^{18}O_P$ and a P pool, $\delta^{13}C$ and/or $\delta^{15}N$. Because the method to analyzing for $\delta^{18}O_P$ is relatively new and very labor intensive, identifying a strong correlation with one of the other factors could provide a mechanism to target specific sampling areas to analyze for $\delta^{18}O_P$.

CHAPTER 2. PHOSPHORUS BUDGETS AND RUNOFF LOSSES FROM LONG-TERM NUTRIENT MANAGEMENT PRACTICES IN THE TEXAS BLACKLAND PRAIRIE

2.1 Introduction

The U.S. poultry industry has rapidly grown over the past twenty years, with broiler meat production increasing by 12% from 8.7 to 9.9 billion broiler birds (NASS, 2020) and a 25% gain in egg production between 2000 and 2019 (NASS, 2001, 2020). Increased production of meat and eggs is accompanied by increased poultry litter, which is often applied to both cultivated fields and pastures as a source of nitrogen (N) and phosphorus (P). Land application of poultry litter can increase the soil organic matter, increase infiltration and water-holding capacity, improve yields, and soil fertility (Hoover, Law, Long, Kanwar, & Soupir, 2019; Lin, Watts, van Santen, & Cao, 2018) ; however, it can also contribute to nonpoint P loss, especially when litter is applied at N-based rates (Qin & Shober, 2018; A. Sharpley et al., 2013; Sims, 1998; Sims, Edwards, Schoumans, & Simard, 2000). The eutrophication of surface water bodies remains the leading cause of water quality impairment in the U.S. and globally, as the number and severity of Harmful Algal Blooms (HABs) and hypoxic zones continue to increase (Ho, Michalak, & Pahlevan, 2019). As increased poultry production and impaired water quality persist, sustainable approaches for managing poultry litter are critically needed.

The effect of poultry litter application on runoff P concentrations and losses has been widely studied with laboratory- (Adeli, Bala, Rowe, & Owens, 2006; Kleinman & Sharpley, 2003) and plot-scale studies (Edwards & Daniel, 1993; Haggard, Vadas, Smith, DeLaune, & Moore, 2005; Harmel, Haney, & Smith, 2011; Pote et al., 2003; Vadas, Harmel, & Kleinman, 2007) using mainly simulated rainfall. For example, Harmel et al. (2004) showed that repeated applications of poultry litter increased extractable P concentration in soil, with increased soil test P concentration likely to increase the risk of P loss (Kingery, Wood, Delaney, Williams, & Mullins, 1994; Pote et al., 1996). Study results showing the impact of nutrient management practices such as application timing (i.e., time of year or time relative to rainfall), application rate, and application placement (i.e., broadcasted vs. incorporated) have been summarized in nutrient management tools including

P indices (DeLaune et al., 2004; Elliott, Brandt, Kleinman, Sharpley, & Beegle, 2006; Kleinman et al., 2006) and numerical models (Collick et al., 2016; Vadas et al., 2007).

Evaluating individual variables under simulated rainfall has been invaluable to the understanding of practice dynamics. Comprehensive assessment of nutrient management strategies that encompass nutrient management (i.e., source, rate, timing, and placement), crop yield, changes in soil nutrient concentration, and water quality from fields and small watersheds under natural precipitation, however, is limited, with datasets greater than 5 years in length uncommon. These long-term data are needed to validate nutrient management tools (Osmond et al., 2012) and improve nutrient management guidelines and recommendations. Further, measuring P losses from a single spatial scale while providing information on local source and transport factors does not allow for assessment of P transport beyond the plot or field. Nested water quality monitoring studies can be useful for understanding how both biogeochemical (source) and hydrologic (transport) factors influence downstream nutrient losses (Bauwe, Tiemeyer, Kahle, & Lennartz, 2015; Lohani, Baffaut, Thompson, & Sadler, 2020) and assessing watershed P buffering capacity (Kusmer et al., 2019). Identifying nutrient sources and evaluating the impact of upland management practices on downstream loading are essential for increasing the efficacy of conservation practice implementation (Williams, King, & Penn, 2018).

In 2000, a long-term nutrient management study was initiated on pastures and cultivated fields at the USDA-Agricultural Research Service (ARS) Grassland, Soil and Water Research Laboratory near Riesel, Texas to determine the effects of converting from an inorganic to an organic fertilization system using poultry litter. Studies investigating nutrient loss in runoff from new poultry litter application sites (Harmel et al., 2004), nutrient loss from repeated poultry litter applications (Harmel et al., 2009), the effect of poultry litter composting on runoff water quality (Harmel, Haney, Smith, White, & King, 2014), soil microbial communities and enzyme activity following poultry litter application (Acosta-Martinez & Harmel, 2006), transformations of soil and manure P after surface application of poultry litter (Vadas et al., 2007), distribution of soil P using sequential fractionation following long-term poultry litter application (Waldrip et al., 2015), on-farm economics of poultry litter application (Harmel, Harmel, & Patterson, 2008), and evaluation of the EPIC (Wang, Harmel, Williams, & Harman, 2006) and SWAT models (Green, Arnold, Williams, Haney, & Harmel, 2007) on fields receiving poultry litter have been published utilizing data from this long-term study. Here, we build upon this previous work using long-term nutrient

management records (i.e., source, rate, placement, and timing of P application) in conjunction with harvest and yield records (1995-2015) to evaluate temporal trends in annual agronomic P budgets for nine monitored fields (6 cultivated; 3 pasture). Specific objectives were to 1) assess relationships among agronomic P budgets, soil test P concentration, and dissolved P concentration in surface runoff from the cultivated and pasture fields receiving different poultry litter application rates (0.0 to 13.4 Mg ha^{-1}); and 2) assess the effect of long-term poultry litter application on downstream dissolved P concentrations and loads in two watersheds using a nested watershed approach.

2.2 Materials and Methods

2.2.1 Site Description

Experimental fields and watersheds monitored in the current study are part of a long-term study to evaluate the effects of poultry litter application on soil properties and environmental quality (Harmel et al., 2014). The study sites are located within the Texas Blackland Prairie ecoregion near Riesel, TX (701440.23 m E, 3484189.47 m N) (Figure 2.1). The Blackland Prairie ecoregion is dominated by Houston Black clay soil (fine, smectitic, thermic, udic Haplustert), which has high potential of shrinking and swelling with moisture fluctuations. Long-term average annual rainfall at the study site is 988 mm, with most rainfall occurring during May, June,

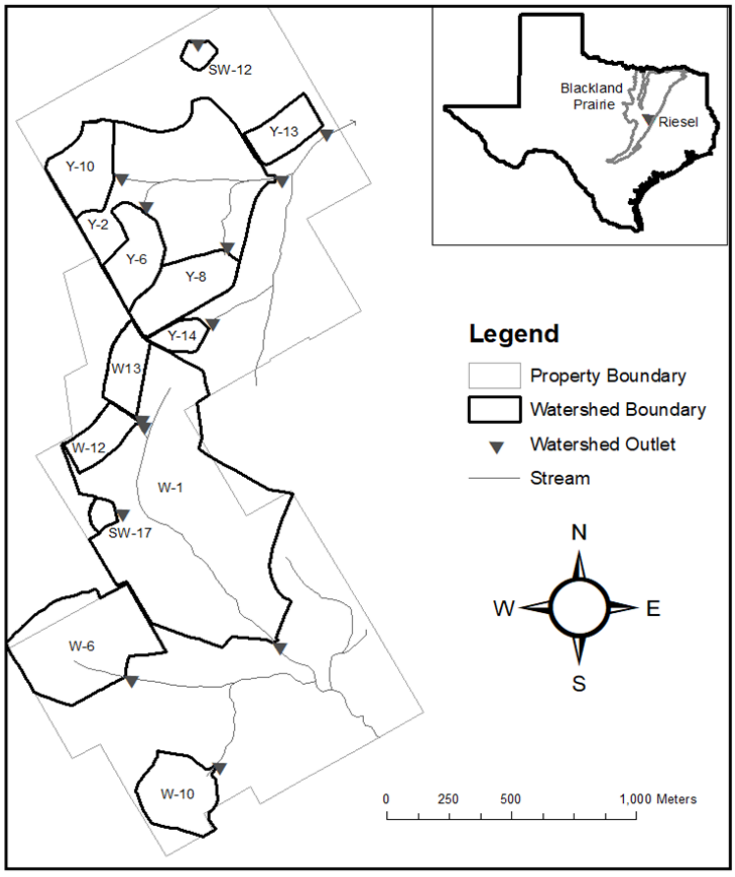

Figure 2.1. Study fields at the USDA Agricultural Research Service Grassland, Soil and Water Research Laboratory, Riesel, TX.

and October. Average annual temperature is 19.2 °C and ranges from 8.2 to 29 °C in January and July, respectively. Management practices within study fields were generally consistent across the study period to avoid confounding differences resulting from varying management, with detailed management information outlined in Harmel et al, (2004, 2009) and Waldrip et al., (2015). Briefly, management practices included tillage, planting, harvest, application and incorporation of poultry litter, supplemental application of inorganic N and P, and pesticide and/or herbicide use.

Cultivated fields (Y6, Y13, Y10, W12, W13, and Y8) were fallow in 2000, and in 2001, a 4-year corn (*Zea mays* L.)-corn-wheat (*Triticum aestivum* L.)-fallow rotation was used until 2010. Oat (*Avena stative* L.) and hay were also used in the rotation after 2010. Each field received an annual application of poultry litter at target rates of 0.0, 4.5, 6.7, 9.0, 11.2, and 13.4 Mg ha^{-1}, respectively. Poultry litter was a mixture of manure and bedding (either wood shavings or rice hulls) obtained from the cleanout of turkey and broiler houses near the study site. Based on litter properties (Waldrip et al., 2015), mean P application rates ranged from 75 to 219 kg P ha^{-1} (Table 2.1). Field Y6 received solely inorganic P fertilizer at an annual mean rate of 18 kg P ha^{-1} (Table 2.1) and supplemental inorganic N was applied to all fields during corn years. Poultry litter was incorporated into the soil after application with a disk or field cultivator. Between 1995 and 2015, cultivated fields were tilled 1-4 times per year.

Table 2.1. Field scale watershed properties and management.

Site	Area (ha)	Slope (%)	Land management	Phosphorus source	Mean P application rate (kg ha^{-1} yr^{-1}) †
Y13	4.6	2.3	Cultivated (Corn-Corn-Wheat)	Poultry litter	75 (*n*=15)
Y10	7.5	1.9	Cultivated (Corn-Corn-Wheat)	Poultry litter	108 (*n*=15)
W12	4.0	1.2	Cultivated (Corn-Corn-Wheat)	Poultry litter	134 (*n*=15)
W13	4.6	1.1	Cultivated (Corn-Corn-Wheat)	Poultry litter	175 (*n*=15)
Y8	8.4	2.2	Cultivated (Corn-Corn-Wheat)	Poultry litter	219 (*n*=15)
Y6	6.6	3.2	Cultivated (Corn-Corn-Wheat)	Commercial fertilizer	18 (*n*=12)
SW17	1.1	1.8	Pasture, hayed (Bermuda/Klein grass)	Poultry litter	107 (*n*=2)
W10	8.2	2.5	Pasture, hayed (Bermuda Grass)	Poultry litter	123 (*n*=7)
Y14	2.3	1.6	Pasture, hayed (Klein grass)	Poultry litter	219 (*n*=9)
Watershed					
W1	71.0	2.2	Cultivated (56%), Pasture/rangeland (44%)		
Y2	53.0	2.6	Cultivated (30%), Pasture/rangeland (70%)		

† Number of years from 1995 – 2015 with documented application rates

Pasture fields were either managed as grazed improved pasture (SW17) or hayed improved pasture (W10 and Y14). The pastures contained a monoculture of coastal Bermudagrass (*Cynodon dactylon* L.) or Klein grass (*Panicum coloratum* L.). SW17 received two surface applications of inorganic fertilizer, while W10 and Y14 each had a combination of 6 kg P ha^{-1} from inorganic fertilizer applications and an annual mean application rate of 123 kg P ha^{-1} over 7 years and 219 kg P ha^{-1} over 9 years, respectively, from poultry litter (Table 2.1). Neither inorganic nor organic fertilizers were incorporated on the pastures. Pasture SW17 was also opened for selective grazing for approximately 8 months each year.

Two small agricultural mixed land use watersheds (Y2 and W1) were also monitored in the current study. Field sites Y6, Y8, and Y10 (total area = 22.5 ha) drain to watershed Y2 (53.0 ha), while sites SW17, W12, and W13 (total area = 9.7 ha) drain to watershed W1 (71.0 ha) (Figure 2.1). Areas outside of the study fields were planted with similar crops (e.g., corn, wheat, oat, hay) and pasture. Only inorganic fertilizers were applied to these fields and pastures, with P applications equivalent to crop P removal rates (est. average annual P application rate = 17 kg P ha^{-1}).

2.2.2 Field management, discharge, and runoff water quality data

Field management, discharge, and water quality data were downloaded from the USDA-ARS Grassland, Soil and Water Research Laboratory website (Harmel et al., 2014; USDA Agricultural Research Service Grassland, 2020). Consistent field management data including dates of field operations, nutrient management (source and rate of application), crop type, and crop yield were available from 1995-2015. Soil samples (0-15 cm) were collected annually in late-fall at each of the study sites (at least one core per 0.4 ha) and were analyzed for Mehlich-3P (Mehlich, 1984; Waldrip et al., 2015). Sub-daily discharge values were downloaded for the period of 2000-2015 to match the period of runoff water quality data availability (Harmel et al., 2014). Fields and watersheds were instrumented with a shaft encoder as the primary water level recording device and flow rates were calculated with known stage-discharge relationships. Automated samplers (Teledyne ISCO, Inc., Lincoln, NE) were used to sample runoff from all storm events, with flow-paced samples composited into a single bottle (Harmel, King, Haggard, Wren, & Sheridan, 2006; Harmel, Richardson, King, & Allen, 2006). All water samples were refrigerated prior to analysis for dissolved nitrate, ammonium, and phosphate concentrations using colorimetric methods with a Technicon Autoanalyzer IIC (Bran-Luebbe, Roselle, IL) or a Flow IV Rapid Flow Analyzer (O.I.

Analytical, College Station, TX). Detailed site metadata including site history and management, instrumentation, and laboratory methods are available from the STEWARDS database (www.nrrig.mwa.ars.usda.gov/stewards/stewards.html).

2.2.3 Estimating agronomic phosphorus budgets

Agronomic P budgets were estimated for each pasture and cultivated field using a crop and soil systems approach (Bundy & Sturgul, 2001), whereby the sum of outputs was subtracted from the sum of inputs for each year between 1995 and 2015. Inputs of P included organic and inorganic fertilizer application, while outputs included only surface loss and crop P removal. Since atmospheric deposition is generally low relative to fertilizer inputs (Hanrahan et al., 2019; Pease et al., 2018), it was not included as an input of P. Phosphorus application rates for poultry litter were calculated by multiplying application rate by manure P concentration. Crop P removal was estimated by multiplying reported crop yield by a P removal factor (Logsdon, Clay, Moore, & Tsegaye, 2008)). Consistent with previous studies, positive balances indicate nutrient accumulation and negative balances indicate nutrient drawdown or reduction, after accounting for all agronomic inputs and outputs.

2.2.4 Data analysis

Daily mean discharge for fields and watersheds was calculated using R Statistical Software (2017) and were concatenated with dissolved P concentration from water quality monitoring stations. Annual flow-weighted mean concentration and P load were then determined for each of the study sites. Trends in annual and cumulative agronomic P budgets were determined and compared to average annual P application rate using linear regression. Relationships among annual (and cumulative) agronomic P budgets, soil test P concentration, flow-weighted mean dissolved P concentration were also evaluated using linear regression. Relationships were assessed for pasture and cultivated fields separately, as well as for all sites regardless of land use. All analyses were considered statistically significant at $p < 0.05$.

To assess the effect of field-scale P management on watershed-scale P losses, a nested watershed approach was utilized. Data from the small watersheds and the field sites within them were analyzed using a variation of the before-after control-impact experimental (BACI) design. A BACI experimental design is often characterized by two fields being managed similarly for a

specified period of time and then a treatment would be implemented on one of the fields while the other field would remain as the control (e.g., King, Williams, Dick, & LaBarge, 2016; Williams et al., 2015). In the current study, we did not have sufficient water quality data before the poultry litter experiment began; however, we use fields within each watershed that maintained a near neutral agronomic P balance as a proxy for a "before" period. Average annual dissolved P FWMC and load were analyzed using analysis of co-variance (ANCOVA) as outlined by (Clausen & Spooner, 1993) to determine if fields and watersheds varied from a neutral P balance. Linear relationships between control and treatment sites were compared, where significantly different slopes indicated a treatment effect.

2.3 Results

2.3.1 Agronomic P budgets

Prior to the initiation of the long-term poultry litter study (1995-2000), inorganic P applications to fields and pastures ranged from 0.0 to 31.2 kg ha^{-1}. Sites SW17, W12, W13, and Y13 received no inorganic P application, sites Y6, Y8, and Y10 received an average annual inorganic P application of 18.5±5.8 kg ha^{-1}, and sites Y14 and W10 received an average annual inorganic P application of 6.6±0.9 kg ha^{-1}. Annual agronomic P budgets for cultivated fields was between -4.7 and -15.7 kg ha^{-1} (average = -6.8±9.9 kg ha^{-1}), while annual P budgets for pastures ranged from -7.4 to 0.5 kg ha^{-1} (average = -3.5±5.1 kg ha^{-1}). Cumulative agronomic P budgets across all sites during this 6-yr period averaged -8.4±9.5 kg ha^{-1} (Figure 2.2A).

From 2001 through 2015, poultry litter was applied to all fields and pastures except for Y6, which only received inorganic P applications (Table 2.1). Across all sites a total of 87 poultry litter applications occurred at an average P rate of 151.8±67.7 kg ha^{-1}, with average P rates for individual sites ranging from 81.1 to 235.1 kg ha^{-1} (Table 2.1). Average annual crop P removal rate over the entire period (1995-2015) was greatest for corn (-17.7±5.6 kg ha^{-1}) compared to hay (-11.1±5.4 kg ha^{-1}), wheat (-10±2.6 kg ha^{-1}), and Klein grass (-9.3±4.4 kg ha^{-1}). Accounting for P inputs and outputs, average annual agronomic P budgets across sites was 61.9±88 kg ha^{-1}, with cultivated fields (105.3±77.1 kg ha^{-1}) tending to have a greater average annual P balance than pastures (58.0±92.6 kg ha^{-1}). Average annual P budgets exhibited a significant positive relationship with average annual P application rate ($R^2 = 0.98$; $p < 0.001$; data not shown).

Cumulative agronomic P budgets increased linearly for most study sites as poultry litter application rate and manure P concentration was fairly consistent across years (Figure 2.2A). Cumulative P budgets for all sites was between -18 and 2980 kg ha^{-1} and averaged 1301±932 kg ha^{-1}. Cultivated fields tended to have greater cumulative P balance (1523±987 kg ha^{-1}) compared to pastures (856±637 kg ha^{-1}), however P application rates tended to be greater on cultivated fields Figure2.2B). For pastures sites W10 and Y14 where poultry litter was applied early in the study period (i.e., 2001-2007) and either no litter or less frequent applications occurred in later years, cumulative P budgets reached an asymptote, as annual crop removal only accounted for a small fraction of the accumulated P (Figure 2.2B).

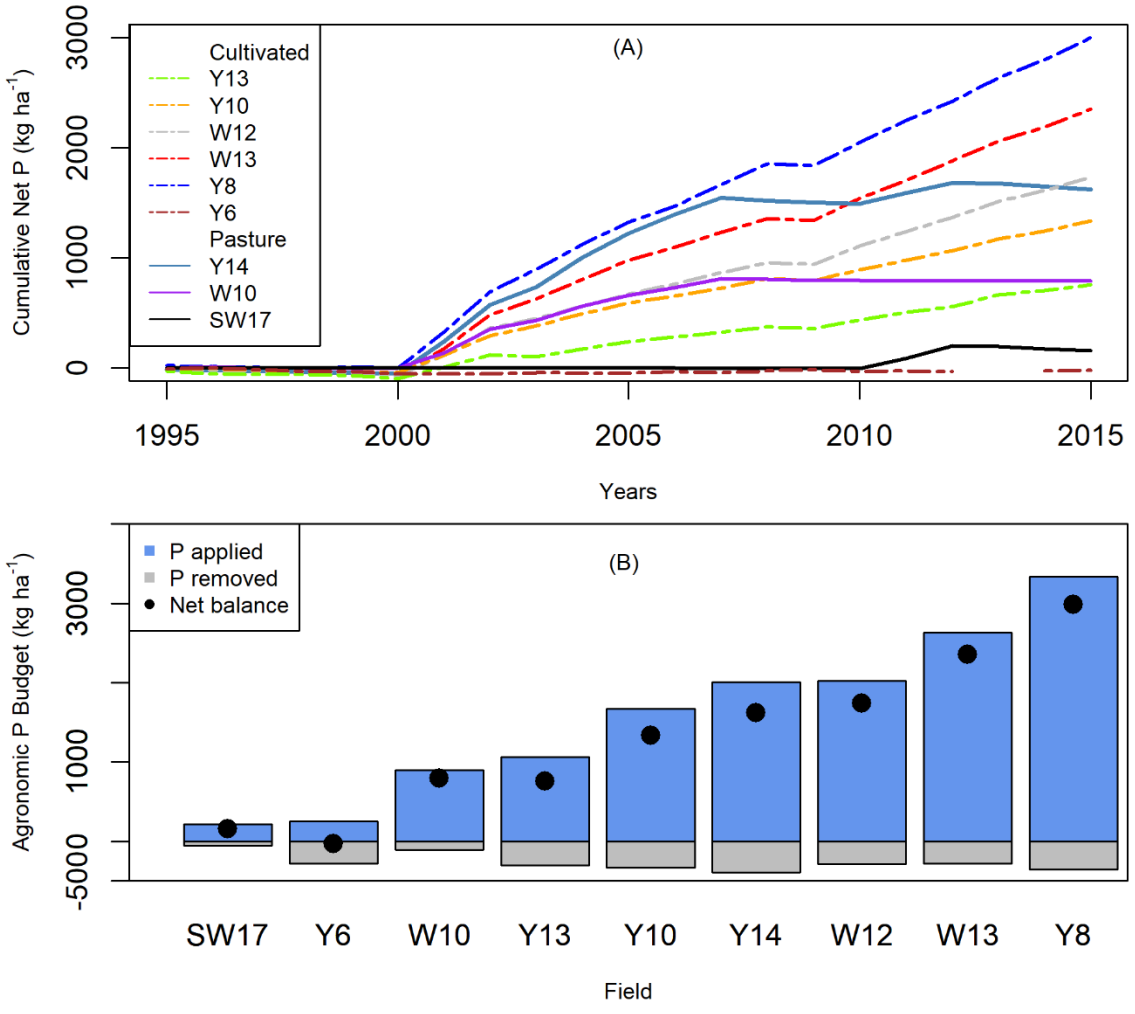

Figure 2.2. Cumulative and agronomic P budgets for cultivated and improved pasture with long-term poultry litter application.

2.3.2 Effect of phosphorus budgets on STP and runoff dissolved phosphorus

Soil samples were collected and analyzed in 2000 to obtain baseline levels of soil test phosphorus (STP) for fields and pastures, which averaged 20.3±3.5 mg kg^{-1} ranging from 15 mg kg^{-1} to 27 mg kg^{-1}. Cultivated fields had a slightly elevated baseline mean of 24.3±2.1 mg kg^{-1} compared to the pasture fields mean STP of 19.0±2.8 mg kg^{-1}. Soil test P levels for Y6 averaged 25±4 mg kg^{-1} throughout the study, while STP at Y8 increased to 59 mg kg^{-1} after a single poultry litter application and further increased over the study period to 236 mg kg^{-1}. Average STP for pastures (SW17, Y14, W10) was 50.3±37.7 mg kg^{-1} whereas the cultivated fields averaged 114.5±49.1 mg kg^{-1} from 2001-2015. All fields combined had an average soil level P of 81.1±56.9 mg kg^{-1}. Soil level P showed a positive correlation with cumulative P balance ($R^2 = 0.76$, $p < 0.001$; Figure 2.3A). The average annual change in STP levels also exhibited a positive correlation with average annual P balance for all sites ($R^2 = 0.88$, $p < 0.001$; Figure 2.3B). A stronger positive correlation was observed among cultivated fields compared to pasture fields, $R^2 = 0.95$ and $R^2 = 0.45$, respectively ($p < 0.001$, $p = 0.60$, Figure 2.3B).

Annual flow weighted mean concentration (FWMC) of dissolved phosphorus averaged 0.6±0.5 mg L^{-1} for all sites from 2001–2015, ranging from 0.01 mg L^{-1} to 2.98 mg L^{-1}. Throughout the study, average annual FWMC fluctuated between 0.01 mg L^{-1} and 2.29 mg L^{-1} for cultivated fields and 0.03 mg L^{-1} and 2.98 mg L^{-1} for pasture fields. During the study, 3 of the 15 years (2004, 2007, 2015) had notably higher phosphorus loading due to increased average rainfall of 1449(±45) mm yr^{-1} compared to the remaining years of mean rainfall of 816±286 mm yr^{-1}. The fall application of poultry litter in 2009 was delayed and applied in January 2010, hence 2 litter applications occurred in 2010 which explains the higher P loading and lower observed rainfall. Strong positive correlations were exhibited between average annual FWMC and average annual P budgets for both pasture and cultivated fields, $R^2 = 0.99$ and 0.95, respectively ($p < 0.05$, $p < 0.001$), whereas the correlation for all fields collectively was much weaker ($R^2 = 0.54$, $p < 0.001$, Figure 2.3C). A strong positive correlation is also observed comparing average annual FWMC mg L^{-1} with average annual STP mg kg^{-1} for pasture fields ($R^2 = 0.992$, $p = 0.16$) and cultivated fields ($R^2 = 0.989$, $p < 0.001$) whilst the correlation for all fields regardless of land management exhibiting a moderate correlation ($R^2 = 0.468$, $p < 0.001$; Figure 2.3D).

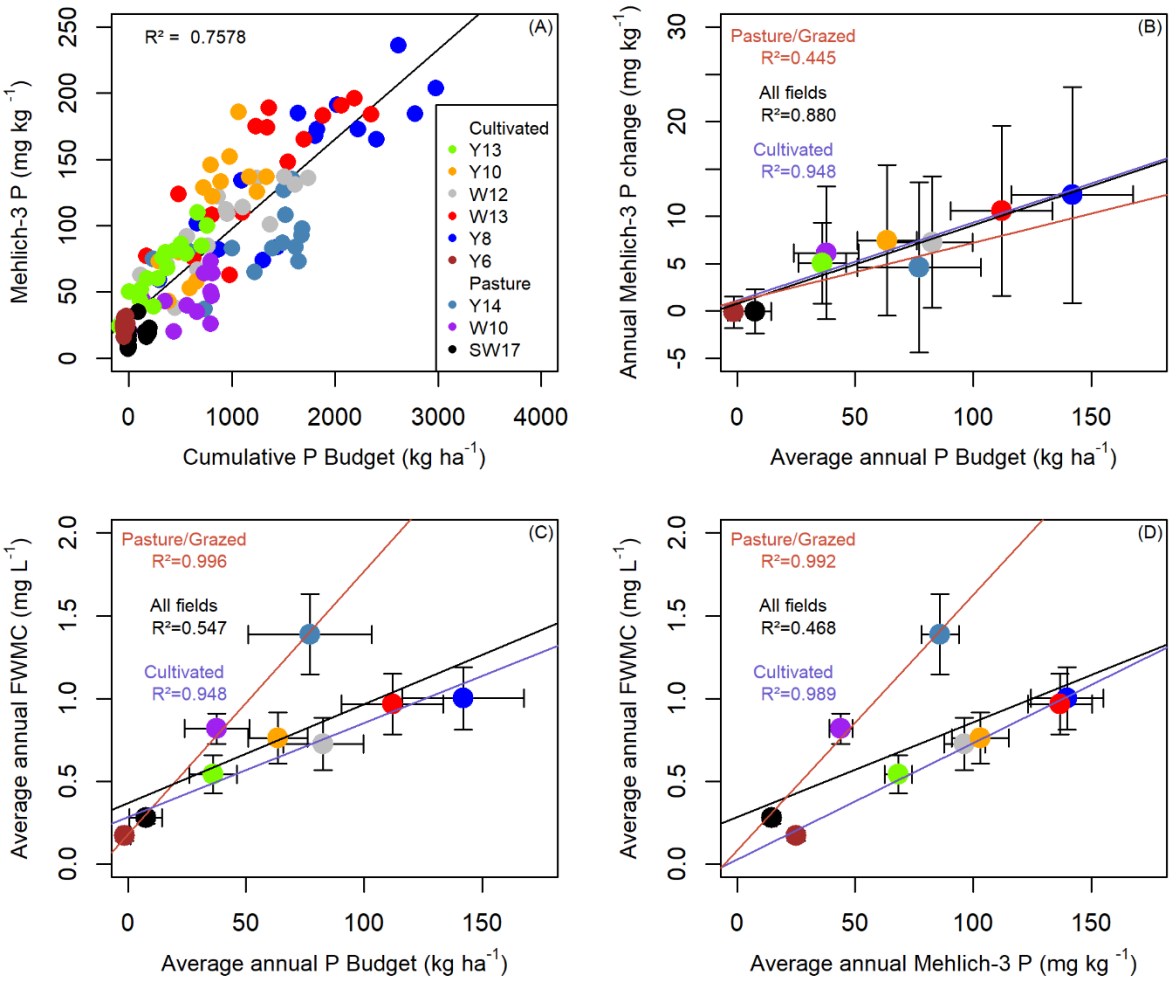

Figure 2.3. Relationships between cumulative P budgets, STP (Mehlich-3P), and DRP FWMC show positive relationships with pasture/grazed fields showing increased risk of elevated DRP FWMC.

2.3.3 Effect of field-scale P management on watershed-scale P losses

Field sites Y6, Y8, and Y10 drain to watershed Y2, while sites SW17, W12, and W13 drain to watershed W1 (Figure 2.1), referred to hereafter as Y and W watershed. Within both Y and W watersheds, one field or pasture (Y6 and SW17, respectively) maintained a near neutral P balance throughout the study period. The relationship between Y6 and SW17 was therefore used to assess if other fields or the watershed differed from a neutral P balance. For average annual FWMC, the slope of the relationship between SW17 and Y6 (m = 0.03) was significantly less than the slope of

the relationship between SW17 and Y10 (m = 0.1, p =.009) and between SW17 and Y8 (m = 0.3, p =.006), indicating that FWMC for Y8 and Y10 were greater than that observed from fields with a neutral P balance. The slope of the relationship between Y6 and SW17 (m = 2.0) was similar to the slope of the relationship between Y6 and W12 (m = 2.1, p = 0.018) and between Y6 and W13 (m = 2.1, p = 0.018). In contrast, the slope of the relationships for both Y (m = 0.1, p = 0.200) and W (m = 0.8, p = 0.387) watersheds was not significantly different from a neutral P balance suggesting that average annual FWMC was not significantly influenced by poultry litter applications to portions of the watershed. Average annual FWMC for the Y and W watershed was 0.34±0.17 mg L^{-1} and 0.25±0.14 mg L^{-1} from 2002 – 2015, respectively. Initial examination of annual P loading relationships between control (Y6 or SW17) and treatment fields and watersheds revealed a large amount of variability. Years 2004, 2007, 2010, and 2015 were grouped together due to 'high rainfall' (HR) 1449(±45) mm yr^{-1} and two litter application during 2010 (i.e., elevated transport or source potential). Remaining years were grouped as 'normal rainfall' (NR) and had an average rainfall of 816±286 mm yr^{-1}. Relationships were subsequently assessed for all years, HR years, and NR years. For the Y watershed, the relationship between SW17 and Y6 (m = 0.3) was significantly different for Y10 (m = 2.9, p < 0.0001), Y8 (m = 3.2, p < 0.0001), and Y2 (m = 1.2, p < 0.0001) when all years were considered. During the NR years, treatment effects of poultry litter application are observed on Y8 (m = 0.6, p = 0.018), Y10 (m = 0.5, p = 0.039), and Y2 (m = 0.5, p = 0.047) as well as the HR years for Y8 (m = 3.9, p = 0.021) and Y2 (m = 1.4, p = 0.022); however, Y10 had no treatment effect (m = 3.7, p=.052) (Figure 2.4). Phosphorus loads in the W watershed did not indicate any treatment effects at W1 for LR, HR, or all years (m = 0.9, p = 0.695; m = 3.4, p = 0.858; m = 2.7, p = 0.981, respectively). Watersheds W12 and W13 (m = 13.5, p < 0.0001; and m = 14.9, p < 0.0001, respectively) showed a treatment effect when assessing all the years together. However, differentiating between the HR years and NR years, W12 and W13 exhibited no treatment effect during the NR years (m = 0.8, p = 0.435; and m = 1.5, p = 0.051) but p values indicated a treatment effect of poultry litter application on P loading during the HR years for both fields: W12 (m = 20.4, p = 0.010) and W13 (m = 21.2, p = 0.002) (Figure 2.4).

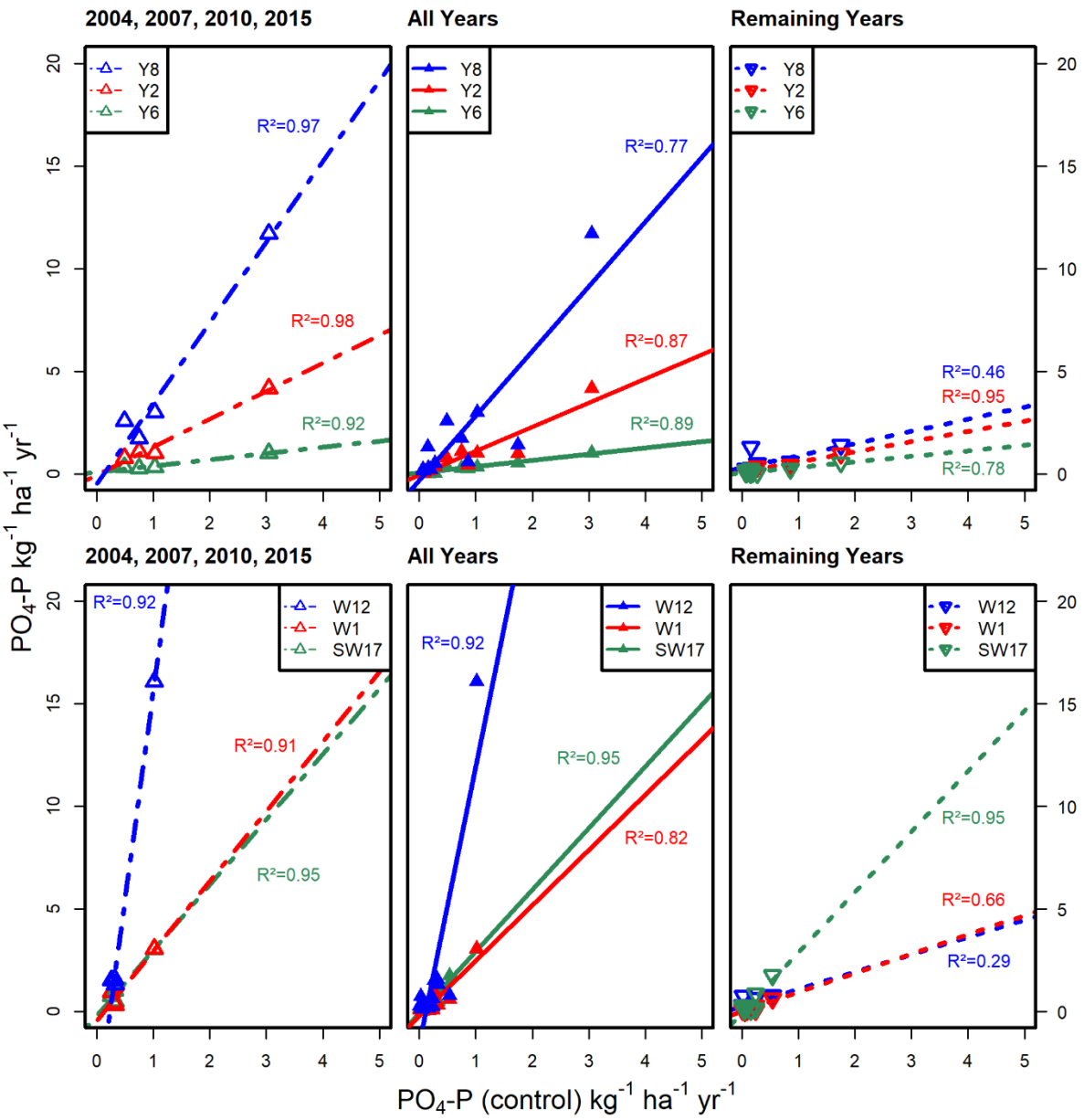

Figure 2.4. Using BACI to determine impacts of poultry litter for W and Y watersheds using P balanced fields (SW17 and Y6) to assess relationship between poultry litter field and the impact at the watershed scale.

2.4 Discussion

2.4.1 Positive agronomic P balances resulted in soil P accumulation and increased DRP concentration in field runoff

Agronomic P budgets determined for pastures and cultivated fields in the current study were strongly influenced by P application rates. Annual P inputs from commercial fertilizer or poultry litter ranged from 0 to 219 kg P ha^{-1} (mean = 124.8±86.3), with P outputs including crop removal (-11.6±6.4 kg P ha^{-1}) and DRP losses in runoff (-1.9±3.8 kg P ha^{-1}) accounting for only a small fraction of P inputs, especially for fields and pastures receiving poultry litter. To maintain a balanced P budget at application rates applied in the current study, poultry litter would only have needed to be applied to fields or pastures every 10±6 years. It should be noted, however, that P application rates exceeded fertility recommendations for the Texas Blackland Prairie region. For example, in 2000, average soil test P for study fields was 23 mg kg^{-1}. Consistent with findings from the current study, previous research at the field (Hanrahan et al., 2019), watershed (Bennett, Reed-Andersen, Houser, Gabriel, & Carpenter, 1999), river basin (Powers et al., 2016) and regional spatial scales (Garnier et al., 2015) have shown that variability in agronomic P budgets was largely dependent on application rate.

Phosphorus inputs in excess of crop P removal (i.e., positive agronomic P balance) resulted in the accumulation of soil P within study fields and pastures, with greater soil P accumulation observed in fields and pastures with greater agronomic P balances. Similar positive relationships between agronomic P budgets and the amount of P remaining in agricultural fields (Domburg, Edwards, Sinclair, & Chalmers, 2000; Messiga, Ziadi, Belanger, & Morel, 2014; Ruane, Treacy, McNamara, & Humphreys, 2014) and regions (Reid & Schneider, 2019) have been reported. For instance, Simpson, Stefanski, Marshall, Moore, and Richardson (2015) found that 96% of P applied to a grazed pasture over a 9-year study was retained within the top 20 cm of the soil profile. While increases in Mehlich-3 P were observed with positive agronomic P balances in the current study, Waldrip et al. (2015) assessed changes among soil P pools between 2002 and 2012 from the same fields using the sequential Hedley fractionation method providing additional insight into soil P accumulation. The authors found that poultry litter application to both cultivated fields and pastures increased concentrations of total soil P in all extractable fractions, especially at high application rates. In cultivated fields (e.g., Y8 and Y10), the H_2O and $NaHCO_3$-P inorganic pools

substantially increased compared to stable pools (i.e., HCl-P) (Waldrip et al., 2015). In contrast, the only increase in soil inorganic P in pastures was observed in the HCl-P fraction when poultry litter was applied at the highest rate (Y14; (Waldrip et al., 2015)).

Elevated STP levels are widely known to increase the risk of DRP loss in surface runoff (e.g., Pote et al., 1996) and are useful for identifying critical source areas (e.g., Duncan et al., 2017). Results from the current study showed similar trends whereby accumulation of STP as the result of positive agronomic P balance resulted in greater average annual DRP FWMC in surface runoff. Indeed, Zopp et al. (2019) using a regression tree analysis found that soil test P concentration was the most important factor in predicting DRP FWMC at the field scale. Despite greater cumulative agronomic P balances, greater accumulation of soil P (as evidenced by increased Mehlich-3 P concentrations), and a large fraction of soil total P in labile fractions (Waldrip et al., 2015), cultivated fields in the current study had relatively lower risk of DRP loss compared to pastures with lower poultry litter application rates, lower soil test P concentrations, and only small changes in labile P pools over time. It is postulated that the difference in annual average DRP FWMC between cultivated fields and pastures was the result of P application method, as poultry litter applied to cultivated fields was incorporated with tillage whereas poultry litter was surface broadcast on pastures. Incorporating applied fertilizer and manures often decreases DRP concentration in surface runoff (e.g., A. N. Sharpley, 1995). It is also possible that increased runoff losses of DRP from pastures resulted in smaller fractions of labile P remaining in the soil compared to cultivated fields (Harmel et al., 2009). Findings from the current study therefore suggest that poultry litter application rates in excess of crop P requirements resulted in accumulation of P within the fields and pastures, and increased DRP FWMC in surface runoff, with pastures receiving surface broadcast applications representing the largest risk of loss.

2.4.2 Effect of field-scale P management on watershed-scale P loss

Assessing the impact of management practices on nutrient loss at the watershed scale is often challenging, as detailed information on land management, such as P inputs and P outputs, that is typically available at the field scale is often difficult to obtain across an entire watershed. Trends in water quality data at the watershed scale can therefore be difficult to interpret, which makes it nearly impossible to examine conservation practice effectiveness at this spatial scale without the aid of numerical models and scenario testing (Choquette, Hirsch, Murphy, Johnson, &

Confesor, 2019; Fanelli, Blomquist, & Hirsch, 2019; Kleinman et al., 2019). Nested watershed approaches are often recommended to overcome these challenges (Bauwe et al., 2015), but there are few examples from the literature that leverage this approach to evaluate the effect of nutrient management changes to individual fields on watershed nutrient loss. In the current study, we utilized a pair of nested watersheds in combination with a BACI experimental design to determine whether watershed DRP FWMC and DRP load varied from a neutral P balance (i.e., P inputs = P outputs). In doing so, we were able to quantify the impact of field scale management practices (i.e., high poultry litter application rates) on watershed concentration and load. The study design employed in the current study could therefore serve as a framework for future work geared toward assessing watershed scale conservation effects.

As a proof-of-concept for the approach, cultivated fields with high poultry litter application rates (Y8, Y10, W12, and W13) were compared to a neutral P balance. Not surprisingly, when all study years were considered, regression slopes for both DRP FWMC and DRP load from these fields differed from fields with a neutral P balance. That is, DRP FWMC and DRP load from the fields with high poultry litter application rates were greater than what would be expected from fields where P inputs equaled P outputs. Examination of DRP FWMC at the outlets of the Y and W watersheds, however, revealed that despite having 30% and 12%, respectively, of the total watershed area with high poultry litter application rate, DRP FWMC was not different from a neutral P balance. Thus, P application rates exceeding crop removal for 15 years did not increase the risk of elevated DRP FWMC at the watershed outlets. In both watersheds, fields with high poultry litter application rate were located at the farthest points from the watershed outlet (Figure 2.1), which likely lessened the impact of the high poultry litter application rates on watershed DRP FWMC compared to a scenario where fields with high application rates were located near the watershed outlet. For instance, in a rainfall simulation study using soil runoff boxes with high and low soil test P levels oriented differently within the boxes, Penn, Bryant, Needelman, and Kleinman (2007) found that DRP concentration in runoff from boxes with low soil test P positioned near the outlet was less than DRP concentration from boxes where high soil test P was positioned near the outlet. Elevated DRP transport in runoff during events from fields with high poultry litter application therefore likely had the opportunity to adsorb to soils with lower soil test P during transport. It is hypothesized that over time P accumulation along flow pathways could

result in increased DRP FWMC at the watershed outlet as these flow pathways and channels become increasingly saturated with P.

In contrast to DRP FWMC, results indicated that DRP loading from the Y watershed was greater than would be expected from a neutral P balance when all years, only NR years, and only HR years were considered. While the regression slope for HR years was substantially greater than a neutral P balance, DRP load during NR years only represented a slight increased risk compared to a neutral P balance. It is hypothesized that during NR years, much of the surface runoff from the high poultry litter rate fields may have infiltrated into the soil along flow pathways prior to reaching the watershed outlet due to drier antecedent conditions compared to HR years with wetter antecedent conditions. Differences in hydrologic connectivity between NR and HR therefore likely resulted in a greater risk of loss from the watershed outlet during HR years. These findings contradict those of Harmel et al. (2009) for the same watershed which concluded that litter application rates of 4.5 Mg ha^{-1} yr^{-1} were unlikely to have an adverse effect on water quality; however, the current study included an additional 7 years of data, which highlights the importance of long-term datasets for assessing conservation practices. For the W watershed, DRP load was not different than a neutral P balance for any of the scenarios tested. A combination of longer flow pathways (1.04 km vs. <0.66 km) and smaller impacted area (12% vs. 30%) likely contributed to the difference in affect observed between W and Y watersheds. Thus, the nested watershed approach with BACI design allowed for the testing of field P balances on watershed response and showed that the risk of downstream DRP loss in this landscape increased under conditions that promoted enhanced transport (i.e., hydrological connectivity) and source (i.e., two poultry litter applications, greater impacted area) factors.

2.5 Conclusion

Non-point source phosphorus contributions from agricultural systems can be reduced by determining phopshorus budgets and minimizing the difference between P inputs and P outputs. Nine field scale watesheds received annual rates of poultry litter ranging between 75 – 219 kg P ha^{-1} yr^{-1} on both cultivated and pasture/grazed fields. Results from cultivated fields showed a lower risk of DRP loss compared to pastures which could be attributed to P application methods. However, regardless of the application rate or land management, results showed net P balances had a positive relationship with DRP FWMC, STP and DRP loads in systems where poultry litter

was the primary nutrient source. This confirms previous findings between the relationship of P balances and STP (Ruane et al., 2014) and the impact legacy P has on increasing hydrologic P losses (Hanrahan et al., 2019). We utilized a pair of nested watersheds using the BACI design to quantify the impact of upstream contributions from high poultry litter applied fields. Hydrological connectivity (i.e., years with high rainfall and increased surface flow) between upstream fields and the watershed outlets enhanced DRP loads conributions but not DRP FWMC at the watershed scale. During years where normal rainfall was observed, treatment effects were not observed for either DRP load or FWMC at the watershed scale which could be attributed to findings by Penn et al. (2007), showing soils with low STP concentrations transport less P than soils with high levels of STP. Contributions from agricultural systems to downstream waterways is influenced by a combination of exisiting STP levels, P application method, tillage, application rate, and distance of flowpath from edge of field to waterbody and are more likely to occur during years where precipitation promotes hydrological connectivity.

CHAPTER 3. UTILIZING ISOTOPIC TRACERS TO EVALUATE PHOSPHORUS FATE IN TEXAS VERTISOL SOILS WITH LONG-TERM POULTRY LITTER APPLICATION

3.1 Introduction

Substantial efforts have been made over the last several decades to reduce agricultural non-point source pollution to waterways, however, elevated levels of phosphorus (P) and nitrogen (N) are still problematic in many areas. These elevated nutrient levels can cause harmful algal blooms (HABs) and hypoxia in surface water bodies such as Lake Erie and the Gulf of Mexico. One of the main challenges to mitigating non-point source pollution is identifying and differentiating among contributing nutrient sources. Management strategies could be improved if phosphate (PO_4) entering a surface water body from agricultural fields could be differentiated: for example, organic fertilizer (poultry litter, cattle manure, etc.) from commercial fertilizer and whether the contributing source is from a recent application or high P soil (i.e., legacy P). If organic and inorganic fertilizer is concurrently applied to an agricultural field to meet nutrient uptake demands (Harmel et al., 2009), the fate and transport of each P source is also unknown. The phosphate stable oxygen isotope ($\delta^{18}O_P$) could potentially help identify different sources of P in both water bodies and agricultural systems, and enable policy makers, researchers, and farmers to make management decisions that are both environmentally and economically beneficial.

To differentiate among potential sources of P, novel methods of analyzing P must be used. Traditional soil extractions such as water extractable P, Bray-P, and Mehlich-3 P are useful in determining the quantity and intensity of available P. Hedley et al. (1982) developed a series of extractions to determine the organic and inorganic fractions of P within the soil; however, these extractions are unable to provide information on the source of P.

Determining the $\delta^{18}O_P$ signature(s) in a soil sample can potentially isolate contributing sources. Biochemists in the 1960s and 1970s initially measured excess ^{18}O in PO_4 by investigating reaction rates of oxygen (O) with water and P (Boyer, 1978; Cohn, 1958). Researchers then showed that biological activity promoted the O exchange between water and PO_4 at typical earth temperatures (Blake et al., 2005; Kok & Varner, 1967; Longinelli & Nuti, 1973). Although a wide range of signatures have been observed, the $\delta^{18}O_P$ provides insight and can be critical in identifying unique sources in contaminated waterways (Paytan & McLaughlin, 2011). Recently, researchers

have found that $\delta^{18}O_P$ signatures may be useful to differentiate between contributing P sources (Granger et al., 2017; Federica Tamburini et al., 2014; Young et al., 2009) and as a tracer of microbial P cycling within the soil profile (Alon Angert et al., 2011; Ford et al., 2018; Larsen et al., 1989; Federica Tamburini et al., 2014; Zohar, Shaviv, Young, et al., 2010).

The $\delta^{18}O_P$ is used because the oxygen molecule is strongly bound to the phosphorus molecule and although ^{31}P is the only stable P isotope (^{32}P and ^{33}P are radioisotopes with relatively short half-life, 14.3 and 25.3 days, respectively), it makes up nearly 100% of the total P on earth (E. Frossard et al., 2011). The stable ^{18}O isotope is strongly bound to P found in soils which provides insight on P cycling by assessing the ratio of the natural abundance of ^{18}O to ^{16}O relative to a ^{18}O to ^{16}O ratio from a Vienna Standard Mean Ocean Water (VSMOW) standard (Emmanuel Frossard et al., 2011; Longinelli & Nuti, 1968).

$$\delta^{18}O_{P-sample} = 1{,}000\left\{\left[\frac{(^{18}O_P{}^{16}O_P)sample}{(^{18}O_P{}^{16}O_P)reference}\right] - 1\right\}$$

Equation 3-1. Determining natural abundance of ^{18}O bound to P (parts per thousand, ‰)

Soil samples from 3 cultivated and 1 pasture field receiving different poultry litter application rates (0.0 to 13.4 Mg ha^{-1}) and 1 native remnant prairie from Riesel, TX were analyzed to 1) determine the potential for using Hedley fractionation pools for ^{18}O isotope analysis ; and 2) investigate the practical aspects of producing Ag_3PO_4 for subsequent use in $^{18}O_P$ isotope analysis on soils with diverse chemical properties. The following sections outline several attempts, failures, and successes of using the Tamburini method to better understand individual chemical reactions, especially the final step of Ag_3PO_4 formation from vertisols.

3.2 Materials and Methods

3.2.1 Site Description

Experimental fields and watersheds monitored in this study were part of a long-term study to evaluate the effects of poultry litter application on soil properties and environmental quality (Harmel et al., 2014). Five soils were collected from the Texas Blackland Prairie ecoregion near Riesel, TX (701440.23 m E, 3484189.47 m N) (Figure 3.1). The Blackland Prairie ecoregion is

dominated by Houston Black clay soil (fine, smectitic, thermic, udic Haplustert), which has high potential for shrinking and swelling with moisture fluctuations. Long-term average annual rainfall at the study site is 935±264 mm. and average annual temperature is 19.2°C.

Three cultivated fields (Y6, Y10, and Y8) each field received an annual application of poultry litter at target rates of 0.0, 6.7, and 13.4 Mg ha^{-1}, respectively between 2001 - 2015. Based on litter properties (Waldrip et al., 2015), mean P application rates ranged from 75 to 219 kg P ha^{-1} (Table 3.1). Field Y6 received solely inorganic P fertilizer at an annual mean rate of 18 kg P ha^{-1} (Table 3.1). Poultry litter was incorporated into the soil after application with a disk or field cultivator. Between 1995 and 2015, cultivated fields were tilled 1-4 times per year.

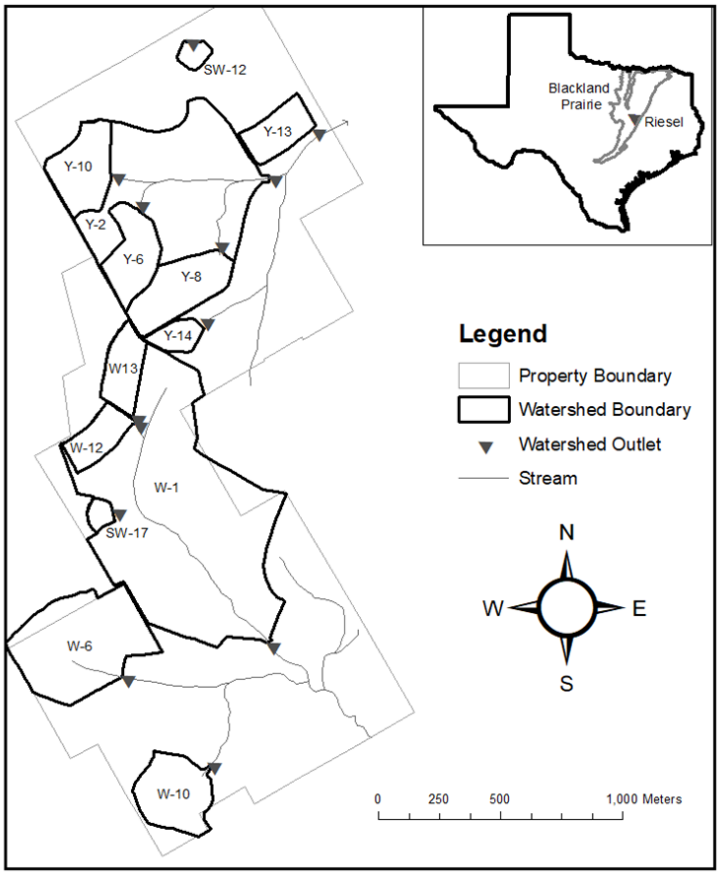

Figure 3.1. Study fields at the USDA Agricultural Research Service Grassland, Soil and Water Research Laboratory, Riesel, TX

The pasture field was managed as hayed improved pasture (W10) and contained a monoculture of coastal Bermudagrass (*Cynodon dactylon* L.) or Klein grass (*Panicum coloratum* L.). A combination of 7 kg P ha^{-1} from inorganic fertilizer applications and an annual mean application rate of 123 kg P ha^{-1} from poultry litter was applied for the first 7 years of the study (Table 3.1). Neither inorganic nor organic fertilizers were incorporated on the pasture, which was opened for selective grazing for approximately 8 months each year.

Table 3.1 Field scale watershed properties and management

Site	Area (ha)	Slope (%)	Land management	Phosphorus source	Mean P application rate (kg ha^{-1} yr^{-1}) †
Y10	7.5	1.9	Cultivated (Corn-Corn-Wheat)	Poultry litter	108 (*n*=15)
Y8	8.4	2.2	Cultivated (Corn-Corn-Wheat)	Poultry litter	219 (*n*=15)
Y6	6.6	3.2	Cultivated (Corn-Corn-Wheat)	Commercial fertilizer	18 (*n*=12)
W10	8.2	2.5	Pasture, hayed (Bermuda Grass)	Poultry litter	123 (*n*=7)
SW12	1.2	3.8	Native remnant prairie	None	N/A

† Number of years from 1995 – 2015 with documented application rates

Soil from a native remnant prairie (SW12) received no fertilizer inputs, organic or inorganic, and according to long term records, has never been tilled, cropped, or disturbed since 1955. Records indicate herbicide applications and removal of hay has been the sole activity since 1990. Between 1955 and 1990, records show SW12 was pasture/meadow, but no harvest or chemical applications were recorded.

3.2.2 Soil Characterization

The Houston Black soil series is derived from calcareous mudstone with runoff potential classified as high when slopes are <1% and very high on soils with 1 – 8% slope. Permeability is very slow when soil is moist, however infiltration increases when soil is dry and cracked (USDA, 2017). A description of winter soil sampling methods and soil properties of each field scale watershed is described by Waldrip et al. (2015). For the purpose of this study, we analyzed carbon and nitrogen, $\delta\,^{15}N$, P fractionation pools using the Hedley Fractionation Method, and isotopic analysis for $\delta^{18}O$ from a precipitated Ag_3PO_4, ultimately produced from an HCl extraction.

3.2.3 Hedley Fractionation

3.2.3.1 Background

The Hedley method has been an accepted sequential extraction for P pools since 1982. This fractionation method distinguishes and quantifies several P pools based on their solubility in water (H_2O-P), sodium bicarbonate P ($NaHCO_3$-P), sodium hydroxide (NaOH-P), and Hydrochloric Acid P (HCl-P) (Hedley et al., 1982). H_2O-P extracts inorganic P available to plants, whereas $NaHCO_3$ extracts the inorganic P which is loosely attached to clay particles in the soil. Iron and Aluminum oxides/hydroxides more strongly associated with P are extracted using NaOH, and all remaining mineral P which is likely associated with less soluble Ca is dissolved during the HCl extraction (Hedley et al., 1982; Federica Tamburini et al., 2014). A time series of soils were

analyzed from five fields (SW12, Y6, W10, Y10, and Y8) from 2002, 2005, 2010, 2014, and 2017 (Table 3.1).

3.2.3.2 Hedley Fractionation Extraction

0.5 g soil were extracted with de-ionized (DI) water at a solid:solution ratio of 1:60 and equilibrated for 16 h on a reciprocating shaker (horizontal, 160 rpm) followed by centrifugation at 5000 g for 20 minutes. Supernatant was filtered through 0.45 µm nylon filter (Fisherbrand) prior to analysis. $NaHCO_3$-P, NaOH-P and HCl-P were extracted using the same protocol, however the NaOH extractions were centrifuged at 10,000 g for 20 minutes. All supernatant was refrigerated and analyzed for phosphate (PO_4) colorimetrically on a Thermo Scientific™ Gallery™ Discrete Analyzer (Waltham, MA).

3.2.4 Isotope Analysis

3.2.4.1 Background

The Hedley fractionation method should be used to determine P availability in each pool to successfully extract the PO_4 and apply the F. Tamburini et al. (2010) method to purify the PO_4 and attach a silver (Ag) molecule to PO_4, forming Ag_3PO_4. These 5 soils had > 250 mg HCl-P kg^{-1} (see Appendix B1-1) whereas F. Tamburini et al. (2010) reported HCl-P values between 82 – 843 mg HCl-P kg^{-1}. Soils with lower exchangeable P will require larger volumes of soil to ensure HCl-P is ideally > 100 mg HCl-P kg^{-1}. Purification, however, proved difficult and although we were successful in forming Ag_3PO_4 from a standard using Phosphoric Acid (H_3PO_4), the soil matrix and impurities in the soil made the formation extremely difficult.

There are currently a few published methods used for isotopic analysis for soils (Granger et al., 2017; Joshi et al., 2016; Kolodny, Luz, & Navon, 1983; F. Tamburini et al., 2010; Federica Tamburini et al., 2012; Weiner et al., 2011) and according to Jiang et al. (2017) the methods that were most effective for complex soil matrices were those of Blake, Chang, and Lepland (2010) and Joshi et al. (2016). To assess the efficacy of the Tamburini method on a series of TX vertisol soils which are high in carbonates, clay content, and organic matter, soils were initially extracted and analyzed as outlined in F. Tamburini et al. (2010). Although they specify that the purification procedure used to obtain Ag_3PO_4 precipitate must be “adapted” for each soil because of the chemical differences among soils, no information was provided as to how to adapt the method,

therefore we initially followed the published protocol. Chemical ratios among published methods were compared by Paytan and McLaughlin (2011) with a main difference of 100 times the $Ag:NO_3:NH_4OH$ molar ratios in the Tamburini method [$P:Ag:NO_3:NH_4OH$ (1:100:300:750)] (Paytan et al., 2002; F. Tamburini et al., 2010) compared to other published methods [$P:Ag:NO_3:NH_4OH$ (1:10:30:75)] (A. Colman, 2002; A. S. Colman, 2002).

The original method (Figure 3.2; but omitting Step A3) consists of a series of extractions and precipitations to purify and ultimately form Ag_3PO_4. The desired final precipitation is Ag_3PO_4 because it is stable which will not fractionate during analysis. Any mass or fractionation resulting in a mass of 28 during analysis would alter analytical results because carbon monoxide gas is used as the carrier gas, which has a mass of 28 g/mol. Hence, the final precipitation cannot have any form of ammonium which could fractionate to either N_2 or NO, interfering with analysis (verbal, Brad Erkkila, YASIC). As a result, the method consists of several steps to purify the final precipitate. Initially, HCl-P is used to extract the P pool from the soil as described in Section 3.2.3, followed by a resin wash (DAX) to remove any organic matter. Our final modifications inserted a resin wash using a cation exchange resin (BioRad) to remove any free cations prior to the subsequent precipitations and dissolutions of Ammonium Phospho-Molybdate (APM) and Magnesium Ammonium Phosphate (MAP). After the dissolution of MAP, an additional BioRad wash is used to remove any remaining cations prior to precipitating the Ag_3PO_4. Sections 3.2.4.2 and 3.2.4.3 details individual steps, difficulties and modifications made to successfully form Ag_3PO_4.

Figure 3.2. Ag_3PO_4 visual method

3.2.4.2 Isotope Method

Step A1: HCl-P extraction

Tamburini: 20-25 g soil extracted with 100 mL 1 M HCl **(1:5 ratio)** – 16 hr. shake
Modified-Tamburini: 10 g soil extracted with 100 mL 1 M HCl **(1:10 ratio)** – 16 - 36 hr shake

Soil samples were weighed (10 g) into a 250 mL Teflon lined centrifuge tube and placed on a reciprocating shaker at low speed (20-25 rpm) with caps vented to release CO_2 from carbonates overnight. On day 2 the samples were tightly capped and vigorously shaken for 16 hr, centrifuged at 5000 g for 20 minutes, filtered through 0.45 µm nylon filter membrane, and transferred into clean 250 mL Teflon lined centrifuge tubes.

Calcareous soils have a high buffering capacity and using a higher soil:extractant ratio resulted in greater P extraction. We adjusted the soil:solution ratio from 1:5 to 1:10 and monitored pH before and after the 16h shake to ensure pH remained <1. For soils with a high pH buffering capacity, a 2-day sequential extraction may be necessary to ensure enough phosphate is dissolved. It is important to achieve a high P extraction efficiency for this step because the mass of P extracted here represents the amount of Ag_3PO_4 that can ultimately be precipitated for final isotopic analysis. After this extraction, calculate the maximum mass of Ag_3PO_4 that could be precipitated based on the amount of P extracted by the HCl solution, and confirm that this amount of Ag_3PO_4 is sufficient for isotopic analysis.

Step A2: Dissolved organic carbon (DOC) removal

Tamburini: Add **20 mL** of resin to the total volume of HCl solution extracted from step 1 and shake for 3 hr followed by filtration.
Modified-Tamburini: Add **30 mL (32 g)** of resin to the total volume of HCl solution extracted from step 1 and shake for 3 hr, filter, and **repeat on the same sample using fresh or re-conditioned resin**.

Prior to precipitating ammonium phospho-molybdate (APM), removing any dissolved organic matter is critical. Supelite^{TM} Dax-8 resin was purchased from Sigma Aldrich, Burlington MA, USA. This resin is mostly non-polar in character and therefore able to preferentially remove

dissolved non-polar solution components without interference from cations or anions. Since pH of the HCl extract is 1 or less, active functional groups on dissolved organic compounds (DOC) will be protonated, and therefore neutral, which maximizes and minimizes their non-polar and polar nature, respectively. The non-polar functional groups have an affinity for the non-polar resin, and minimization of polarity reduces their ability to partition to solution. DAX was initially conditioned as suggested by rinsing with HPLC grade methanol (MeOH) for 15 minutes and rinsing with DI water for an additional 10-15 minutes (F. Tamburini et al., 2010). Although efforts were made with vacuum filtration to separate DAX from MeOH or water, filtration was very slow, so decanting was employed. In addition, if conditioning new DAX, omit the MeOH shake and just rinse twice with water, decant, and use 30 mL per sample.

Although not disclosed in F. Tamburini et al. (2010) spent DAX-8 resin must be eluted with hydroxide solution before re-use. Briefly, due to the non-polar nature of DAX and the compounds that sorb to it, polar solutions such as methanol and water will do little to remove those compounds. Instead, hydroxide is always utilized for elution by increasing pH, thereby causing active functional groups to de-protonate, making the compound more polar and therefore able to partition to the polar solution phase instead of the solid non-polar phase (i.e. DAX). After elution with hydroxide, treatment with an acidic solution will ensure that addition of a new sample will permit dissolved organic compounds remain protonated, therefore minimizing polarity.

The Tamburini method suggests extracting DOC from solution using the DAX-8 resin with a 3 hr equilibration time, filtration with 0.2 µm polycarbonate filter, followed by rinsing resin with 10 mL of DI water (F. Tamburini et al., 2010). A single DAX extraction as outlined in the Tamburini method proved insufficient to remove enough DOC for proper Ag_3PO_4 formation. Therefore, it was conducted sequentially for a total of two extractions (3 hr each) whilst increasing the amount of DAX to 30 mL. This more vigorous extraction of DOC improved Ag_3PO_4 precipitation. In greater detail, the modification is as follows: addition of 30 mL DAX resin to the total extracted solution volume from Step A1, and 3 hr equilibration on a shaker followed by filtration with 0.45 µm nylon filter membrane to separate the majority of DAX resin. Filtrate is added to new DAX resin (30 mL) for the second 3 hr extraction. After the second DAX extraction, the resin-solution mixture was filtered through 0.45 µm nylon filter membrane followed by a final "polishing" filtration with a 0.2 µm polycarbonate filter. After each sequential filtration, DAX resin was treated with 10 mL of DI water to displace entrained solution remaining in the resin pore

volume, as outlined by F. Tamburini et al. (2010); the subsequent sample was combined with the previously collected solution sample i.e. 100 mL 1 M HCl + 10 mL DI from first DAX extraction + 10 mL DI from second DAX extraction).

Solution was transferred to a clean 250 mL Teflon lined centrifuge tube before proceeding to Step A3.

Step A3: Cation Removal

Tamburini: N/A

Modified-Tamburini: Equilibrate sample with **30 mL** of conditioned **BioRad** resin to remove free cations.

Solutions needed: (same as Step A6)

Solution 9: 7 M HNO_3 for BioRad Resin conditioning

BioRad Resin was purchased from Bio-Rad, Hercules CA (AG 50W-X8 Cation Exchange Resin, analytical grade, 100-200 mesh, H^+ form: PN 1421441) and pre-saturated with protons while displacing any cations through equilibration in 7 M HNO_3 (Solution 9) for approximately 16 hr. Resin was separated from BioRad resin by vacuum filtration using a 90 mm filtration apparatus and 0.45 nylon 90-mm filter membrane and rinsed by passing a minimum of 1-2 L of water through the filtration apparatus. Add 30 mL of resin slurry to a centrifuge tube containing the DOC-free solution from step A2, cap and place on reciprocal shaker for 16h. Separate resin from solution with vacuum filtration (0.2 μm polycarbonate filter) and rinse resin twice with 2 mL of DI water, and combine with sample solution. Transfer sample to a 200 mL Erlenmeyer flask for subsequent APM precipitation in step A4.

Although not part of the original Tamburini method, this additional cation exchange step was added to ensure that the HCl soil extract was free of cations in order to reduce potential interferences with precipitation of APM and MAP and other subsequent steps. This was necessary for our calcareous soil used as it produced high concentrations of Ca^{2+} from dissolution of free carbonates.

Step A4: Precipitation of ammonium phospho-molybdate (APM) from sample solution, followed by dissolution.

Tamburini method: no modifications were made to this step.

Solutions needed:

Solution 1: 4.2 M Ammonium Nitrate Solution: 4.2 M NH_4NO_3 (336.2 g of NH_4NO_3 DI in 1 L (measured pH 4.64).

Solution 2: 0.09 M Ammonium Molybdate Solution: 110 g of $(NH_4)_6Mo_7O_{24}{\cdot}4H_2O$ DI in 0.99 L (measured pH 5.47).

Solution 3: 0.6 M Ammonium Nitrate Solution: 0.6 M NH_4NO_3 (48 g of NH_4NO_3 DI in 1 L.

Solution 4: 0.09 M Ammonium citrate solution: 10 g citric acid was added to 140 mL concentrated NH_4OH and 300 mL DI water.

All sample volume from Step A3 was transferred to a 200 mL Erlenmeyer flask and 25 mL of 4.2 M ammonium nitrate solution (Solution 1) was slowly added to it. The original Tamburini method specified a 50ºC water bath for this step; similarly, we utilized a temperature controlled environmental shaker set to 50ºC and gentle shake speed (80 rpm). After Solution 1 was added, pH was determined to be 1.1±0.06.

After samples were placed on the shaker, 40 mL of 0.09 M ammonium molybdate (Solution 2) was slowly added whilst being swirled. Formation of APM was observed based on the immediate color reaction. Among soils that received high rates of poultry litter (Y10 and Y8), a green and/or yellow solution immediately formed (Figure 3.2) but soils possessing less HCl extractable P (Indiana mollisol, W10, SW12) required more time, as APM precipitated overnight.

Formation of APM with soil samples containing 200 - 800 mg/kg of HCl-extractable P was consistent and repeatable. However, it is worth noting for future reference the variable texture of the yellow APM crystals formed. Although we were not able to identify influential factors, texture of the APM was either soft and cake-like or crystalline in structure (Figure 3.2; Step A4b). As shown in Figure 3.2, the brightness of yellow varied between soil types. The brightest yellow was observed for the laboratory control (CTL-a), followed by a TX vertisol and a very pale and more sponge-like APM from an Indiana mollisol.

All APM precipitate samples were vacuum filtered with a 0.2 µm polycarbonate filter and rinsed 3 times with 4 mL of 0.6 M ammonium nitrate (Solution 3). Precipitate was carefully transferred to a 100 mL Erlenmeyer flask and dissolved in 30 mL of 0.09 M NH_4-citrate solution (Solution 4). The pH of the dissolved samples remained basic at 10.48±0.09. Dissolution of APM crystals should be consistent and quick (<10 minutes) and should result in a colorless liquid before proceeding to Step A5.

Step A5: Magnesium ammonium phosphate (MAP) precipitation followed by dissolution with nitric acid

Tamburini method: **Adjust pH** of sample solution from Step A4 with 3.65 M ammonium hydroxide (Solution 6).
Modified-Tamburini: **Do not adjust pH**.

Solutions needed:

Solution 5: Magnesia solution (Mg-ammonium chloride): 50 g of $MgCl_2 \cdot 6H_2O$ and 100g NH_4Cl dissolved in 500 mL of DI water. Adjust pH to 1 with 12 M HCl and bring to 1 L (should be made fresh as precipitation occurs within 1 week regardless of storage conditions).

Solution 6: 3.65 M ammonium hydroxide solution (1:1 NH_4OH:DI): slowly add 50 mL concentrated NH_4OH (28-30% NH_3 basis) to 50 mL of DI water.

Solution 7: 0.7 M ammonium hydroxide solution (1:20 NH_4OH:DI): slowly add 5 mL of concentrated NH_4OH (28-30% NH_3 basis) to 100 mL of DI water.

Solution 8: 0.5 M Nitric Acid: add 2.86 mL of 70% HNO_3 to 90 mL of DI water.

Please note that concentrated NH_4OH stock solutions can vary as purchased from various manufacturers. For the experiments described here, it was found that more concentrated NH_4OH of ~30% was more effective than 20-22% stock solutions.

The dissolved APM from Step A4 remains in a 100 mL Erlenmeyer flask and 25 mL of Magnesia solution (Solution 5) is added and placed on a magnetic stir plate overnight forming magnesium ammonium phosphate (MAP, struvite). pH should be checked to ensure it is 8.5 – 10.0 and adjust with 3.65 M ammonium hydroxide (Solution 6) if necessary. Tamburini suggested

adding 7-15 mL of 0.7 M ammonium hydroxide to adjust to pH 8-9 (F. Tamburini et al., 2010), however, in several successful attempts at precipitating MAP, the measured pH was initially ~ 9.7, requiring no pH increase. During Experiment 3, we attempted to decrease initial pH from 9.7 to 8.5 by adding 14-16 mL of concentrated 12 M HCl, which resulted in no visible MAP crystals and samples were discarded (see Experiment 3).

All successfully precipitated MAP crystals were vacuum filtered through 0.2 µm cellulose nitrate filter membranes. 0.7 M ammonium hydroxide (Solution 7) was used to rinse the MAP crystals by slowly pipetting 30 mL over the crystals whilst under vacuum. This rinsing step is critical to remove any excess chloride from the sample to prevent formation of AgCl in the final step (F. Tamburini et al., 2010).

The filter membrane was carefully removed from the filtration base and whilst holding the membrane over a 50 mL centrifuge tube, 20 mL of 0.5 M nitric acid (Solution 8) was pipetted over the membrane, physically displacing all crystals or residue from the filter. The nitric acid solution also dissolved the MAP. Alternatively, the filter membrane was directly placed in a clean 50 mL centrifuge tube followed by addition of 20 mL of 0.5 M nitric acid, capped and gently shaken (by hand) for 1 minute before removing membrane with tweezers. This option was preferred when no visible precipitate was formed.

Results varied as to the quantity, color, and visibility of the MAP crystals formed. One trial resulted in no visible crystals on the membrane and failure was assumed, but once the membranes dried, a faint residual of crystals were visible, so we proceeded to dissolve them with nitric acid by the latter method as outlined above. Visible MAP precipitate varied from white, blue/grey, or cream; regardless of color, we proceeded to Step A6.

Step A6: Cation removal

Tamburini method: add about **6 mL** of BioRad resin slurry and shake 16 hr
Modified-Tamburini: add **10-12 mL** of BioRad resin slurry and shake 16 hr

Solutions needed:
Solution 9: 7 M HNO_3 for BioRad Resin conditioning

This cation removal step is intended to replace the solution Mg from the previously dissolved MAP, and any other cations from the original HCl extraction, with protons. This is necessary for the final step of silver phosphate precipitation in order to prevent precipitation of other minerals, especially those that contain oxygen

BioRad Resin was purchased from Bio-Rad, Hercules CA (AG 50W-X8 Cation Exchange Resin, analytical grade, 100-200 mesh, H^+ form: PN 1421441) and pre-saturated with protons while displacing any cations through equilibration in 7 M HNO_3 (Solution 9) for approximately 16 hr. BioRad resin was separated by vacuum filtration using a 90 mm filtration apparatus and 0.45 nylon 90-mm filter membrane. Although Tamburini (2010) recommended washing with deionized water until pH is neutral, we were unable to achieve a neutral pH with DI water. After washing BioRad Resin with approximately 20 L of DI water, pH remained around pH 5 which is consistent with the pH of the water before passing through the BioRad Resin. One should not expect to achieve neutral pH through equilibration with DI water, since pure water in equilibrium with atmospheric CO_2 is approximately 5.5. The difference in pH was accepted and we proceeded with the method as described.

Ten-mL of conditioned resin slurry was added to the dissolved MAP precipitate from Step A5. Samples were capped and horizontally placed on a shaker for approximately 16 hr, and vacuum filtered with 0.2-μm polycarbonate filter followed by rinsing twice with 2 mL of DI water, which was collected and combined with the sample solution. The filtered solution transferred to a clean 50 mL centrifuge tube, capped and stored at room temperature until the final step of silver phosphate precipitation (A7) was initiated.

Step A7: Ag_3PO_4 precipitation

Tamburini method: Add ~ 5 mL of Ag-ammine solution (Solution10) to sample from Step A5 and place in 50ºC overnight for **2-3** days.

Modified-Tamburini: **Adjust pH of sample to 7.5** with concentrated NH_4OH, add 5 mL of Ag-ammine solution and place in 50ºC overnight for **1-2** days or until yellow crystals have formed.

Solutions needed:

Solution 10: Silver ammine solution: Add 10.2 g of $AgNO_3$ and 9.6 g NH_4NO_3 to 81.5 mL of DI water. Dissolve and slowly add 18.5 mL of concentrated NH_4OH [Final solution: 0.6 M $AgNO_3$ & 1.1 M NH_4NO_3].

Solution 11: Concentrated NH_4OH (28-30% NH_3 basis)

Two approaches were investigated to precipitate Ag_3PO_4 in this final step and ultimately, the modified-Tamburini includes a critical step which was derived from the Firsching method. An overview of each method is as follows:

Tamburini method: add approximately 5 mL of Solution 10 to the dissolved MAP and equilibrate in an oven at 50ºC for several days. Samples should be checked regularly, and DI water added to maintain a constant volume. When crystals form, vacuum filter with 0.2 µm polycarbonate filter and wash 3-4 times with DI water (F. Tamburini et al., 2010).

Firsching method (FM):

Solution FM1: 1.3 mM H_3PO_4, 0.5 mL concentrated NH_4OH, and 25 mmoles of NH_4NO_3 adjusted to volume of 100 mL with DI water (place FM1 in a 200 mL beaker).

Solution FM2: 15 mmoles $AgNO_3$, 3 mL concentrated NH_4OH adjusted to volume of 75 mL.

Place Solution FM1 on a stir plate and whilst stirring, slowly add Solution FM2. After equilibration a clear solution should result, however a precipitate may form if pH is too low. If brown/grey precipitate develops, add more concentrated NH_4OH until the solution turns clear. Remove stir bar and place on heat plate. Sample should be checked regularly to maintain volume of 175 mL with DI water. Precipitation should occur within 3-4 hr and once the pH is < 7.5 the precipitate can be vacuum filtered and rinsed 3-4 times with 2 mL of DI water (Firsching, 1961).

The Modified-Tamburini comprises of adjusting pH as outlined by Firsching but uses the precipitation chemistry and methodology from Tamburini. pH strips were used to determine pH on the sample from the previous step (dissolved MAP treated for cation removal). Concentrated NH_4OH (Solution 11) was added in 0.1 mL increments to raise sample pH to 7.5±0.5. Five-mL of Ag-ammine solution (Solution 10) was then added to the sample and the mixture equilibrated at

50ºC in an oven for 1-2 days. When crystals form within the solution, vacuum filter with 0.2 µm polycarbonate filter and wash 3-4 times with DI water. Filtration and storage of samples in dark conditions will promote yellow crystal preservation, however further investigation is required to explore impacts of UV light on $\delta_{18}O_P$ results (see 3.3.1.3.5).

Step A8: Ag_3PO_4 oven dry: first drying step

Tamburini method: 50ºC overnight
Modified Tamburini: 50ºC for 24 hr

Filter membrane and precipitate from Step A7 were transferred to a 2 mL vial and equilibrated at 50º C in an oven for 24–48 hr. A yellow crystalline structure should indicate pure Ag_3PO_4 was precipitated but due to trace amounts of trapped water and NH_4, the sample must be dried ("Advances in Agronomy, Vol 125," 2014). Procedures for drying silver phosphate crystals vary from 50ºC overnight (McLaughlin et al., 2004) to 110ºC for 24 hr (Bi et al., 2018). The recommended oven dry is 24 – 48 hr at 50ºC for the first drying step.

Step A9: Ag_3PO_4 vacuum furnace dry: second drying step

A two-step drying process is recommended: oven dry (Step A8) followed by a vacuum furnace cycle at 550ºC for 3 - 5 minutes (S. J. Chang & Blake, 2015). Samples were sent to Yale Isotope Laboratory for analysis and further purification in the vacuum furnace at 550ºC for 5 minutes. Drying the crystals under vacuum (1.3×10^{-5} mbar) at a high heat (400 - 450 ºC) removes any structural water molecules, trace contaminant organic compounds and inorganics with a gaseous phase, drives off any sorbed alcohol, breaks down and drives off any nitrate, and converts any AgO to elemental silver reducing the potential for oxygen not found in phosphate to be present during analysis ("Advances in Agronomy, Vol 125," 2014).

Step A10: Sample analysis

Phosphate O-isotope analyses was performed at the Yale Analytical and Stable Isotope Center (YASIC), Yale Institute for Biospheric Studies, New Haven, CT. Online high-temperature thermal decomposition using a Thermo-Chemolysis Elemental Analyzer (TC/EA) coupled to a

Delta +XL continuous flow isotope ratio monitoring mass spectrometer (Thermo-Finnigan, Bremen, Germany) was used for analyzing silver phosphate. Phosphate O-isotope ratios ($\delta^{18}O_P$) were calibrated using different silver phosphate standards with a ±0.3‰ precision and were reported relative to the Vienna Standard Mean Ocean Water (VSMOW) standard in per mil (‰) (Jaisi & Blake, 2010).

3.2.4.3 Method Experimentation

This section outlines the numerous attempts at refining and modifying the method to successfully form Ag_3PO_4. An experiment was defined by initiating a new approach using new samples or a new objective (see Table 3.2).

Experiment 1: Resin-P pool

Many published Ag_3PO_4 precipitation methods use HCl-P, however, very little HCl-P is plant available or soluble and therefore may not represent the most important P pools in the context of bioavailability and transport of dissolved P to surface waters. Hence, attempts were made to use an Anion Exchange Material (AEM) from Sorbtech Technologies, Inc (Norcross, GA) to extract a labile-P pool, which is available for uptake and fairly soluble. Sheets of AEM (20x20 cm; 200 µm, polyester backed, mixed layer of silica get with strongly basic anion exchange resin: p/n 1324026) were purchased and cut into strips. Unfortunately, the AEM material flaked at edges when cut, however we proceeded to add it to 100 mL of a 100 mg P L^{-1} solution. After a 3 hr shake, the resin had completely separated from the backing and essentially disintegrated into solution. As a result, we abandoned the Resin-P pool for isotopic analysis and opted for the Hedley fractions.

Experiment 2: First Tamburini method attempt

The Hedley method provided background soil P concentrations to determine the mass of soil needed for obtaining enough P for ultimately measuring ^{18}O isotopes. The sequential Hedley fractionation method was performed on 20 grams of soil utilizing a 1:5 ratio (soil:solution) of DI water, 0.5 M $NaHCO_3$, 1 M NaOH, and 1 M HCl following the sequential procedure outlined in section 3.2.3. However, difficulties in both centrifugation and filtration of the Na based solutions resulted in elimination of those respective pools and then focus solely on the H_2O-P and HCl-P

Table 3.2. Experimental outline of method development and modifications.

			Hedley P fractions					DAX		Purification & Precipitation				Ag_3PO_4		Drying/Purify				
STEP			A1					A2		A3	A4	A5	A 6	A7			A8	A9	A10	
Experiment #	Soil (g)	1 M H_3PO_4 (mL)	H_2O (mL)	Resin-P†	$NaHCO_3$ (mL)	NaOH (mL)	HCl (mL)	Wash 1 grams / hr	Wash 2 grams / hr	BioRad (mL) Shake hr	APM	MAP	BioRad (mL)	Tamburini	Firsching	H_2O_2	Oven	Vacuum	Analysis	FOCUS / RESULTS
1		100*	25	X																Resin strip disintegrated
2	20		100		100	100	100	20 g 3 hr			X									Conditioned DAX:MeOH APM Membranes dissolved
3a	20		100		100	100	100	20 g 3 hr††			a	X								Condition DAX:NaOH No MAP crystals formed
3b											b	Δ pH SP	6	50ºC				X		MAP Δ pH Precipitate fused to quartz tube (A9)
3c											c	ES	6	50ºC				X		MAP no Δ pH Precipitate fused to quartz tube (A9)
4a	5						25													(A1) pressure build Day 1 = pressure release

Table 3.2 (continued)

			Hedley P fractions					DAX		Purification & Precipitation				Ag_3PO_4		Drying/Purify				
STEP			A1					A2		A3	A4	A5	A 6	A7			A8	A9	A10	
Experiment #	Soil (g)	1 M H_3PO_4 (mL)	H_2O (mL)	Resin-P[†]	$NaHCO_3$ (mL)	NaOH (mL)	HCl (mL)	Wash 1 grams / hr	Wash 2 grams / hr	BioRad (mL) Shake hr	APM	MAP	BioRad (mL)	Tamburini	Firsching	H_2O_2	Oven	Vacuum	Analysis	FOCUS / RESULTS
4b							25													Buffer prevented P exchange Day 2 = P Exchange
5	5						25	0 – 4 washes												Assess DAX efficacy
6a	10						100													Soil:HCl Ratio 1:10 P Extract 1
6b	10						100	30 g 3 hr	30 g 3 hr		ICP		6	X						P Extract 2 Add DAX wash MAP pH not adjusted
7		25[*]					100				50		6							APM Heat source compared
8	10														Y					Firsching on 6b and 7
9																				P Affinity/Titrations
10a		1.3					100				50		10	Y						Firsching versus Tamburini (F1)
10b		1.3					100				50		10		Y					Firsching versus Tamburini (F2)

Table 3.2 (continued)

			Hedley P fractions					DAX		Purification & Precipitation				Ag_3PO_4		Drying/Purify				
STEP			A1					A2		A3	A4	A5	A 6	A7			A8	A9	A10	
Experiment #	Soil (g)	1 M H_3PO_4 (mL)	H_2O (mL)	Resin-P[†]	$NaHCO_3$ (mL)	NaOH (mL)	HCl (mL)	Wash 1 grams / hr	Wash 2 grams / hr	BioRad (mL) Shake hr	APM	MAP	BioRad (mL)	Tamburini	Firsching	H_2O_2	Oven	Vacuum	Analysis	FOCUS / RESULTS
10c		1.3					100				50	312 mg	10							Paused after dissolution of APM (F3)
11a														50ºC					Y	Time and Ag_3PO_4 stability of 10a (6 hr and 3 day)
11b																			Y	Time and Ag_3PO_4 stability of 10b (5 hr and 7 day)
11c														50ºC					Y	6 months (A6→A7)
12																			Y	Ag_3PO_4→AgOH → Ag_3PO_4 (using 10b)
13	10	1.3					100	30 g 3 hr	30 g 3 hr		50		12		X					Tamburini (A1–A6) Firsching Ag_3PO_4 (A7)
14a	10	1.3					100	90 g 3 hr	90 g 3 hr	30 mL 16 hr	50		10	50ºC					Y	Cation wash (A3) Adjust pH (pre-A7) No H_2O_2 + filtered in light

Table 3.2 (continued)

			Hedley P fractions					DAX		Purification & Precipitation				Ag_3PO_4		Drying/Purify				
STEP			A1					A2		A3	A4	A5	A 6	A7			A8	A9	A10	
Experiment #	Soil (g)	1 M H_3PO_4 (mL)	H_2O (mL)	Resin-P†	$NaHCO_3$ (mL)	NaOH (mL)	HCl (mL)	Wash 1 grams / hr	Wash 2 grams / hr	BioRad (mL) Shake hr	APM	MAP	BioRad (mL)	Tamburini	Firsching	H_2O_2	Oven	Vacuum	Analysis	FOCUS / RESULTS
14b	10	1.3					100	90 g 3 hr	90 g 3 hr	30 mL 16 hr	50		10	50ºC					Y	Adjust pH (pre-A7) H_2O_2 + filtered in light
14c	10	1.3					100	90 g 3 hr	90 g 3 hr	30 mL 16 hr	50		10	50ºC					Y	Adjust pH (pre-A7) Filtered in dark
14d		1.3					100				50		10	50ºC					Y	Resumed F3 (see 10c) Adjust pH (pre-A7) Filtered in dark
15	10	1.3					100	90 g 3 hr	90 g 3 hr	30 mL 16 hr	50		10	50ºC					Y	Repeat Experiment 14c
16	10	1.3					100	90 g 3 hr	90 g 3 hr	30 mL 16 hr	50		10	50ºC					Y	Final Method

* mg L^{-1}; †Not part of original Hedley Fractionation Method; ††DAX conditioned in 0.1 M NaOH remove potential organic matter; SP = Stir plate; ES = Environmental Shaker; X = Experiment stopped at this step; Y = Experiment was successfully analyzed for Ag_3PO_4.

extractions. A literature review indicated the majority of Ag_3PO_4 results are derived from using the HCl extractable P pool (Amelung et al., 2015; Bi et al., 2018; F. Tamburini et al., 2010; Zohar, Shaviv, Klass, Roberts, & Paytan, 2010), which is mostly non-labile. However, a more labile pool such as H_2O-extractable P might be more suitable for our context of nutrient transport. Note that DAX-8 resin for DOC removal was conditioned with methanol for this experiment (step A2).

Although the APM precipitate was successfully formed by following the Tamburini method, dissolution did not occur after addition of citric acid (solution 4). Addition of an extra 20 mL citric acid did not improve dissolution. Precipitate plus filter membrane equilibrated for 16 hr; precipitate produced from H_2O-P pool dissolved but the HCl-P APM precipitate did not dissolve. Unfortunately, all samples were discarded because the filter membranes added with precipitant in both the HCl and H_2O extractants dissolved, compromising the chemistry of the solutions.

Experiment 3: pH for precipitation of MAP

Based on Experiment 2, we hypothesized that the extracted solutions were still rich in DOC, thereby preventing precipitation of pure APM in Step A4, or preventing citrate (solution 4) from complexing Mo in APM (Alcock et al., 1990). Three Texas soils were weighed (20 g) and the Hedley fractionation was conducted with 100 mL of the respective extractant solutions. DAX-8 resin was conditioned with 0.1 M NaOH for 3 hr to improve DOC removal during Step A2. During Step A2, all but the HCl-P pools were abandoned due to filtration difficulties and logistics difficulties with excessive samples (n=16; 4 soils x 4 Hedley fractions).

Methodology for APM precipitate was followed as outlined in Step A4. Ample amounts of APM were precipitated and then divided into 3 subsets to create triplicate samples for further exploration throughout the method. The first set of APM replicates was dissolved in citrate solution (solution 4). All samples measured pH 8-9 using Fisherbrand pH strips and Magnesia solution (solutions 5) was added to precipitate MAP. No MAP crystals were visible and replicate 1 samples were discarded (see Table 3.2; 3a).

The remaining 2 sets of APM precipitate were dissolved in 50 mL of NH_4-citrate solution (solution 4) and 25 mL of magnesia solution (solution 5) was added. We determined that pH strips were not accurate enough for this step so a calibrated pH meter was used to ensure pH was between 8 – 9 as suggested by F. Tamburini et al. (2010). Our results, however, were contradictory to those of Tamburini because our samples measured pH 9.8 which would require an acid to adjust to target

pH 8 – 9 and Tamburini suggested a base (1:1 H_2O:NH_4OH) for increasing pH. Replicate 2 samples (see Table 3.2; 3b) were acidified using 12 M HCl to reach the target pH and placed on a magnetic stir plate (SP), whereas replicate 3 samples (see Table 3.2; 3c) were not adjusted for pH and placed in the environmental shaker (SH).

No visible MAP crystals were visible in either Rep 2 or Rep 3 samples, however, we proceeded with dissolution and cation removal (steps A5 – A7) as prescribed in the Tamburini method. Results showed a slight yellow color, indicating successful Ag_3PO_4 crystal formation in the final precipitant produced from 3 soils; however, after filtration of the yellow Ag_3PO_4, it turned black before being placed in a 50ºC oven to be dried. Samples were sent to Yale Isotope Laboratory for analysis and further purification in a vacuum furnace at 550ºC for 5 minutes. This resulted in fused crystals to the quartz tube; although yellow hints remained in the tube, no residual could be recovered for $\delta^{18}O_P$ analysis. We hypothesize that because of excess Na from the $NaHCO_3$ and NaOH extractions with the Hedley fractionation, the sample became saturated with Na, causing the crystals to fuse to the glass, similar to the process of "soda glass" production. Although the method incorporates a cation removal step, there was not enough BioRad Resin added to remove Na^+ cations based on the CEC and mass of resin utilized. We recommend that any sodium-based solutions used for Ag_3PO_4 precipitation, implement additional BioRad resin treatment to ensure complete cation removal.

Experiment 4a: Carbonates and pH buffering capacity of TX soils

Abandoning the Hedley fractions and focusing solely on an HCl extraction, the high carbonates in these soils caused excessive pressure buildup in tubes as well as a neutralization of the pH during P extraction. As a result, Step A1 was modified to a 2 day process: 5 g of three TX soils were weighed and 25 mL of HCl was added on day 1, samples were left overnight on a reciprocating shaker (~40 rpm) with lids vented to drive off any carbonates and reduce pressure buildup in the sample bottle. On Day 2 the samples were tightly capped and shaken vigorously overnight as outlined in the Hedley method.

Using a 1:5 soil:solution ratio, it was evident that pH did not respond similarly between soils. For example, after adding 25 mL of 1 M HCl to 5 g of soil, supernatant for the native soil (SW12) had an initial pH of 5.27 compared to 1.02 for the extraction solution. Y10 and Y6 had a pH of 1.06 and 1.04, respectively, immediately after adding 25 mL of 1 M HCl. After a 16 hr shake,

pH for SW12 remained at 6.6 whereas Y10 and Y6 were 0.92 and 0.91 suggesting the native remnant prairie soil (SW12) had a much higher pH buffering capacity.

Experiment 4b: Sequential extraction

High pH buffering for sample SW12 suggested that perhaps P extraction was inefficient. Phosphorus extractions with HCl are intended to dissolve P-rich minerals through dramatic reduction in pH. Therefore, a second sequential 25 mL 1 M HCl extraction to the 5 g soil pellet from SW12 was conducted. Samples were centrifuged at 5000 g for 15 minutes and filtered through a GF/F filter. After 2 subsequent extractions, P concentrations in solution from SW12 increased from 0.14 to 51.40 mg/L of P. For samples Y10 and Y6, > 95% of P was extracted in the initial extraction, suggesting that a single extraction was enough for those cultivated soils but the highly pH-buffered SW12 required a second extraction.

Experiment 5: DAX-8 resin extraction of DOC

Additional efforts were made to verify the complete removal of DOC from the HCl-P solution by exploring the efficacy of the DAX resin extraction. Five replicates of each soil were weighed out (5 g each) and extracted with 25 mL of 1 M HCl. Sequential DAX extractions were performed on the HCl soil extract up to four times. Five-mL of DAX resin was added to each solution sample and processed as described in step A2.

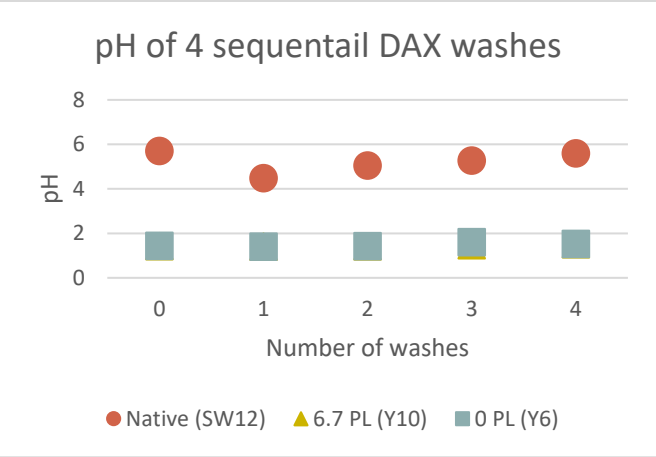

Figure 3.3. pH response to sequential DAX washes

DAX resin extraction had a negligible effect on sample pH (Figure 3.3). Attempts to verify complete removal of DOC were attempted by analyzing subsamples of the HCl-P solution pre and post DAX extraction, however, methanol associated with DAX-resin interfered with analytical analysis making quantitative results unavailable for verification. Assumptions had to be made that a standard method change to all subsequent attempts

would include 2 DAX washes whilst increasing the amount of DAX to 30 mL (32 g) for each extraction. Using 2 DAX extractions with a minimum 3:1 resin (g):soil (g) ratio was used or all subsequent attempts.

Experiment 6: Soil:HCl ratio

Results from Experiment 4 warranted a modification to the soil:solution ratio used during initial extraction (Step A1). Four TX soils (SW12, W10, Y10, and Y6) were weighed (10 g) and 100 mL of 1 M HCl was added, including SW12, which as explained in Experiment 4, had a high pH buffering capacity. This experiment was designed to test the soil:HCl ratio by changing it from 1:5 to 1:10 and extracted as described above under experiment 4 using a sequential two-day extraction. Both extractions (i.e. day 1 and 2) were composited for a 200 mL composite sample.

The mean pH was 0.75±0.03 prior to the first 16 hr shake and 0.96±0.09 after. The second extraction had an initial mean pH of 0.83±.01 and after a 16 hr shake, mean pH was still low at 1.15±0.09, indicating effectiveness. ICP analysis was performed on the 2-day HCl-P extractions, confirming sufficient extraction of P with an average 226 mg P kg^{-1}.

Previous investigation (Experiment 4) showed the pH from SW12 was buffered to 6.6 suggesting P extraction, mostly through dissolution, was minimized when using a 1:5 soil:HCl ratio. These calcareous soils have a high pH buffering capacity and use of a greater soil:solution ratio resulted in a greater extraction potential. All subsequent attempts used 10 g soil:100 mL 1 M HCl and pH was monitored to ensure values <1 before and after a 16 hr shake to confirm adequate P extraction. Changing the soil:solution ratio from 1:5 to 1:10 successfully extracted sufficient P while minimizing extraction time: 10 g of soil in 100 mL of 1 M HCl.

Adjustments to the DAX resin extractions were made based on previous results. Assumptions were made based on Experiment 5 for improving DOC removal from samples by utilizing 2 DAX washes and larger amount of DAX resin (30 mL-32 g). Samples were extracted for DOC as described under experiment 5. Efforts were made to ensure pH remained ~ pH 1; after the sequential DAX extractions, the 4 TX soils had a mean pH 1.06±0.03.

APM precipitate formed immediately (and turned green) after Solutions 1 & 2 were added. Samples were placed on the environmental shaker (speed 2) at 50ºC for ~ 16 hr. An average of 2.43 g of APM precipitate was collected and divided into subsamples. A small subsample (50 mg) was removed from APM [$(NH_4)_3PMo_{12}O_{40}$] precipitate and dissolved in 10 mL of NH_4-citrate

solution (Solution 4). The solute was then analyzed on the ICP for Al, P, Mo, As, B, Ca, Cd, Cr, Cu, Fe, K, Mg, Mn , Mg, Na, Ni, S, Si, and Zn. Results showed all elemental analysis to be Below Detection Limit (BDL) except for Mo and Al.

Remaining APM was dissolved in 30 mL of NH_4-citrate and 25 mL of Magnesium Chloride (Magnesia, Solution 5) was added in proceeding to step A5. Although Tamburini suggested adjusting pH with 1:1 H_2O:NH_4OH (Solution 6) to achieve pH 8.5, average pH prior to adding Solution 6 was 10.48±0.06 and was 9.79±0.03 after. Stratful, Scrimshaw, and Lester (2001) and Wang, Qiu, and Hu, showed that MAP optimally formed between pH 8.5 – 10 and 7.5-10, respectively, which is in accord with thermodynamic equilibrium calculations, therefore, no HCl was used to adjust pH as was previously done in Experiment 3. It is important to note that in the pH range of 7.5 – 10, Mg hydroxide and Mg phosphate may also precipitate, depending on pH and concentrations. Samples were placed on a stir plate for ~ 16 hr for precipitation of MAP. pH did not change overnight, and samples were vacuum filtered through 0.2 µm cellulose nitrate filter membranes. Diluted NH_4OH (Solution 7) was used to rinse the MAP crystals by slowly pipetting 30 mL over the crystals and membrane whilst under vacuum. The rinsing step is critical to remove any excess chloride from previous steps, which will prevent the formation of AgCl in the final step (F. Tamburini et al., 2010).

Filter membranes containing MAP precipitate were placed in 50 mL centrifuge tubes and 20 mL of 0.5 M HNO_3 (Solution 8) were pipetted over the membranes. Tubes were gently swirled, and membranes removed with tweezers. Cation removal (Step A6) was achieved by adding 6 mL of conditioned BioRad Resin and shaking ~ 16 hr. Samples were removed from the shaker and vacuum filtered with 0.2 µm polycarbonate filter and washed twice with 2 mL of DI water, which was composited with the sample solution.

After completing Step A6 to remove cations, sample pH was found to be consistent with a mean of 1.17±0.10. However, in proceeding to Ag_3PO_4 precipitation (Step A7), adding 5 mL of silver ammine solution (Solution 10) to samples resulted in a mean pH of 5.83±2.92, with a range from 1.37 on the native soil (SW12) to 9.12 on the grazed pasture (W10) (see Table 3.3). No crystals formed overnight with heating, so pH was measured again and adjusted accordingly. SW12 measured pH 0.65 which required ~14 mL of concentrated NH_4OH to reach target pH 7. The grazed field (W10) and the cultivated field with PL (Y10) reached the target pH with 5 and

22 drops, respectively, whereas the cultivated control (Y6) required approximately 6 mL to adjust the pH from 4.56 to 7.00.

Table 3.3. Influence of 5 mL of Silver ammine solution on TX vertisols

Field	pH		Precipitate
	Pre	Post	
Native (SW12)	1.2	1.37	No visible (until filtered)
Grazed (W10)	1.3	9.12	None
Poultry Litter (Y10)	1.16	7.6	~ 3 mL (grey)
Inorganic Fertilizer (Y6)	1.02	5.25	~ 1 mL (grey/black)

Samples with adjusted pH were equilibrated at 50ºC overnight in an oven and vacuum filtered with 0.2 µm polycarbonate filter and wash 3-4 times with DI water (F. Tamburini et al., 2010). Ag_3PO_4 precipitation resulted in 4 varying precipitates – none of which were yellow (Figure 3.4). Samples were discarded and not analyzed. It is unknown if the precipitants contained Ag_3PO_4 or not.

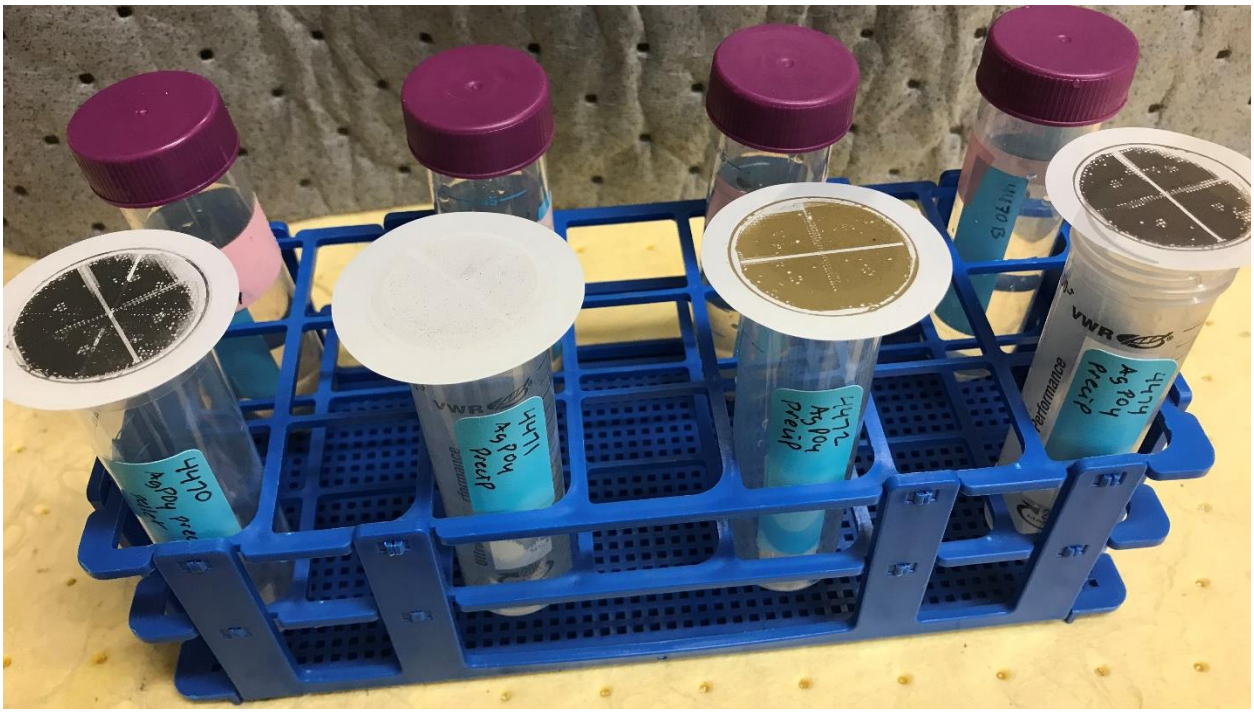

Figure 3.4. Variation in Ag_3PO_4 precipitate from SW12, W10, Y10 and Y6 (left to right) prior to method modification of adding Step A4 (cation removal after Step A3).

Experiment 7: APM Heat Source

Four heat sources were compared to assess APM formation: an oven set to 50ºC, a heated stir plate at 50ºC, heated sonicator bath (without sonication), and the environmental shaker at 50ºC (60 rpm). Instead of soil extracts, a known solution of 25 mg L^{-1} of PO_4 in 100 mL of 1 M HCl was made using ion chromatography analytical standard (RICCA Chemical, Arlington TX). Use of this standard P solution is indicated as a "laboratory control". The heated sonicator bath (without sonication) was unsuccessful because the desired temperature could not be reached, and water evaporation proved problematic. Results showed the other heat sources did not influence precipitation hence, all samples were placed on the environmental shaker for APM precipitation. Most attempts of resulted in a soft spongy precipitate (Figure 3.2; Step A4b).

Experiment 8*: Use of Firsching method instead of Tamburini for precipitation of Ag_3PO_4*

Precipitate formed during Step A7 (forms of grey and black) from previous attempts (soils in Experiment 6b and control from Experiment 7) were dissolved and then precipitated using the Firsching method. The original precipitant was dissolved with 0.5 mL concentrated NH_4OH, and 25 mmoles of NH_4NO_3 adjusted to volume of 100 mL with DI water and pH increased with concentrated NH_4OH until solution turned clear and there was no visible precipitate. Initial pH for SW12, Y10, and control samples was 6.21, 7.02, and 6.40, respectively and adjusted to pH 9.66. Samples were then placed on a hot plate at 55ºC (PC-351, setting 'low'). After 3-4 hr no precipitate had formed, however after ~ 16 hr white crystals had formed in SW12 (4470), and yellow in Y10 (4472) and the laboratory control whilst pH had dropped to 6.58, 6.74, and 6.34, respectively. The decrease in pH is due to NH_4 volatilization and according to Firsching (1961), filtration of silver phosphate precipitate can be conducted after pH <7 at room temperature. It appears that the slow heating step, either by oven or hot plate, is necessary to slowly drive the pH back down towards the ideal pH for Ag_3PO_4 precipitation, but not permitting AgOH to form. AgOH preferentially forms over Ag_3PO_4 at high pH, but the presence of NH_3 prevents AgOH formation through complexation of Ag. With heating, NH_3 is lost and decreases pH:

$$NH_{3(aq)} \longleftrightarrow NH_{3(g)}$$

Equation 3-2. NH_3 converting from aqueous to gas thus decreasing pH.

As NH_3 is lost with heating, NH_4 is driven to further de-protonate, decreasing the pH:

$$NH_4 \longleftrightarrow H^+ + NH_{3(aq)}$$

Equation 3-3. De-protonation of NH_4, thus decreasing pH.

The simultaneous decrease in pH and NH_3 promotes Ag_3PO_4 formation.

Experiment 9: Silver phosphate precipitation/dissolution under various solution conditions

After several failed attempts of precipitating Ag_3PO_4 and much variability among soils and replications, an in-depth investigation on Ag_3PO_4 solubility/formation in the final step (A7) was necessary. The objective was to understand how variations in solution composition, specifically how pH and competing anions, would impact Ag_3PO_4 formation. Phosphoric Acid was used to make a 1 M H_3PO_4 solution enabling us to forego the time-consuming steps of extracting and purifying the phosphate solution, in addition to utilization of a known P concentration with no interferences. Both Tamburini and Firsching methods were explored to better understand the chemical processes involved in formation of Ag_3PO_4. Results over a series of solution titrations showed that adjusting the pH **prior** to adding the silver ammine solution is imperative to silver phosphate formation. These titration tests are discussed individually below.

Titration 1: Impact of NH_4^+ and pH on Ag precipitation with no P present

The objective was to determine the reaction of the OH^- groups, in a solution containing 0 mg/L PO_4, 20 mL of 0.5 M HNO_3, and 5 mL of $AgNO_3$. The initial titration (Table 3.4; 1a) solution omitted the NH_4^+ hydroxide normally used to increase pH, and instead 5 M NaOH was used in order to determine the effect of raising pH with no potential for forming the Ag-NO_3 solution complex. Observations indicated that with a limited amount (0.1 mL) of 5 M NaOH, grey precipitate immediately formed as the NaOH drop entered the Ag solution and dissolved in the clear solution as pH changed from 0.83 to pH 0.74. However, a stable precipitant was formed at pH 1.9 while a total of 2 mL of 5 M NaOH was incrementally added, raising the pH to 3.52. The addition of NaOH reacts with the $AgNO_3$ forming hydrated silver oxides [$AgNO_3(aq) + NaOH(aq) = AgOH(s) + NaNO_3$] when no NH_4 was present. Next, with the presence of the AgOH precipitant, NH_4 was then added with base (Table 3.4; 1b) causing the precipitant to darken until pH 11.46 when the solution lightened considerably and turned clear at pH 11.84. At this high pH, NH_4 is de-

protonated into NH_3, which is a strong complexing agent with Ag, thereby dissolving the solid AgOH. Relevant reactions:

$$NH_4 \longleftrightarrow H^+ + NH_3$$
$$Ag^+ + NH_3 \longleftrightarrow AgNH_{3(aq)}$$

Equation 3-4. De-protonated NH_4 into NH_3, a complexing agent with Ag

Titration 2: Phosphorus titrations for Ag_3PO_4 precipitation and impact of pH

To observe the effect of P on the Ag_3PO_4 precipitation, a solution comprised of 20 mL of 0.5 M HNO_3 and 5 mL of silver ammine solution (Solution 10) from the Tamburini method was combined. An initial pH of 5.83 was recorded (see Table 3.4; 2a) with no visible precipitation in solution. The addition of 0.002 mL of 1 M H_3PO_4 immediately precipitated light yellow precipitate and continued to increase with further P addition. After precipitation of Ag_3PO_4, titration of concentrated NH_4OH was conducted. After a total of 0.8 mL concentrated NH_4OH (see Table 3.4; 2b) lightened the yellow precipitate, turning it to brown and eventually clear at pH 7.89. We hypothesized that the increased pH created unstable conditions for Ag_3PO_4 and more favorable conditions for the formation of solid AgOH, causing the Ag_3PO_4 to dissolve. Notice that formation of AgOH is clearly favored by an increase in pH:

$$Ag^+ + 2H_2O \longleftrightarrow AgOH + H^+$$

Equation 3-5. Formation of AgOH in unstable conditions when pH increases.

Titration 3: Kinetics of Ag_3PO_4 precipitation and effect of light exposure

The objective was to determine if adding the P solution in a single aliquot, rather than incrementally as in Titration 2, would produce similar results. 1 mM P standard was added to 20 mL of 0.5 M HNO_3 and initial pH was 0.71. Five mL of Solution 10 (silver ammine solution) was added and yellow precipitate formed immediately (see Table 3.4; 3). However, within 5 minutes the yellow precipitate turned brown. This observation is confirmed by McLaughlin et al. (2004) and is likely due to reduction of the Ag (Baxter & Jones, 1910), where light exposure promotes electrical reduction of Ag^{1+} (in the Ag_3PO_4) to Ag^0. This is illustrated in the reaction below, where "h^+" indicates UV light.

$$4Ag_3PO_4 + 6H_2O + 12h^+ + 12e^- \longleftrightarrow 12Ag + 4H_3PO_4 + 3O_2$$

Equation 3-6. UV light promotes electrical reduction of Ag^{1+} to Ag^0

Figure 3.5 and Results 3.3.1.3.5 shows the effect of light on silver phosphate crystals: crystals turning yellow to black within 24 hr of light exposure compared to crystals remaining yellow when left in a dark environment (oven) 72 hr.

Titration 4: Effect of presence of NH_4^+ on Ag_3PO_4 precipitation while increasing pH

The objective of this titration was to assess the role of NH_4^+, hence no ammonium was present in this iteration of titrations. A solution containing 20 mL of 0.5 M HNO_3, 5 mL of solution 10, 60 mg L^{-1} of P was made. Initial pH was 0.7 and 5 M NaOH was added in 0.1 mL increments for a cumulative addition of 2.05 mL whilst pH changed from 0.7 to pH 8.28 over 16 minutes (see Table 3.4; 4a). Brown flakes started immediately started forming and dissolving when 0.1 mL of 5 M NaOH was added. Dissolution of the brown flakes slowed after 1 mL of titrations (pH 0.86) and stopped dissolving after 1.925 mL of 5 M NaOH was added (pH 2.71). More NaOH continued to add brown precipitate but no yellow precipitate formed when NH_4^+ was omitted.

Titrations were continued on solution from titration 4a but switching the titration solution to 0.6 M NH_4NO_3 (see Table 3.4; 4b) and added in 50 µl increments. The brown precipitate remained in solution until 1.55 mL of 0.6 M NH_4NO_3 was added which turned the solution clear. pH, however remained constant at 8.85 throughout. Based on these observations and knowing that NH_3, which is the dominant form of NH_4 at high pH, it appears that NH_3 reduces the potential for Ag to be precipitated as AgOH. This is important because AgOH is a less soluble and therefore more stable mineral than Ag_3PO_4. Standard state equilibrium reactions between Ag and NH_3 show that the two can form a stable solution complex (shown above), which is why further addition of NH_4 solution is able to dissolve any Ag precipitant if the pH is sufficiently high to allow for NH_3.

Titration 5: Effect of increasing pH on Ag_3PO_4 formation with limited NH_4

The objective of titration 5 was to assess precipitation of Ag_3PO_4 in a solution containing high P and low NH_4^+. Titrations of 0.1 mL increments of 5 M NaOH was added to a solution containing 20 mL of 0.5 M HNO_3, 60 mg L^{-1} of P, 5 mL of silver ammine solution, and 10 mL of 0.6 M NH_4NO_3. pH was monitored and changed from an initial pH 2.30 to 7.35 after incremental additions of 5 M NaOH totaling 2.0 mL. Results showed brown precipitate formed at pH 3.17 but

quickly dissolved. pH slowly changed from 2.3 to 3.95 with 1.9 mL of 5 M NaOH, but quickly jumped to 7.37 with an additional 0.1 mL (total = 2 mL) forming yellow precipitate, which later dissolved with time.

Titration 6: Effect of increasing pH on Ag_3PO_4 formation with abundant NH_4

The objective of titration 6 was to investigate the influence of pH with abundant NH_4^+ in solution. An equivalent NH_4^+ from the silver ammine solution (solution 10) and the concentrated NH_4OH in the Tamburini method was added to 5 mL $AgNO_3$ and 20 mL of 0.5 M HNO_3. This equivalent was a 5 M NH_4NO_3 solution (10.04 g NH_4NO_3 in 25 mL) and the initial solution had a pH of 1.25. A titration solution of 5 M NaOH was added in 0.1 mL increments which slowly raised the pH to 9.89 after a cumulative addition of 18.16 mL. Observations showed faint yellow precipitation beginning at pH 5.01 and continued until pH 9.15 when solution went clear.

Table 3.4 P affinity study and titration results

		P affinity / Ag_3PO_4 Precipitation Titrations						
	mg L^{-1} P	HNO_3 (mL)	NH_4OH	5 M NaOH (mL)	$AgNO_3$ (mL)	Ag-ammine (mL)	0.6 M NH_4NO_3	Result
1a	0	20	--	T†	5	--	--	Brown
1b	0	20	T†	2.1	5	--	--	Brown → clear
2a	T†	20	--	--		5	--	Yellow
2b	90	20	T†	--		5	--	Yellow → brown → clear
3	60	20	--	--		5		Yellow → brown (< 5 minutes)
4a	60	20	--	T†	5	--		Brown → clear → brown
4b	60	20	--	2.05	5	--	T†	Clear → brown
5	60	20	--	T†		5	10	Brown → yellow → clear
6	60	20	--	T†	5	--	T††	Clear → yellow (pH 5 – 5.24) → clear

† Titration solution;

†† An equivalent 5 M NH_4NO_3 was used to provide enough NH_4 equal to NH_4 from Ag-ammine solution and concentrated NH_4OH

Experiment 10: Firsching versus Tamburini: Ag_3PO_4 precipitate

In an attempt to refine this final step (A7), a comparison between the Tamburini Ag_3PO_4 method was compared to the Firsching method of Ag_3PO_4 precipitation from 1961 (Firsching, 1961; F. Tamburini et al., 2010). For an overview of each method, see 3.2.4.2; Step A7. Triplicate controls were made by adding 1.3 mL of 1 M H_3PO_4 to 100 mL of 1 M HCl (labeled F1, F2, and F3). Steps A2 – A3 were eliminated and instead proceeded immediately to Step A4 (precipitation of APM) and continued through removal of cations in Step A6. Additional efforts were made throughout this attempt to quantify precipitate from APM and MAP. In Step A4, APM precipitation was visible within 5-10 minutes but still allowed to equilibrate ~ 16 hr on the environmental shaker. APM 'wet weight' was estimated to be around 3.8 g (filter membrane + vacuum filtered APM). Because MAP precipitate is less visible, we opted to air dry F3 after Step A5 to determine a true dry weight of 312 mg (see Table 3.2; 10c) whilst F1 and F2 continued through the method.

Step A7 was initiated on F1 using the Tamburini method and F2 using the Firsching method. Silver phosphate immediately formed in both approaches (see Table 3.2; 10a and 10b) confirming both methods could successfully form Ag_3PO_4.

Experiment 11: Ag_3PO_4 stability with time

Successful formation of Ag_3PO_4 in Experiment 10a and 10b in conjunction with previous attempts had revealed the sensitivity of time, light, and temperature after Ag_3PO_4 had been formed. The objective of this experiment was to evaluate the time required for Ag_3PO_4 to form during Step A7 using both the Tamburini and Firsching Method.

Sample from Experiment 10a (F1) formed precipitate immediately but was left in a 50ºC oven and a subsample was removed after 6 hr and vacuum filtered with 0.2 µm polycarbonate filter and washed 3-4 times with DI water. Crystals were transferred to a 2 mL glass vial and placed in oven according to Step A8. The remaining solution was left in the oven and volume maintained with DI water for a total of 3 days. Sample was removed from the oven and processed the same as the 6-hr sample that produced the initial crystals. Samples were sent to Yale for Steps A9 – A10 and successful analysis was performed (see Table 3.2; 11a) (see 3.3.1.3.4 for results).

Sample from Experiment 10b (F2) also formed precipitate immediately following the comparative Firsching method (1961). Using a similar approach, a subsample was removed from F2 at 5 hr and the remaining sample was left to further precipitate Ag_3PO_4 in the oven for 7 days (see Table 3.2; 11b). Respective samples were removed from the heat plate and vacuum filtered with 0.2 µm polycarbonate filter and washed 3-4 times with DI water. Crystals were transferred to a 2 mL glass vial and placed in oven according to Step A8. Samples were sent to Yale for Steps A9 – A10 and successful analysis was performed (see 3.3.1.3.4 for results).

Sample from Experiment 10b (F3) was left as dissolved MAP for 6 months at room temperature and then was resumed, beginning at Step A6. The Tamburini method was used and samples were sent to Yale Isotope Laboratory for Steps A9 – A10 (see 3.3.1.3.4 for results).

Experiment 12: $Ag_3PO_4 \rightarrow AgOH \rightarrow Ag_3PO_4$

Observations made when combining the Firsching with the Tamburini approach led us to modify Step A7 by adjusting the pH to 7-8 prior to adding $AgNO_3$. Remaining Ag_3PO_4 crystals from Experiment 11b were used to investigate the possibility of reversing the reaction, adjusting pH and then converting back to Ag_3PO_4. A subsample was taken from 11b and dissolved in HNO_3 before repeating the precipitation procedure using the Tamburini approach (see 3.3.1.3.4 for results). This procedure resulted in successful re-precipitation of Ag_3PO_4 after dissolution of the crystals.

Experiment 13: Tamburini Extraction and Firsching Precipitation

To compare the effect of soil properties, a mollisol to a vertisol were selected to determine if soil types would produce different results through the procedure. Duplicate samples of one Indiana Mollisol and one Texas Vertisol were extracted for P as described in Step A1 and Experiment 4 at a 1:10 soil:1 M HCl solution ratio. Two controls were included as 1.3 mL of 1 M H_3PO_4 in 100 mL of 1 M HCl. After HCl extraction, pH was measured at 0.72±0.11, which based on Experiment 4, suggests soil buffering capacity did not inhibit exchangeable P. DAX-8 resin was rinsed with DI water (omitting the MeOH conditioning) and decanted prior to DOC removal (Step A2). Extraction of DOC was conducted twice for a total of two 30-gram resin extractions at 3 hr each, however, sample discoloration prompted a third extraction which made no visible

difference. Steps A4 – A5 proceeded as expected. Results varied for MAP characteristics between the IN, TX, and control samples where the control sample had about 1/16" of white precipitate, the IN soil had a slight residual of an off-white precipitate and the TX soil had a blue/grey precipitate. We hypothesize the blue/grey precipitate may be Calcium Carbonate (Garcia-Guinea, Correcher, Benavente, & Sanchez-Moral, 2015) but regardless, we continued onto cation removal in Step A6.

Cation removal followed the protocol outlined in Step A6 increasing the BioRad resin to 12 mL. Ag_3PO_4 precipitation (Step A7) was conducted using the Firsching method (see 3.2.4.2; Step A10) but placed in the oven as described by Tamburini, instead of a using a hot plate. Ag_3PO_4 initially formed on the control within 4-5 hr whereas the TX soil required about 12 hr to produce visible precipitate. We opted to filter one rep of the control and TX samples after 12 hr and ironically, when the TX sample was removed from oven to proceed with filtration, the sample turned more yellow whilst preparing filtration equipment but within 5 minutes the crystals all turned black. The replicate control and TX samples were removed after 24 hr in the oven and all yellow crystals turned black within 1-2 minutes. The IN soil never precipitated any crystals. The transformation of the yellow Ag_3PO_4 is likely indicative of the electrical reduction of Ag, induced by UV light, as previously mentioned (Baxter & Jones, 1910) and/or a combination of the pH not reaching optimum (7.0±0.5) at the end of Step A7 which may have caused incomplete precipitation of the silver phosphate (McLaughlin et al., 2004).

Experiment 14: Additional cation removal (Step A3) and refining Step A7: Adjust pH, H_2O_2 purification, and light

The objective of this experiment was to further investigate the impact of pH prior to adding Ag-ammine solution in Step A7, light versus dark exposure during the final filtration, and evaluate H_2O_2 to remove organic matter contaminants. In addition, we added an additional BioRad resin wash after organic matter removal (Step A2) but before the APM precipitation (Step A4).

This attempt followed Experiment 13 methodology except an additional BioRad resin wash for cation removal was included (i.e. added Step A3) and for Step A2, improved DOC removal by increasing DAX resin to 90 grams. Note: if using "new" DAX resin with water only, then only 30 mL resin is required. However, in this case spent DAX resin (i.e. reconditioned with MeOH for 15 minutes and rinsed 3x with DI) and tripled the normal amount to compensate for potential

inefficiencies in the DOC extraction. The 90-g DAX resin extraction for DOC was repeated twice before adding 30 mL of conditioned BioRad cation resin to shake for ~ 16 hr. In retrospect, spent DAX resin should have been reconditioned with a hydroxide solution to removed previously held organics, followed by equilibration in acid solution. See the previous discussion under Step A2.

The additional cation removal extraction was included because of the previous observation of calcium carbonate formation during MAP precipitation for the TX soil (Experiment 13). Precipitation conditions for MAP is also ideal for calcium carbonate, if Ca is present. Since the TX soil was especially rich in Ca and because it is highly soluble in the HCl extraction solution, it was necessary to include the additional cation removal step. The additional cation removal (Step A3) before APM precipitation (Step A4) showed immediate improvement in the clarity, consistency, and colors of the APM and MAP precipitates and the ease in which they each dissolved.

Method modifications were also made to Step A7 by adjusting pH prior to adding the Ag-ammine solution from the Tamburini method. Using pH strips, about 1.0 mL of concentrated NH_4OH was added in 0.1 mL increments to raise sample pH to 7.5±0.5. No immediate reaction occurred when 5 mL of the Ag-ammine solution (Solution 10) was added however after 24 hr in a 50ºC oven, crystals were present in both the soil and the control samples. One replicate of each soil and control sample was removed from oven for filtration and no color change was observed in the control sample, however crystals precipitated from the soil extract changed from yellow to brown within 15 minutes (Experiment 13 was <5 minutes) (see Table 3.2; 14a) due to light exposure. Separated crystals were placed in 2 mL vials and oven dried at 50ºC for 5 hr and removed from oven to be subsampled for further exploration (see Experiment 14b). The remaining silver phosphate (not used for Experiment 14b) was left on the counter all night and within 24 hr had turned black due to light exposure. These samples were sent to Yale for further purification in a vacuum furnace and $\delta^{18}O_P$ analysis (see results in 3.3.1.3.5).

Efforts were made to further eliminate DOC in samples by taking subsamples from Experiment 14a (laboratory control and soil) and adding 0.5 mL of 30% H_2O_2 (see Table 3.2; 14b) (Bi et al., 2018; Zohar, Shaviv, Klass, et al., 2010). No visible reaction was observed by adding H_2O_2 and samples were placed back into the oven to evaporate and were sent to Yale for further purification in a vacuum furnace and $\delta^{18}O_P$ analysis (see results in 3.3.1.3.6).

Previous results indicated that light was converting our crystals from yellow to black so we opted to remove the second set of samples and filter them in complete darkness to assess the impact of UV light (see Table 3.2; 14c). Samples were filtered according to Step A7 and precipitate (including filters) were placed in 2 mL vials and re-placed in the oven at 50ºC for ~16 hr. Crystals remained yellow and vials were immediately wrapped with foil to avoid discoloration and were shipped to Yale for further purification in a vacuum furnace and $\delta^{18}O_P$ analysis (see results in 3.3.1.3.5).

During Experiment 10, sample F3 was left as dissolved APM for nearly 6 months and resumed as part of Experiment 14 by adjusting the pH prior to adding Ag-ammine solution (see Table 3.2; 14d). Although crystals did form and remained yellow due to limited UV light exposure, $\delta^{18}O_P$ varied from other control results (see results in 3.3.1.3.4).

Experiment 15: Repeatability of success from additional cation removal and pH adjustment prior to silver ammine addition

The objective of this attempt was to assess the repeatability of observed success in Experiment 14. Results from Experiment 14b showed H_2O_2 increased $\delta^{18}O_P$ variability, presumable due to formation of an additional oxide, so this was omitted. All silver phosphate precipitate was filtered in the dark. Four TX soils were weighed (10 g) and 2 laboratory controls for a total of 6 samples. This run followed the modified Tamburini method (derived from Experiment 14c); results for $\delta^{18}O_P$ from Yale Isotope lab were promising (see results in 3.3.1.4).

Experiment 16: Final method

The last experiment was a confirmation of the modified-Tamburini method on soils. The modified-Tamburini method (see Appendix A) was used for this experiment. Samples were submitted for analysis to the Yale Isotope Laboratory, but due to Covid-19, analysis has not been completed at time of this submission.

3.3 Results and Discussion

3.3.1 Silver phosphate

The role of microbes in different P pools and their role in mobilizing P to make it available for plants is poorly understood, largely due to limitations in methodology (Bi et al., 2018). Using oxygen isotope ratios in phosphate ($\delta^{18}O_P$) is one approach that has been used as a P tracer in soils (A. Angert et al., 2012; Bi et al., 2018; Elsbury et al., 2009; Federica Tamburini et al., 2014). Following the F. Tamburini et al. (2010) method for soils, our results were limited, however, modifying the method to incorporate an additional cation removal step and adjusting the pH prior to adding the silver ammine solution produced viable data. We will discuss several contributing factors to achieving repeatable and reliable results during the silver phosphate precipitation step such as pH, time, and light exposure as well as actual results obtained from 5 uniquely managed soils from Riesel, TX (see Table 3.1). Due to implications from Covid-19, results from the last extraction are awaiting analysis and are unlikely to be completed for purposes of this thesis.

3.3.1.1 Laboratory controls

A critical component of any analysis is the ability to have reproduceable results on a laboratory control. Several approaches were made to confirm formation of Ag_3PO_4 using phosphoric acid as the source comparing the Firsching and Tamburini methods (A7). Bypassing Steps A1-A6 and adding H_3PO_4 to 1 M HCL and proceeding directly to Step A7 resulted in signatures from $\delta^{18}O_P$ of 13.03±1.61‰ and 13.84±0.36‰, respectively. The modified-Tamburini method had a signature of 12.12±1.28‰ (n=4; triplicates analyzed), which we consider to be the target signature as it went through Steps A1-A10. Additional controls have been submitted for analysis, however, due to Covid-19 pandemic, results are unlikely to be acquired in a timely manner to confirm the target signature of the laboratory control.

Calcareous soils have a high buffering capacity and using a higher soil:extractant ratio resulted in greater P extraction. We adjusted the soil:solution ratio to 1:10 and monitored pH before and after the 16 hr shake to ensure pH remained <1. For soils with a high pH buffering capacity, a 2-day sequential extraction may be necessary to ensure enough phosphate is dissolved. It is important to achieve a high P extraction efficiency for this step because the mass of P extracted here represents the amount of Ag_3PO_4 that can ultimately be precipitated for final isotopic analysis. After this extraction, calculate the maximum mass of Ag_3PO_4 than could be precipitated based on

the amount of P extracted by the HCl solution, and confirm that this amount of Ag_3PO_4 is sufficient for isotopic analysis.

3.3.1.2 Magnesium ammonium phosphate (MAP, struvite) pH

According to F. Tamburini et al. (2010), the dissolved APM solution needs to be alkaline and adjusted to pH 8-9 using Solution 6 (1:1 NH_4OH) for optimum MAP precipitation. Our results, however, were contradictory to those of Tamburini because measured pH of our samples was pH 9.8 which would require an acid to adjust to target pH 8 – 9 and Tamburini suggests a base (1:1 H_2O:NH_4OH). Based on thermodynamic equilibrium and an in-depth study by Stratful et al. (2001), optimum MAP precipitation occurs when: pH > 8.5 in the presence of non-limited NH_4^+ and Mg_2^+. Specifically, when NH_4^+ concentrations > 110 mg/L. However, other studies have shown that MAP is rarely pure as the conditions that favor its precipitation also produce Mg-P and MgOH minerals (Yan, Li, & Meng, 2018). Based on these results and a failed attempt of adjusting pH using 1 M HCl, we monitored pH to ensure it was >8.5 but never adjusted it.

According to Stratful et al. (2001), MAP crystallization size ranged from 0.1 mm to 3 mm in length from 1 minute to 180 minutes, respectively, and was an elongated crystal, however precipitate from this study was a fine powder varying from white, cream, and blue/grey in color. Assumptions were initially made that after undergoing HCl extraction, removal of dissolved organic matter, APM and MAP precipitation and dissolution, the precipitation would be free from contaminants and chemical interferences. However, from our repeated observations, the formation of pure MAP is difficult and is complicated by potential presence of fulvic and humic acids and other interfering compounds. However, the additional cation removal (Step A3) decreased variability in this step through removal of excess Ca, which was rich in the TX soils tested. Conditions favoring MAP precipitation will also produce calcium carbonate if calcium is not previously removed. Similarly, excessive DOC in samples will interfere with APM precipitation and subsequent dissolution with citrate, prior to MAP precipitation. For this reason, a more vigorous DOC extraction with DAX-8 resin may be warranted in OM-rich soils.

$$HPO_4^{3-} + Mg^{2+} + NH_4^+ + 6H_2O \rightarrow MgNH_4PO_4 \cdot 6H_2O \downarrow + H^+$$

Equation 3-7. Map (struvite) formation (Stratful, Scrimshaw et al. 2001)

3.3.1.3 Silver phosphate precipitation and pH

Steps prior to A7 is approximately 8-10 days of extractions, precipitations, DOC and cation removal. One of the conclusions from this research is that the final Ag_3PO_4 precipitation step is critical and finding the balance between free NH_4^+, pH, temperature, and concentrations of both PO_4 and $AgNO_3$ is challenging. Merging the Firsching and Tamburini method by adjusting to pH 7-8 using concentrated NH_4OH prior to adding the 5 mL of silver ammine solution successfully produced silver phosphate crystals, regardless of the soil initially extracted. This modification, in conjunction with the additional cation removal using the BioRad Resin prior to APM formation (Step A4) stabilized the pH throughout the extraction process and promoted successful silver phosphate crystal formation.

3.3.1.3.1 Influence of solution pH buffering capacity on final Ag_3PO_4 precipitation

Assumptions that soils which have gone through Steps A1 – A6 will behave similarly at the final step should not be made due to the variable pH buffering capacity of these soils. The buffering capacity of extracted soils was not considered in the early attempts to successfully precipitate silver phosphate. Essentially, because Ag_3PO_4 precipitates under specific pH and solution conditions, it was necessary to first adjust pH prior to addition of Ag ammine at the final precipitation step. Otherwise, addition of Ag ammine will result in variable pH levels, which may not be favorable for precipitation of Ag_3PO_4 (Table 3.3). For example, 4 soils (SW12, W10, Y10, and Y6) were taken through Steps A1 – A6 (see Experiment 6) and had an average pH 1.17±0.1 before proceeding to Step A7. Following the Tamburini method, the addition of 5 mL of Silver Ammine solution was added resulting in an average pH of 5.83±2.92 ranging from 1.37 for SW12 and 9.12 for W10. Samples were left 16 hr (overnight) and pH had dropped to an average of 4.69±2.51 ranging from 0.65 for SW12 to 6.98 or W10. No visible Ag_3PO_4 crystals were formed in these samples, likely because the pH was too low which according to Firsching (1961), solutions with pH between 4 and 7 results in minimal silver phosphate precipitation.

3.3.1.3.2 Ag_3PO_4 dissolution/precipitation under various conditions

Firsching assessed two approaches to silver phosphate precipitation: ammonia volatilization and urea hydrolysis, each beginning to form precipitation at pH 8.5 and pH 2.8, respectively. Tamburini's approach uses ammonia volatilization and states: "adjust the

concentrations of the necessary components to the concentration of PO_4^{3-} in [*the*] soil extracts" (F. Tamburini et al., 2010), however clarification on what needs 'adjusting' and how to adjust it is lacking.

Conclusions from the titration experiments confirmed that adjusting pH prior to addition of Ag ammine, using a combined approach of both Tamburini and Firsching methods would improve the final step of silver phosphate precipitation. Successful precipitation of silver phosphate is affected by the amount of NH_4NO_3 added to the sample solution, because this controls the concentration of NH_3, which complexes Ag. For example, 9 mmoles of NH_4NO_3 will precipitate Ag_3PO_4 at pH 8 whereas 55 mmoles precipitates at pH 7 (Firsching, 1961); a lower pH is required to precipitate Ag_3PO_4 with greater NH_3 because of the greater Ag-NH_3 complexation, which is helpful in that it reduces formation of AgOH at higher pH levels. It is critical to adjust pH prior to Ag ammine addition and also ensure sufficient NH_4^+ is in solution by adding concentrated NH_4OH until any precipitate in solution turns clear and target pH 7.5-8 has been reached (Firsching, 1961).

Conclusions from the titration study confirm that lack of NH_4^+ in solution would produce only brown precipitate (i.e. AgOH, see Table 3.4; 4a), and Ag_3PO_4 precipitate was proportional to the amount of P and NH_4^+ in solution. For example, Titration 2a had limited NH_4^+ and the yellow precipitate gradually increased as the amount of P increased but turned to brown and eventually clear when more NH_4OH was added (Titration 2b). Time was a factor when limited NH_4^+ and high P were in solution as yellow precipitate turned brown within 5 minutes (Titration 3). pH was influential on Ag_3PO_4 precipitation between 5 and 9 when higher amounts of P and NH_4^+ were in solution (Titrations 5 & 6). Results show a delicate balance between pH, free NH_4^+, PO_4^- in solution, and time. This phenomenon may explain the highly varied precipitate that resulted from following Steps A1 – A7 as outlined by F. Tamburini et al. (2010).

3.3.1.3.3 Variability in Ag_3PO_4 precipitate

Repeated attempts of Step A7 produced highly variable results. The original Tamburini method on 4 uniquely managed soils (SW12, W10, Y10, and Y6; Table 3.1) produced highly variable precipitate: black, none, light brown, and dark brown, respectively (Figure 3.4).

3.3.1.3.4 Ag_3PO_4 Stability

Impact of time was observed at various stages and for the most part was a non-issue. However, potential mineral transformation was observed on control samples where Ag_3PO_4 was formed using the Firsching Method beginning at Step A7 and analyzed at day 0 and day 7 of precipitate while remaining in the $AgNO_3$ solution. Triplicate P isotope analysis showed 14.4‰ for day 0 and 13.8‰ for day 7 for a difference of 0.56±0.48‰. Minimal signature change was observed in Step A7 comparing a 6 hr to a 3-day precipitation period using the Tamburini method, averaging 14.01‰ and 13.67‰, respectively (see Experiment 10 & 11). However, average standard deviation for triplicate analysis of all analyzed samples was 0.21‰ suggesting that a 0.34‰ difference for a 6 hr versus a 3-day sample may be indicative of Ag_3PO_4 transformation. Results suggest a potential reduction in signature, hence future research should investigate the impact of time allowed for Ag_3PO_4 crystal formation. The final step in F. Tamburini et al. (2010) states that crystal formation occurs within 2 or 3 days whereas Firsching (1961) predicted crystal formation within 3 to 4 hr.

During Experiment 10, sample F3 was left as dissolved APM for nearly 6 months and resumed as part of Experiment 14 (see Table 3.2; 14d). Phosphorus isotope results were 10.34‰ compared to an average 13.98‰ from Experiments 11a and 11b suggesting that unreliable results may occur if excessive time lapses are allowed between Steps A6 and A7. We hypothesize that evaporation resulted in an increase in ^{18}O or over time causing a discrepancy in signatures.

An additional experiment exploring the stability of the Ag_3PO_4 molecule tested the ability to reverse the reaction from $Ag_3PO_4 \rightarrow AgOH \rightarrow Ag_3PO_4$. A subsample from Ag_3PO_4 precipitate was taken (see Table 3.2; 11b) and results show the $\delta^{18}O_P$ to be similar to other results using the Tamburini approach in Step A7 with average $\delta^{18}O$ to be 13.75±0.32‰. This successful reverse reaction was informative because it demonstrates the repeatability and stability of this last, yet critical step.

3.3.1.3.5 Light Exposure

Impurities, DOC, and other components found in the soil matrix frequently turned Ag_3PO_4 crystals brown/black with time and light exposure (Figure 3.5). Jiang et al. (2017) suggested drying silver phosphate crystals at 110 ºC and then storing in a desiccator in a dark environment until analysis. Observations during the separation of Ag_3PO_4 crystals from solution showed

immediate transformation from yellow crystals to black during the 2-3 minutes of filtration whereas a sample removed from the oven with limited light exposure (i.e. filtration in dark room and cover sample tubes with foil) maintained the yellow color (see Table 3.2; 14). We hypothesize this conversion is a redox reaction caused by light. The Ag_3PO_4 molecule contains an oxidized form of Ag^+ and PO_4^- is reduced creating a stable salt. When exposed to light, the Ag^+ oxidizes a reducing agent such as water, converting Ag^+ to Ag^0 causing the yellow to change to brown-grey-black in color.

Figure 3.5. Silver Phosphate crystals from left to right: TX vertisol (72h dark), CTL (72h dark), TX vertisol (24h light), CTL (24h light).

3.3.1.3.6 H_2O_2 as an Ag_3PO_4 purifier

Precipitating pure silver phosphate proved difficult so efforts to purify the Ag_3PO_4 prior to analysis is essential. Efforts were made in Experiment 14 to assess the efficacy of using H_2O_2 to purify the precipitate prior to analysis (Bi et al., 2018; Zohar, Shaviv, Klass, et al., 2010). Limited results suggested Ag_3PO_4 crystals purified with H_2O_2 was 0.75‰ lower than crystals not treated with H_2O_2 for cultivated soils whereas control samples were 0.49‰ higher in treated samples compared to those not treated. Variability introduced through using H_2O_2 prevented us from using this approach for purification. The vacuum furnace (Step A9) was more consistent and less variable than using H_2O_2.

3.3.1.4 Soil Results

Soil samples were collected in 2017 from five fields with unique management strategies and were analyzed using the modified-Tamburini method. Average $\delta^{18}O_P$ for Y10 and Y8, each receiving poultry litter for 15 consecutive years (Table 3.1), had a mean $\delta^{18}O_P$ of 18.0±0.25‰ ranging from 17.75‰ for Y10 and 18.26‰ for Y8 (see Experiment 15). Animal manure (goose droppings) was characterized by Young et al. (2009) to range between 15.7 – 18.3‰ and bat guano was 20.7‰ so $\delta^{18}O_P$ of 18.0‰ for soils amended with high rates of poultry litter is comparable.

The cultivated control (Y6) never had organic fertilizer applied based on long-term management records dating back to early 1980s and resulted in a $\delta^{18}O_P$ value of 17.09‰. W10 is an improved pasture with cattle grazing (~8 months of the year) and had poultry litter from 2001 – 2007 (Table 3.1) and had a $\delta^{18}O_P$ of 17.20‰. Poultry litter had not been applied for 10 years which suggests that $\delta^{18}O_P$ results between 2001 – 2007 would likely be closer to that of Y8 whereas after 10 years, the result was only 0.1‰ higher than Y6. Ranges summarized by Federica Tamburini et al. (2014) confirm our results are within the expected range for fertilizers (14.8 - 27‰) (Gruau et al., 2005; McLaughlin, Cade-Menun, et al., 2006; Young et al., 2009) and HCl extractable P (8.2 – 21.3‰) (A. Angert et al., 2012), however further characterizing specific fertilizer sources with long-term management records will provide essential baseline values in further studies using $\delta^{18}O_P$ results as phosphorus tracers.

Soils were also extracted for Ag_3PO_4 from the same fields collected in 2002, however, due to Covid-19 laboratory analysis was not completed. Results comparing signatures changes from 2002 to 2017 will help determine signature change over time. Equilibrium was calculated using Equation 1-1 to assess potential significance of the obtained results. Annual soil temperature and $\delta^{18}O_w$ from 2012 – 2013 were obtained from Okafor (2014) which are representative of the area but not specific to this study period or fields resulting in high uncertainty. The calculated equilibrium for $\delta^{18}O_P$ in water resulted in 17.68‰ which suggests the systems could have been in an equilibrated state by comparing the $\delta^{18}O_P$ in water (17.68‰) with the $\delta^{18}O_P$ from the soil. Long term poultry litter applications on Y10 and Y8 were slightly higher than equilibrium by 0.04±0.04‰ and 0.58±0.11‰, respectively whereas Y6 resulted in a signature -0.60±0.04 and W10 was -0.50±0.02‰ lighter than equilibrium. Signatures from these 4 field are similar to that of equilibrium suggesting the P potentially came into equilibrium with the soil water, however,

comparing signatures from 2002 soils and additional analysis will provide valuable insight to the long-term trends in signatures in soils amended with poultry litter.

3.3.1.5 P balance and $\delta^{18}O_P$

Phosphorus accumulation occurred due to poultry litter application for 15 consecutive years on 2 cultivated fields (Y10 and Y8) and 7 years on an improved pasture (W10) whereas the native remnant prairie (SW12) and cultivated control (Y6) maintained a neutral P balance throughout the study period (Figure 3.6). Results for the low PL rate field (Y10) for $\delta^{18}O_P$ was 17.75‰ whereas the high PL field (Y8) was 18.26‰ suggesting a positive correlation between P accumulation from poultry litter and $\delta^{18}O_P$ signatures. Collectively, comparing average P accumulation (2001-2015) to $\delta^{18}O_P$ among soils collected in 2017 exhibits a positive correlation (R^2=0.943, p=0.02, Figure 3.7) suggesting that long-term management data and unique nutrient sources during the study period will enable further characterization of fertilizer signatures to provide more refined $\delta^{18}O_P$ values in tracing P cycling in agricultural soils. Further analysis is necessary to determine statistical significance; however, our limited results suggest there is a $\delta^{18}O_P$ separation between poultry litter, cattle grazed, and inorganic nutrient sources.

3.3.1.6 Conclusion

Using phosphate stable oxygen isotope ($\delta^{18}O_P$) to differentiate organic and inorganic fertilizers and P transport in an agricultural system could improve management strategies to reduce PO_4 entering a surface water body from agricultural fields. This research expanded the ability of future researchers to successfully determine the isotopic signature of the phosphate molecule using the $\delta^{18}O_P$ in a variety of soil samples using the modified-Tamburini method. This signature can be used as a tracer of microbial P cycling within the soil profile (Alon Angert et al., 2011; Ford et al., 2018; Larsen et al., 1989; Federica Tamburini et al., 2014; Zohar, Shaviv, Young, et al., 2010).

Five soils from USDA Research plots in Riesel, TX were characterized and extracted for $\delta^{18}O_P$ using the modified-Tamburini (2010) method. The HCl-P had sufficient extractable P to convert to Ag_3PO_4 for isotopic analysis averaging 493±264 mg kg^{-1}. The HCl-P pool proved to be the simplest extractable P for isotopic analysis due to the high amounts of phosphates and the lack of cations in the extractant solution.

Extensive efforts were made to refine the Tamburini method (2010) and our inability to obtain results due to the Covid-19 pandemic closing down analytical laboratories, our $\delta^{18}O_P$ limited results fall within expected published results for animal manure and fertilizers (Federica Tamburini et al., 2014). Fields (Y8 and Y10) receiving 15 consecutive years of poultry manure (Table 3.1) had a mean $\delta^{18}O_P$ of 18.0±0.25‰ whereas the cultivated control (Y6) had a lighter $\delta^{18}O_P$ value of 17.09‰. A positive correlation was exhibited (Figure 3.7) when comparing the net P balance with the isotopic signatures. Using the phosphate stable oxygen isotope ($\delta^{18}O_P$) could potentially help identify unique sources of P in both water bodies and agricultural systems, and enable policy makers, researchers, and farmers to make management decisions that are both environmentally and economically beneficial.

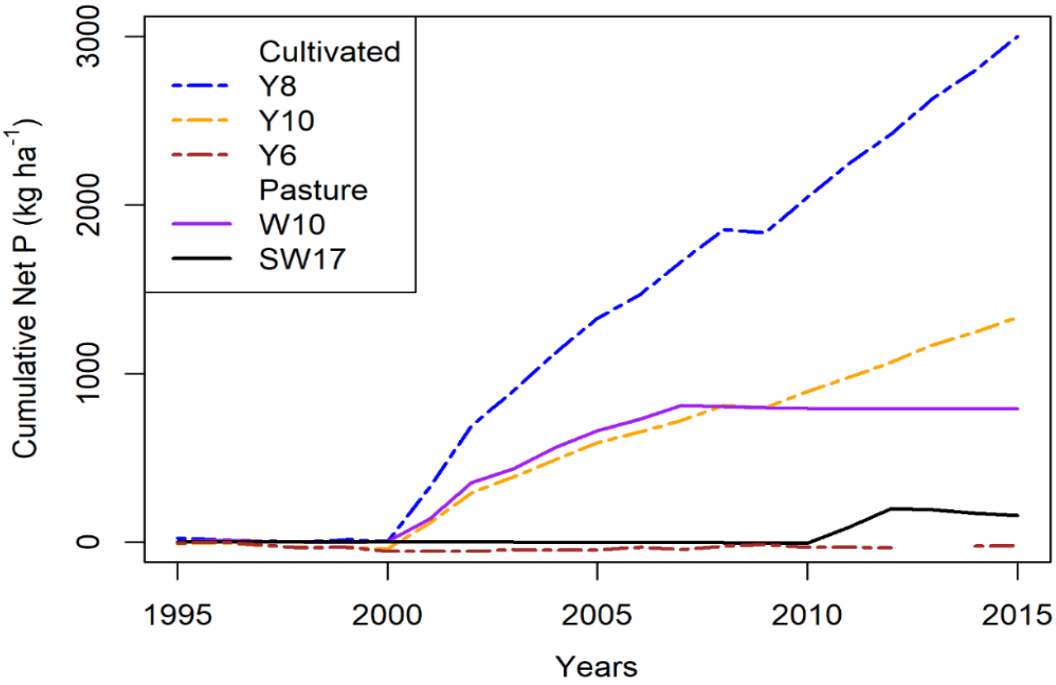

Figure 3.6. Cumulative net P for cultivated fields, improved pasture, and native prairie from USDA plots in Riesel TX

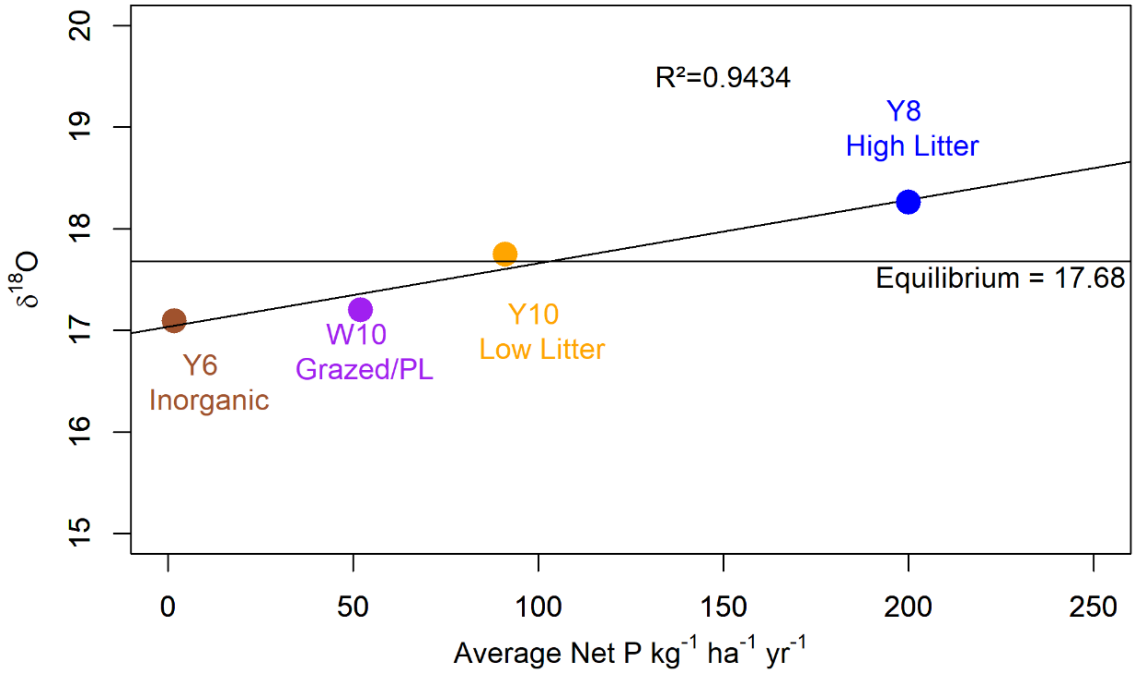

Figure 3.7. Average net P (2001 – 2015) has a positive relationship with $\delta^{18}O$ for soils (2017).

APPENDIX A. MODIFIED-TAMBURINI METHOD (PRINTABLE)

Ag_3PO_4 precipitation for isotopic analysis (Printable)

Materials and Method

The procedure for converting HCl-P to Ag_3PO_4 consists of 7 steps that takes nearly 2 weeks to complete. It is recommended the number of samples to run in a single batch is between 4-6 (including the laboratory control).

1. Extract P using 1 M HCl
2. Remove organic matter using DAX
3. Remove cations using BioRad Resin
4. Precipitate Ammonium phospho-molybdate (APM)
5. Convert APM to Magnesium ammonium phosphate (MAP, struvite)
6. Remove cations using BioRad Resin
7. Precipitate $AgPO_4$ using silver nitrate and NH_4OH

The objectives of this document is to prepare a detailed outline of the procedure using the modified F. Tamburini et al. (2010) procedure for precipitating $AgPO_4$ for isotopic analysis.

Isotopic P extraction method:

Day 1

Step A1**: Hydrochloric Acid P (this may need to be a 2-day process if soils are high in $CaCO_3$)**

1) Weigh out 10 g soil into a 200 mL Teflon lined centrifuge bottle
2) Make 1 M HCl
    a. Fill a 1 L volumetric flask with approximately 500 mL of nanopore water
    b. Slowly add 83 mL of 12 M HCl (concentrated HCl) **IN FUME HOOD**
    c. Bring to volume of 1 L
3) Use a graduated cylinder to measure out 100 mL of 1 M HCl
4) SLOWLY add HCl **samples high in carbonate will effervesce causing potential build-up of pressure so to prevent excessive pressure in centrifuge bottles, an additional step must be taken for safety reasons:
    a. (OPTIONAL) Gently shake overnight in a hood – vented caps releasing C from high carbonate soils (skip for normal $CaCO_3$ levels in soils).

5) Ensure pH~1
6) Attached caps, place on shaker and shake for 16 hr/overnight

Day 2

7) Remove from shaker, tighten caps and centrifuge @ 5000 g for 15 minutes
8) Measure pH: ensure pH remains ~ 1.0 (calcareous soils will lower pH limiting P exchange and may require subsequent extractions)
9) Vacuum filter substrate using 0.45 µm nylon filter membranes to prevent larger clay particles entering solution

Condition BioRad resin (AG50W-X8 cation resin (H^+ form, 100–200 mesh))

1) Add approximately 100 mL of BioRad resin to bottle
    a. Add 180 mL of 7 M HNO_3 (80 mL 70% HNO_3 + 100 mL DI water)
    b. Transfer solution to a 500 mL Erlenmeyer flask – label and stopper
2) Wash conditioned BioRad resin thoroughly with DI water until pH of DI is reached (pH 5-7) → 1-2 Liters
3) Cap and store conditioned Resin for cation removal on Days 3 and 6

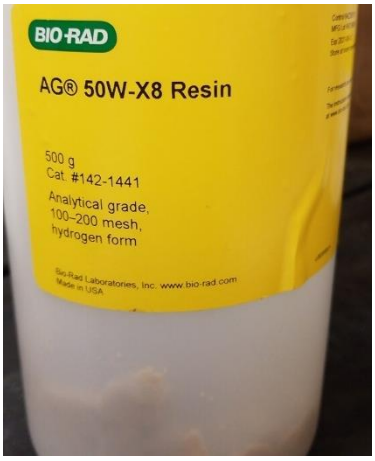

Figure A1-1. BioRad Resin for cation removal

Day 3

Step A2**: Dissolved organic matter removal**

Condition DAX

1) Wet 20 mL of "new/fresh" DAX resin with DI (omit MeOH wash as noted in F. Tamburini et al. (2010) and shake 20 minutes
2) After shake, let settle and decant as much DI water as possible. Add clean DI and repeat 20-minute shake. Let settle and decant as much as possible. (If DAX is moist when added to HCl solution – that's okay but minimize amount of water added with DAX).

Organic matter removal (DAX wash x2)

1) Add ~ 30 g of resin slurry into sample bottle and shake for 3 hr
2) Filter first wash through 0.45 µm nylon using 90 mm filter unit (use stainless steel inserts if available – NOT glass frits to expedite filtration)
3) Rinse resin with 10 mL of DI water which was collected with the sample
4) Transfer solution back to 250 mL Teflon lined centrifuge bottle
5) Add ~30 g of resin slurry into sample bottle and shake for 3 hr
6) Filter first with 0.45 µm nylon to remove DAX using the 90 mm stainless steel insert filter assembly
7) Filter again through 0.2 µm polycarbonate filter (Millipore) using the 47 mm assembly unit
8) Rinse resin with 10 mL of DI water which was collected with the sample
9) Transfer sample to 250 mL Teflon line centrifuge bottle.

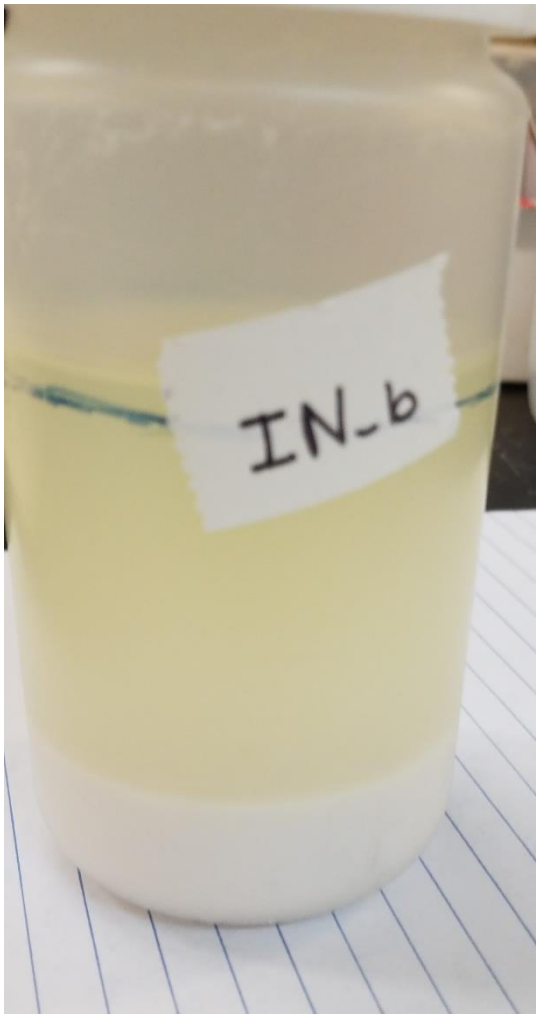

Figure A1-2. DAX wash to remove organic matter

Step A3**: Cation removal**

1) Add 10 mL of the BioRad resin slurry to the sample and leave on shaker overnight

Day 4

2) Filter solution with 0.2 µm polycarbonate filter and wash 2 times with 2 mL of DI water, which was collected with the sample solution
3) Transfer filtrate to 500 mL Erlenmeyer flask – label and stopper

Step A4**: Ammonium Phospho-molybdate (APM) precipitation and dissolution**

Solution 1: Ammonium Nitrate Solution: 4.2 M NH_4NO_3 (336.2 g of NH_4NO_3 was added to 500 mL of DI water, dissolved and brought to volume of 1 L (measured pH 4.64).

Solution 2: Ammonium Molybdate Solution: 110 g of $(NH_4)_6Mo_7O_{24}{\cdot}4H_2O$ was added to 500 mL of DI water and brought to volume of 0.99 liters (measured pH 5.47) ** Make fresh to avoid precipitation**.

Solution 3: Ammonium Nitrate Solution: 0.6 M NH_4NO_3 (48 g of NH_4NO_3 was added to 500 mL of DI and brought to volume of 1 liter.

1) Add 25 mL of Solution 1: Ammonium nitrate solution to each Erlenmeyer flask.
2) Place Erlenmeyer flasks in Environmental Shaker, stabilizing to avoid breakage.
    a. Set speed to "2" (~ 60 rpm) and temperature to 50º C
3) Pick up each flask and whilst swirling slowly add 40 mL of Solution 2: Ammonium molybdate solution
    a. Leave solutions in environmental shaker, shaking overnight to promote APM crystals to form – place flasks in box and separate with adsorbent pads to stabilize **shake should be gentle enough to not 'move' the flasks**

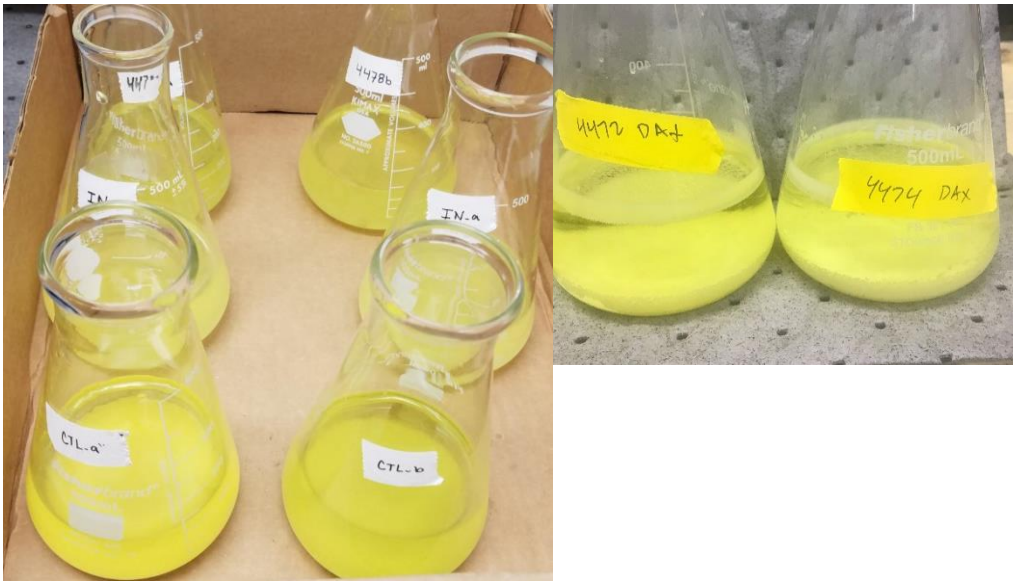

Figure A1-3. APM crystal formation: Step A4

Day 5

4) Separate the yellow APM precipitate from solution by using a 0.2 µm filter and rinse 2-3 times (10 mL each) with Solution 3: 0.6 M NH_4NO_3 solution
5) Carefully transfer precipitate to a 100 mL Erlenmeyer flask

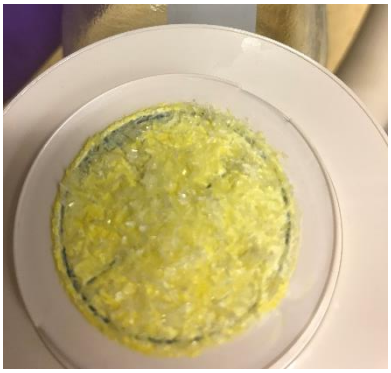

Figure A1-4. APM crystals

Note: crystals may be sponge like OR crystalline in structure -- both should be fine

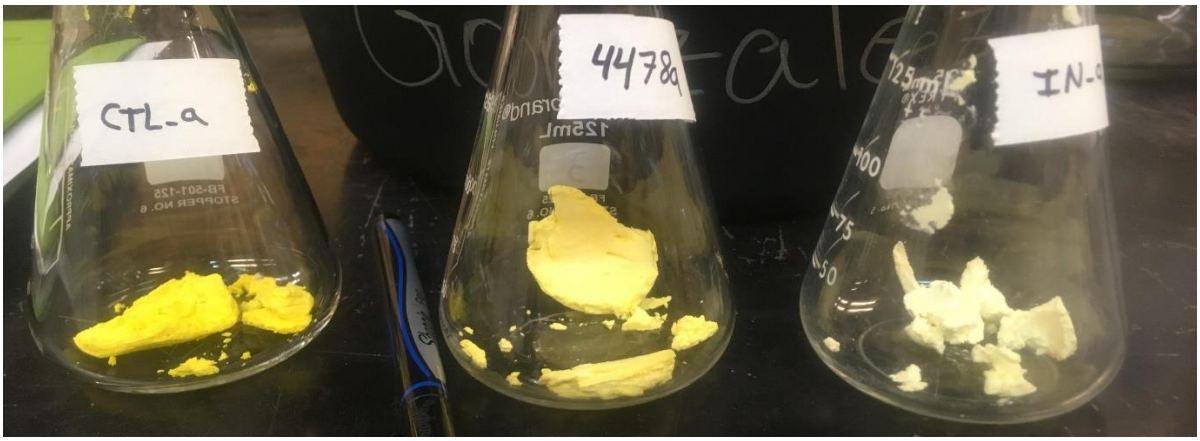

Figure A1-5. APM precipitate ready for dissolution.

Step A5**: Magnesium ammonium phosphate (MAP, struvite) precipitation and dissolution**

Solution 4: Ammonium citrate solution: 10 g citric acid was added to 140 mL concentrated NH_4OH and 300 mL of DI water.

Solution 5: Magnesia solution: 50 g of $MgCl_2 \cdot 6H_2O$ and 100g NH_4Cl is dissolved in 500 mL of DI water. This solution is adjusted to pH 1 with 12 M HCl and then adjust the volume to 1 L (should be made fresh as precipitation occurs within 1 week regardless of storage conditions).

Solution 6: 1:1 ammonium hydroxide solution: a solution of 1:1 NH_4OH:DI: slowly add 50 mL concentrated NH_4OH to 50 mL of DI water.

Solution 7: 1:20 ammonium hydroxide solution: a solution of 1:20 NH_4OH:DI: slowly add 5 mL of concentrated NH_4OH to 100 mL of DI water.

Solution 8: 0.5 M Nitric Acid: add 2.86 mL of 70% HNO_3 to 90 mL of DI water.

1) Add 30-50 mL of Solution 4: citric acid-NH_4OH to 100 mL flask to dissolve APM crystals
    - Should take 1-15 minutes
2) Add 25 mL of Solution 5: magnesia solution
3) Swirl solution and check pH: IF pH is <8, slowly add Solution 6: 1:1 NH_4OH/DI water solution until pH 8–9, otherwise, leave pH unadjusted
    - the optimum pH for MAP precipitation
4) Place solution overnight on a magnetic stir plate (with stir bar & speed = medium)

Figure A1-6. MAP formation after 24 hr on magnetic stir plate

Day 6

1) Filter the white MAP crystals on 0.2-µm cellulose nitrate filters
2) Rinse 2-3 times (10 mL each washing) with a Solution 7: 1:20 NH_4OH/DI water solution

NOTE: Thorough washing is extremely important because the presence of chloride from the 1 M HCl and from the Mg solution will induce co-precipitation of AgCl with the Ag_3PO_4. If thoroughly washed, the MAP crystals are free of excess chloride and no AgCl will form at the end of the procedure.

Figure A1-7. APM post filtration. Quantity and texture may vary.

3) Place filter in 50 mL centrifuge tube and add 20 mL of Solution 8: 0.5 M HNO_3
4) Swirl for 2-3 minutes dissolving any precipitate on paper. Remove filter membrane with clean tweezers for disposal.

Step A6**: Cation Removal**

1) Add approximately 10 mL of the conditioned resin slurry to the sample and leave on shaker overnight

Day 7-8

2) Filter solution with 0.2 µm polycarbonate filter and wash 2 times with 2 mL of DI water, which was collected with the sample solution
3) Transfer filtrate to 50 mL centrifuge tube

Step A7**: Precipitation of silver phosphate**

Solution 9: Silver ammine solution: Add 10.2 g of $AgNO_3$ and 9.6 g NH_4NO_3 to 81.5 mL of DI water. Dissolve and slowly add 18.5 mL of concentrated NH_4OH (~30%).

1) Measure pH of sample -- adjust to pH 7.5 by slowly adding 0.1 mL intervals of concentrated NH_4OH

- Add 5 mL of Solution 9: silver ammine solution

  NOTE: Should be clear, but if grey precipitate forms, add more concentrated NH_4OH until solution becomes clear

2) Place sample in oven (50 ºC) -- crystals form between immediate and 2-3 days (add DI to compensate for evaporation as needed)

   NOTE: The more NH_4 in the solution, the longer it will take

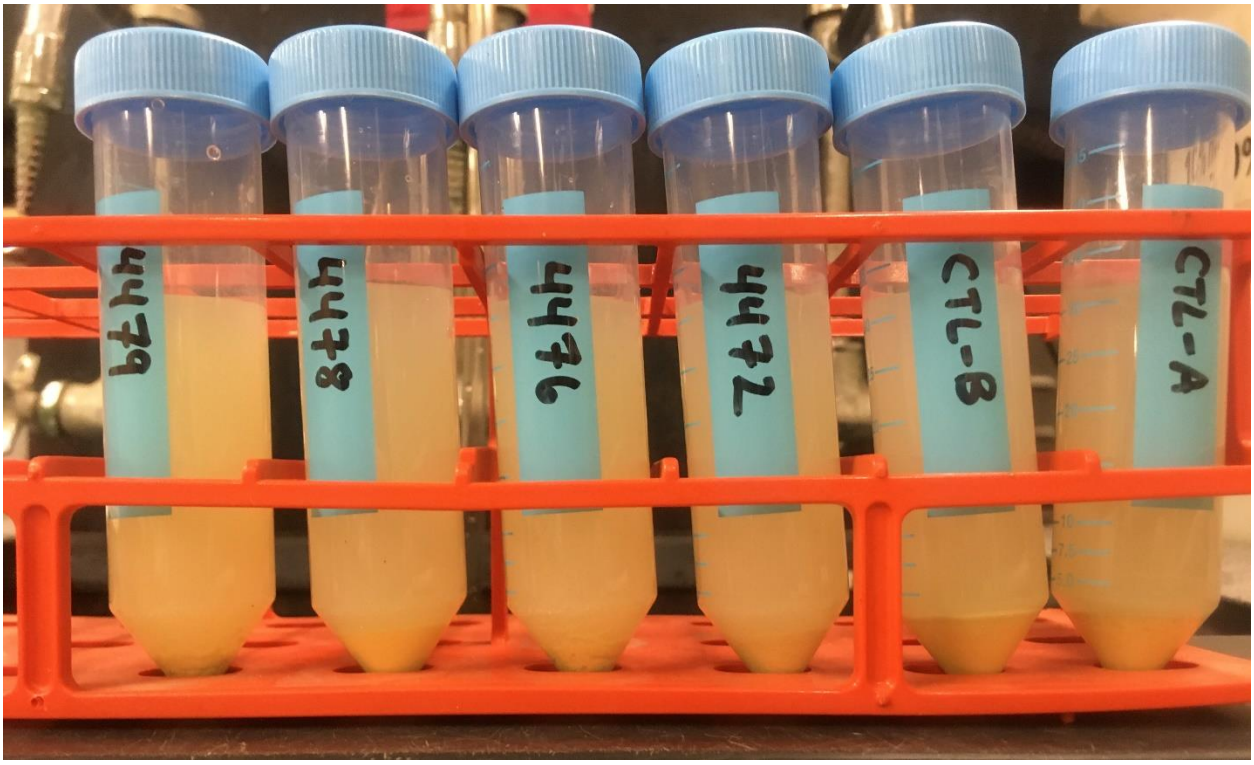

Figure A1-8. Ag_3PO_4 crystal precipitation

3) Vacuum filter Ag_3PO_4 crystals using 0.2 µm polycarbonate filter

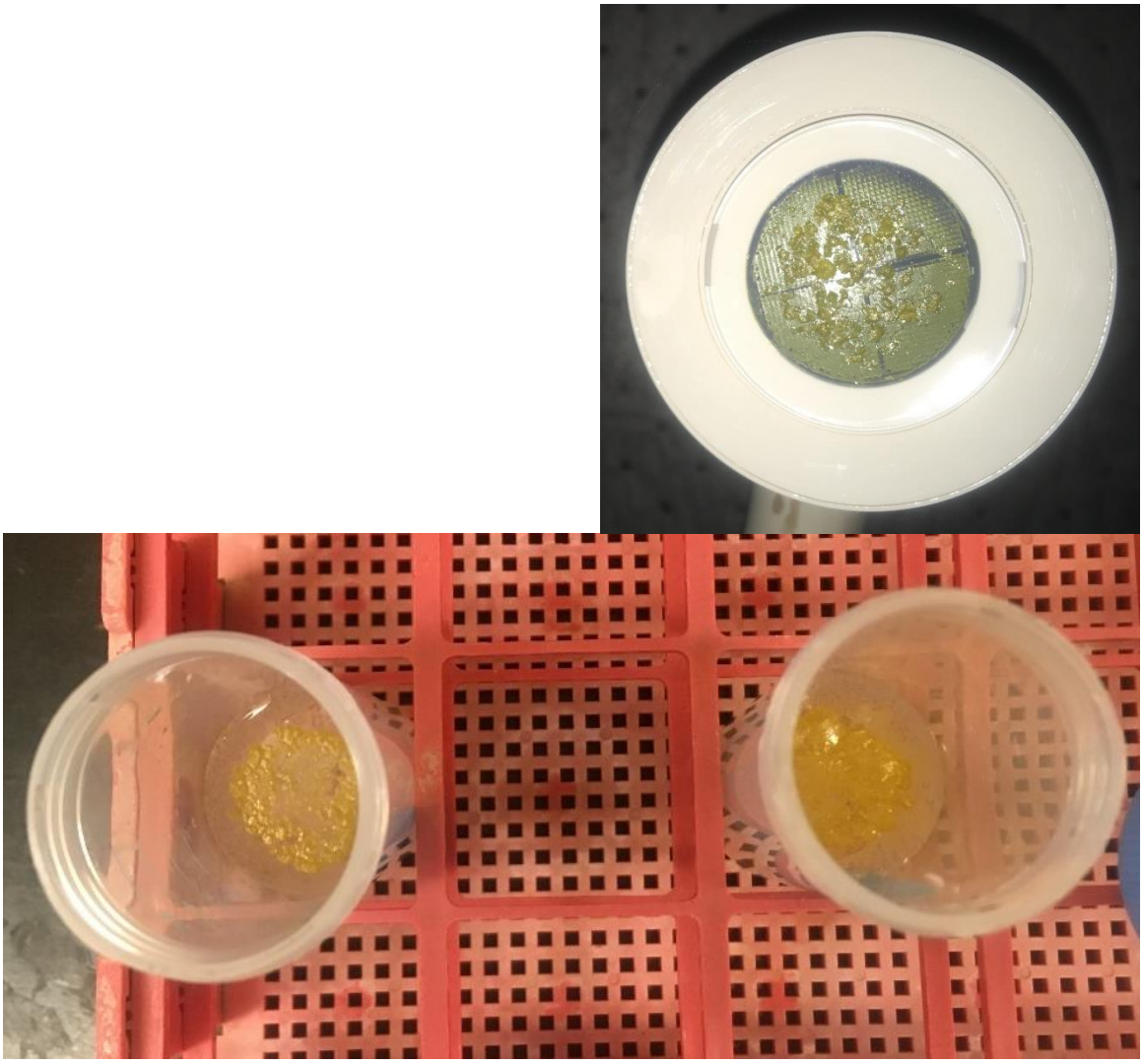

Figure A1-9. Silver Phosphate after 2-3 days in oven and post filtration.

Step A8**: Oven dry Ag_3PO_4 crystals**

1) Carefully remove filter membrane (with crystals) and place in 2 mL glass vial
2) Place vial in 50ºC overnight
3) Once samples have dried, they should separate from filter membrane more easily, but if not, precipitant and filter membrane can be shipped together in the 2 mL vials

Figure A1-10. Drying Ag_3PO_4 crystals in 2 mL vials overnight

Figure A1-11. Silver phosphate ready for transport to YASIC for vacuum furnace and isotopic analysis.

Step A9**: Vacuum Oven dry Ag_3PO_4 crystals**

1) Place sample in vacuum furnace at 550ºC for 5 minutes

Step A10**: δ^{18}O-P Analysis**

1) Analyze at Yale Analytical and Stable Isotope Center (YASIC), Yale Institute for Biospheric Studies, New Haven, CT.

   Online high-temperature thermal decomposition using a Thermo-Chemolysis Elemental Analyzer (TC/EA) coupled to a Delta +XL continuous flow isotope ratio monitoring mass spectrometer (Thermo-Finnigan, Bremen, Germany) was used for analyzing silver phosphate. Phosphate O-isotope ratios ($\delta^{18}O_P$) were calibrated against conventional fluorination using different silver phosphate standards with a ±0.3‰ precision. O-isotope data are reported relative to the Vienna Standard Mean Ocean Water (VSMOW) standard in per mil (‰) (Jaisi & Blake, 2010).

2) Analyze in duplicate or triplicate, if enough Ag_3PO_4 is available.

APPENDIX B. SOIL CHARACTERIZATION

Carbon/Nitrogen analysis, results, and discussion

Total soil C and total N were determined by dry combustion (Tru-Mac CN Analyzer, LECO, St. Joseph, MI) using air-dried, ground soil at 1350 ºC. Due to high soil carbonates making LECO results unreliable for measuring organic C, an acid hydrolysis approach was used on a subset of samples to determine soil carbonate content using a gravimetric approach (Sparks, 1996). In brief, 1.0-gram air dried soil was added to 10 mL 6 M HCl + $FeCl_2$, then hand-shaken and weighed every 15 minutes until weight did not change by more than 1 or 2 milligrams. This allowed carbon dioxide to be lost, thus decarbonating the soil which is then rinsed, dried, and re-analyzed on the LECO for total carbon.

The Houston Black soil series is highly carbonated soil, yet the carbon to nitrogen (C:N) ratio is relatively low. Based on results reported by Waldrip et al. (2015), average C:N was 7.1±0.3 in 2002 for SW12, Y6, Y10, and Y8, however in 2012 average C:N ratios were 8.9±1.75 ranging from 6.11 at Y10 to 10.4 at SW12. Using the acid hydrolysis gravimetric method (Sparks, 1996) for soils from 2014, our results complimented the time series analyzed by Waldrip, with an average C:N ratio of 12.19±0.7. The overall trend of the C:N ratios nearly doubles from 7.1±0.3 in 2002 to 12.19±0.7 in 2014 and based on a meta-analysis done by Lin et al. (2018), this increase can be attributed to the litter applications. Carbon results from the acid hydrolysis method have a consistent %C for the three cultivated soils (Y6, Y10, and Y8) with a mean C of 2.6%±0.84% whereas the remnant native prairie (SW12) had 6% carbon. An in-depth analysis of SW12 and Y10 show the soil organic carbon (SOC) in cultivated soils (Y10) seriously degraded compared to the native prairie (SW12) and that SOC in vertisols improved at a faster rate when cultivated soils were returned to grass production (Stott, Karlen, Cambardella, & Harmel, 2013).

Due to the soil being about 17% $CaCO_3$ of the parent material (Waldrip et al., 2015), C:N ratios of untreated soils ranged from 21 to 32 which was on average 55% higher than the soils analyzed using an acid hydrolysis gravimetric method to de-carbonate the soils prior to the C:N analysis. It is hypothesized that the high carbonates in these soils impacted the efficacy of the

Hedley fractionation, and the formation of APM and MAP in the Isotopic P method because of the impact carbonates has on the pH, which is critically important in the methodology.

δ ^{15}N analysis, results and discussion

Annual mean nitrogen application rates (Harmel et al., 2009) from applied poultry litter averaged 231 and 338 kg N ha^{-1} for Y10 and Y8, respectively and were cultivated 2.4 (±1.3) times yr^{-1}. Inorganic fertilizer was applied to Y6 at an annual mean rate of 146 kg N ha^{-1} yr^{-1} and was cultivated 2.4 (±1.5) times yr^{-1}. SW12 is a native remnant prairie that has never been tilled or fertilized and was used as an experimental control to compare δ ^{15}N signatures among treatments (see Table 3.1). Stable δ ^{15}N isotope analyses on soils from 2002, 2005, 2010, 2012, 2014, and 2017 were conducted on a PDZ Europa Elemental Analyzer interfaced to Sercon Ltd. 20-22 isotope ratio mass spectrometer (EA-IRMS) at the Purdue Stable Isotope Laboratory, Purdue University, West Lafayette, IN, USA. Our objective was to perform a field scale spatial analysis of $\delta^{15}N$ on four watershed soils to evaluate the change in $\delta^{15}N$ signatures from 2002 - 2017 comparing organic (Y10 and Y8) and inorganic (Y6) nitrogen sources to a native soil (SW12) within an agricultural system. Unique $\delta^{15}N$ signatures were obtained for 4 nitrogen sources: a native remnant prairie (SW12) with no added nitrogen fertilizer was +4.7±0.29‰, results where different rates of poultry litter was the sole nutrient source (Y10 and Y8) had a mean $\delta^{15}N$ signature of +11.1‰±0.2‰, and inorganic fertilizers (Y6) was in between with a mean $\delta^{15}N$ signature of +8.04±0.45‰ (Figure A2-1).

Hedley P fractionation results and discussion

Phosphorus pools are indicative of soil health and potential plant uptake availability. The sources of P found in the water-soluble pool are typically readily available for plant uptake and becomes respectively less available in the $NaHCO_3$, NaOH, and HCl extractable P pools. As expected, the control treatment (SW12) showed very little available P in the water-soluble extractable P as well as relatively low levels of P in the cultivated control (Y6) and the grazed field (W10). A mean application of 18 kg ha^{-1} of P was applied on Y6 from commercial fertilizer but 0 kg ha^{-1} applied from poultry litter (Table 3.1). The time series data for PO_4-P from the monitored field sites show spiked levels of phosphorus across P pools in years 2004, 2007, 2010, and 2015

compared to the other years, even though 6.7 and 13.4 Mg ha^{-1} of P had been applied annually for 15 years (Figure A2-2). This anomaly is likely due to a double poultry litter application in 2010 and elevated average rainfall of 1449±45 mm yr^{-1} during 2004, 2007 and 2015 compared to average rainfall of 988±261 mm yr^{-1}. On average, the number of rainfall events for all the monitored sites was 161±148 ranging from 12 to 528 yr^{-1}, however in 2004, 2007, 2010, and 2015 the number of events increased to 196, 388, 257, and 528, respectively.

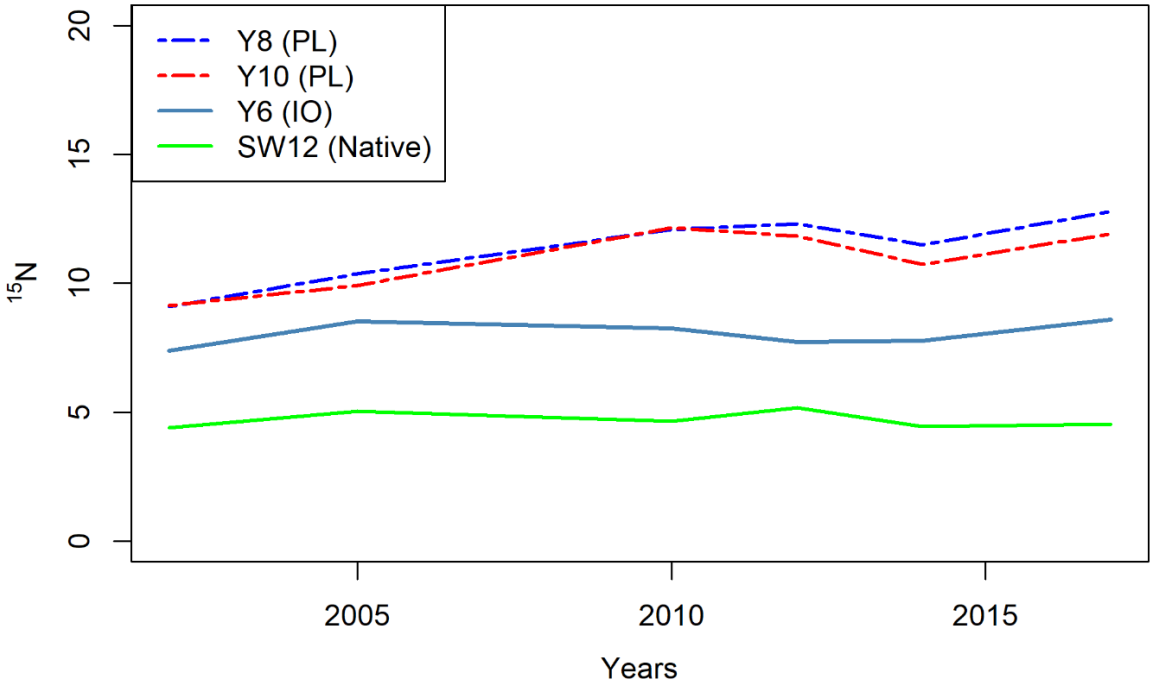

Figure A2-1. $\delta^{15}N$ from 4 TX vertisol soils . Poultry litter (PL) + cultivation (Y8 and Y10) had similar signatures regardless of application rate. Inorganic fertilizer + cultivation (Y6) and a native remnant prairie (SW12) each exhibited unique signatures throughout the study period.

Comparatively, the HCL-P between 2002 – 2017 averaged 84% higher than the other pools with an average of 493±264 mg kg^{-1} ranging from 291 mg kg^{-1} at SW12 to 685 mg kg^{-1} at Y8. The NaOH-P was less variable with an average of 48±14 mg kg^{-1} ranging from 35 mg kg^{-1} at Y6 to 64 mg kg^{-1} at Y8. The $NaHCO_3$-P ranged from 6 mg kg^{-1} at SW12 to 102 at Y8 with an average of 44±45 mg kg^{-1}. The water extractable P was negligible at SW12 where only one reading was above the detectable limit (0.2 mg kg^{-1}) whereas Y10 and Y8 received annual litter applications and averaged 20 and 30 mg kg^{-1}, respectively over the study period (see confirm that of Waldrip et al.

(2015) that poultry litter application increases phosphorus concentrations in all measured pools, regardless of tillage or land use. Results from a Welch Two). Our results confirm that of Waldrip et al. (2015) that poultry litter application increases phosphorus concentrations in all measured pools, regardless of tillage or land use. Results from a Welch Two Sample t-test (R Core Team, 2017) comparing organic to inorganic applied nutrients for both water soluble P and $NaHCO_3$-P had p-values 0.0001 and 0.0002, respectively. Results from both the water-soluble P and $NaHCO_3$-P extractions suggests the plant available P is increased by application of poultry litter. Phosphorus levels in pools that are tightly bound and unavailable to plants, extractable by NaOH and HCl, is higher in soils that used poultry litter as the nutrient source (p=0.001, Figure A2-2).

Table A2-1. Average phosphorus fractionations for time series extractions for soils from 2002, 2005, 2010, 2012, 2014, 2017 using Hedley fractionation.

	SW12	Y6	W10	Y10	Y8
			mg P kg^{-1}		
H_2O-P	0.2±0.2	1.6±0.7	3.3±1.6	21±13	30±15
0.5 M $NaHCO_3$	6±5	13±8	24±12	55±27	102±52
0.1 M NaOH	43±9	35±7	46±9	53±13	64±16
1 M HCl	291±94	324±55	498±330	668±243	685±249

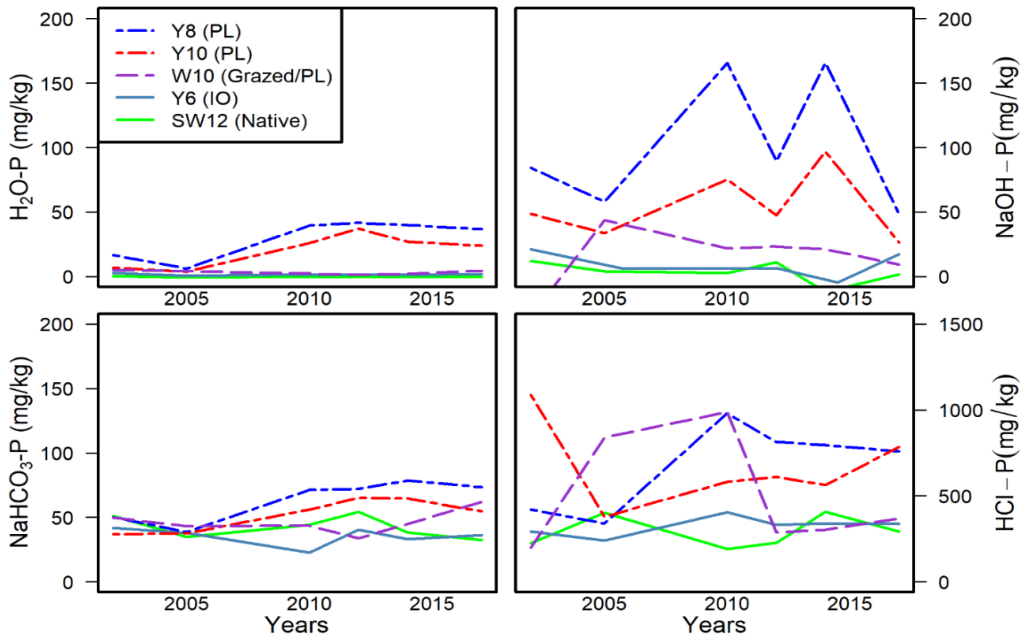

. Figure A2-2. Hedley Fractionation of phosphorus pools

REFERENCES

Acosta-Martinez, V., & Harmel, R. D. (2006). Soil microbial communities and enzyme activities under various poultry litter application rates. *J Environ Qual, 35*(4), 1309-1318. doi:10.2134/jeq2005.0470

Adeli, A., Bala, F. M., Rowe, D. E., & Owens, P. R. (2006). Effects of drying intervals and repeated rain events on runoff nutrient dynamics from soil treated with broiler litter. *Journal of Sustainable Agriculture, 28*(1), 67-83. doi:10.1300/J064v28n01_07

Advances in Agronomy, Vol 125. (2014). In D. L. Sparks (Ed.), *Advances in Agronomy, Vol 125* (Vol. 125, pp. 1-310).

Alcock, N. W., Dudek, M., Grybos, R., Hodorowicz, E., Kanas, A., & Samotus, A. (1990). COMPLEXATION BETWEEN MOLYBDENUM(VI) AND CITRATE - STRUCTURAL CHARACTERIZATION OF A TETRAMERIC COMPLEX, K4 (MOO2)4O3(CIT)2 .6H2O. *Journal of the Chemical Society-Dalton Transactions*(2), 707-711. doi:10.1039/dt9900000707

Amaizah, N., Cakmak, D., Saljnikov, E., Roglic, G., Mrvic, V., Krgovic, R., & Manojlovic, D. (2012). Fractionation of soil phosphorus in a long-term phosphate fertilization. *Journal of the Serbian Chemical Society, 77*(7), 971-981. doi:10.2298/jsc110927208a

Amelung, W., Antar, P., Kleeberg, I., Oelmann, Y., Lücke, A., Alt, F., . . . Barej, J. A. M. (2015). The δ18O signatures of HCl-extractable soil phosphates: methodological challenges and evidence of the cycling of biological P in arable soil. *European Journal of Soil Science, 66*(6), 965-972. doi:10.1111/ejss.12288

Anderson, D. M., Burkholder, J. M., Cochlan, W. P., Glibert, P. M., Gobler, C. J., Heil, C. A., . . . Vargo, G. A. (2008). Harmful algal blooms and eutrophication: Examining linkages from selected coastal regions of the United States. *Harmful Algae, 8*(1), 39-53. doi:10.1016/j.hal.2008.08.017

Angert, A., Weiner, T., Mazeh, S., & Sternberg, M. (2012). Soil phosphate stable oxygen isotopes across rainfall and bedrock gradients. *Environ Sci Technol, 46*(4), 2156-2162. doi:10.1021/es203551s

Angert, A., Weiner, T., Mazeh, S., Tamburini, F., Frossard, E., Bernasconi, S. M., & Sternberg, M. (2011). Seasonal variability of soil phosphate stable oxygen isotopes in rainfall manipulation experiments. *Geochimica et Cosmochimica Acta, 75*(15), 4216-4227. doi:10.1016/j.gca.2011.05.002

Association, Ohio Travel (2015). *Tourism and Algal Blooms: Economic Impact Fact Sheet 2015*. Retrieved 7/6/2018

Ayliffe, L. K., Veeh, H. H., & Chivas, A. R. (1992). Oxygen isotopes of phosphate and the origin of island apatite deposits. *Earth Planet. Sci. Lett., 108*, 119.

Baker, D. B., & Richards, R. P. (2002). Phosphorus budgets and riverine phosphorus export in northwestern Ohio watersheds. *J Environ Qual, 31*(1), 96-108.

Bauwe, A., Tiemeyer, B., Kahle, P., & Lennartz, B. (2015). Classifying hydrological events to quantify their impact on nitrate leaching across three spatial scales. *Journal of Hydrology, 531*, 589-601. doi:10.1016/j.jhydrol.2015.10.069

Baxter, G. P., & Jones, G. (1910). A revision of the atomic weight of phosphorus. First paper. The analysis of silver phosphate. *Journal of the American Chemical Society, 32*, 298-318. doi:10.1021/ja01921a003

Bennett, E. M., Reed-Andersen, T., Houser, J. N., Gabriel, J. R., & Carpenter, S. R. (1999). A phosphorus budget for the Lake Mendota watershed. *Ecosystems, 2*(1), 69-75. doi:10.1007/s100219900059

Bi, Q. F., Zheng, B. X., Lin, X. Y., Li, K. J., Liu, X. P., Hao, X. L., . . . Zhu, Y. G. (2018). The microbial cycling of phosphorus on long-term fertilized soil: Insights from phosphate oxygen isotope ratios. *Chemical Geology, 483*, 56-64. doi:10.1016/j.chemgeo.2018.02.013

Blake, R. E., Alt, J. C., & Martini, A. M. (2001). Oxygen isotope ratios of PO4: An inorganic indicator of enzymatic activity and P metabolism and a new biomarker in the search for life. *Proc. Natl. Acad. Sci.U.S.A., 98*, 2148.

Blake, R. E., Chang, S. J., & Lepland, A. (2010). Phosphate oxygen isotopic evidence for a temperate and biologically active Archaean ocean. *Nature, 464*(7291), 1029-U1089. doi:10.1038/nature08952

Blake, R. E., O'Neil, J. R., & Garcia, G. A. (1997). Oxygen isotope systematics of biologically mediated reactions of phosphate: I. Microbial degredation of organophosphorous compounds. *Geochim. Cosmochim. Acta, 61*, 4411.

Blake, R. E., O'Neil, J. R., & Surkov, A. V. (2005). Biogeochemical cycling of phosphorous: Insights from oxygen isotope effects of photoenzymes. *Am. J. Sci., 305*, 596.

Boyer, P. D. (1978). Isotope exchange probes and enzyme mechanisms. *Accounts of Chemical Research, 11*(5), 218-224. doi:10.1021/ar50125a007

Brooker, M. R., Longnecker, K., Kujawinski, E. B., Evert, M. H., & Mouser, P. J. (2018). Discrete Organic Phosphorus Signatures are Evident in Pollutant Sources within a Lake Erie Tributary. *Environmental Science & Technology, 52*(12), 6771-6779. doi:10.1021/acs.est.7b05703

Bundy, L. G., & Sturgul, S. J. (2001). A phosphorus budget for Wisconsin cropland. *Journal of Soil and Water Conservation, 56*(3), 243-249.

Carpenter, S. R., Caraco, N. F., Correl, D. L., Howarth, R. W., & Sharpley, A. H. (1998). Nonpoint pollution of surface waters with phosphorus and nitrogen. *Ecol. Applications., 8*, 559.

Chang, S. C., & Jackson, M. L. (1957). FRACTIONATION OF SOIL PHOSPHORUS. *Soil Science, 84*(2), 133-144.

Chang, S. J., & Blake, R. E. (2015). Precise calibration of equilibrium oxygen isotope fractionations between dissolved phosphate and water from 3 to 37 degrees C. *Geochimica et Cosmochimica Acta, 150*, 314-329. doi:10.1016/j.gca.2014.10.030

Choquette, A. F., Hirsch, R. M., Murphy, J. C., Johnson, L. T., & Confesor, R. B. (2019). Tracking changes in nutrient delivery to western Lake Erie: Approaches to compensate for variability and trends in streamflow. *Journal of Great Lakes Research, 45*(1), 21-39. doi:10.1016/j.jglr.2018.11.012

Clausen, J. C., & Spooner, J. (1993). *Paried Watershed Study Design*. (841-F-93-009). Washington, D.C. Retrieved from https://www.in.gov/idem/nps/files/iwpg_paired_watersheds.pdf.

Cohn, M. (1958). PHOSPHATE-WATER EXCHANGE REACTION CATALYZED BY INORGANIC PYROPHOSPHATASE OF YEAST. *Journal of Biological Chemistry, 230*(1), 369-379.

Collick, A. S., Veith, T. L., Fuka, D. R., Kleinman, P. J. A., Buda, A. R., Weld, J. L., . . . Easton, Z. M. (2016). Improved Simulation of Edaphic and Manure Phosphorus Loss in SWAT. *J Environ Qual, 45*(4), 1215-1225. doi:10.2134/jeq2015.03.0135

Colman, A. (2002). The oxygen isotope composition of dissolved inorganic phosphate and the marine phosphorus cycle.

Colman, A. S. (2002). *Geology & Geophysics*.

Colman, A. S., Blake, R. E., Karl, D. M., Fogel, M. L., & Turekian, K. K. (2005). Marine phosphate oxygen isotopes and organic matter remineralization in the oceans. *Proc. Natl. Acad. Sci.U.S.A., 102*, 13023.

Commission, F. F. a. W. (2018). HAB Monitoring Database: Routine Monitoring. Retrieved from http://myfwc.com/research/redtide/monitoring/database/

Cross, A. F., & Schlesinger, W. H. (1995). A LITERATURE-REVIEW AND EVALUATION OF THE HEDLEY FRACTIONATION - APPLICATIONS TO THE BIOGEOCHEMICAL CYCLE OF SOIL-PHOSPHORUS IN NATURAL ECOSYSTEMS. *Geoderma, 64*(3-4), 197-214. doi:10.1016/0016-7061(94)00023-4

DeLaune, P. B., Moore, P. A., Carman, D. K., Sharpley, A. N., Haggard, B. E., & Daniel, T. C. (2004). Development of a phosphorus index for pastures fertilized with poultry litter - Factors affecting phosphorus runoff. *J Environ Qual, 33*(6), 2183-2191. doi:10.2134/jeq2004.2183

Domburg, P., Edwards, A. C., Sinclair, A. H., & Chalmers, N. A. (2000). Assessing nitrogen and phosphorus efficiency at farm and catchment scale using nutrient budgets. *Journal of the Science of Food and Agriculture, 80*(13), 1946-1952. doi:10.1002/1097-0010(200010)80:13<1946::Aid-jsfa736>3.0.Co;2-q

Duncan, E. W., King, K. W., Williams, M. R., LaBarge, G., Pease, L. A., Smith, D. R., & Fausey, N. R. (2017). Linking Soil Phosphorus to Dissolved Phosphorus Losses in the Midwest. *Agricultural & Environmental Letters, 2*(1), 5. doi:10.2134/ael2017.02.0004

Echikson, T. (2014). Do You Need To Permit Your Stormwater Discharge? *Environmental Law Insights*.

Edwards, D. R., & Daniel, T. C. (1993). EFFECTS OF POULTRY LITTER APPLICATION RATE AND RAINFALL INTENSITY ON QUALITY OF RUNOFF FROM FESCUEGRASS PLOTS. *J Environ Qual, 22*(2), 361-365. doi:10.2134/jeq1993.00472425002200020017x

Elliott, H. A., Brandt, R. C., Kleinman, P. J. A., Sharpley, A. N., & Beegle, D. B. (2006). Estimating source coefficients for phosphorus site indices. *J Environ Qual, 35*(6), 2195-2201. doi:10.2134/jeq2006.0014

Elsbury, K. E., Paytan, A., Ostrom, N. E., Kendall, C., Young, M. B., McLaughlin, K., . . . Watson, S. (2009). Using Oxygen Isotopes of Phosphate To Trace Phosphorus Sources and Cycling in Lake Erie. *Environmental Science & Technology, 43*(9), 3108-3114. doi:10.1021/es8034126

EPA. *Clean Water Act Section 502(14)*. EPA.GOV Retrieved from https://www.epa.gov/cwa-404/clean-water-act-section-502-general-definitions.

EPA, Ohio. (2010). *The Ohio EPA Ohio Lake Erie Phosphorus Task Force Final Report*. Retrieved from https://www.epa.state.oh.us/portals/35/lakeerie/ptaskforce/Task_Force_Final_Executive_Summary_April_2010.pdf

Fanelli, R. M., Blomquist, J. D., & Hirsch, R. M. (2019). Point sources and agricultural practices control spatial-temporal patterns of orthophosphate in tributaries to Chesapeake Bay. *Science of The Total Environment, 652*, 422-433. doi:10.1016/j.scitotenv.2018.10.062

Firsching, F. (1961). PRECIPITATION OF SILVER PHOSPHATE FROM HOMOGENEOUS SOLUTION. *Analytical Chemistry, 33*(7), 873-&. doi:10.1021/ac60175a018

Ford, W. I., Williams, M. R., Young, M., King, K. W., & Fischer, E. (2018). Assessing intra-event phosphorus dynamics in drainage water using phosphate stable oxygen isotopes. *Transactions of the ASABE, 61*(7), 1379-1392.

Frossard, E., Achat, D., Bernasconi, S., Bünemann, E., Fardeau, J.-C., Jansa, J., . . . Oberson, A. (2011). The Use of Tracers to Investigate Phosphate Cycling in Soil–Plant Systems. In (pp. 59-91).

Frossard, E., Achat, D. L., Bernasconi, S. M., Bunemann, E. K., Fardeau, J. C., Jansa, J., . . . Oberson, A. (2011). The Use of Tracers to Investigate Phosphate Cycling in Soil-Plant Systems. In E. K. Bunemann, A. Oberson, & E. Frossard (Eds.), *Phosphorus in Action: Biological Processes in Soil Phosphorus Cycling* (Vol. 26, pp. 59-91).

Garcia-Guinea, J., Correcher, V., Benavente, D., & Sanchez-Moral, S. (2015). Composition, Luminescence, and Color of a Natural Blue Calcium Carbonate from Madagascar. *Spectroscopy Letters, 48*(2), 107-111. doi:10.1080/00387010.2013.857692

Garnier, J., Lassaletta, L., Billen, G., Romero, E., Grizzetti, B., Nemery, J., . . . Dorioz, J. M. (2015). Phosphorus budget in the water-agro-food system at nested scales in two contrasted regions of the world (ASEAN-8 and EU-27). *Global Biogeochemical Cycles, 29*(9), 1348-1368. doi:10.1002/2015gb005147

Glibert, P. M., Landsberg, J. H., Evans, J. J., Al-Sarawi, M. A., Faraj, M., Al-Jarallah, M. A., . . . Shoemaker, C. (2002). A fish kill of massive proportion in Kuwait Bay, Arabian Gulf, 2001: the roles of bacterial disease, harmful algae, and eutrophication. *Harmful Algae, 1*(2), 215-231. doi:https://doi.org/10.1016/S1568-9883(02)00013-6

Gooddy, D. C., Lapworth, D. J., Ascott, M. J., Bennett, S. A., Heaton, T. H. E., & Surridge, B. W. J. (2015). Isotopic Fingerprint for Phosphorus in Drinking Water Supplies. *Environmental Science & Technology, 49*(15), 9020-9028. doi:10.1021/acs.est.5b01137

Goovaerts, P. (1998). Geostatistical tools for characterizing the spatial variability of microbiological and physico-chemical soil properties. *Biology and Fertility of Soils, 27*(4), 315-334. doi:10.1007/s003740050439

Granger, S. J., Harris, P., Peukert, S., Guo, R., Tamburini, F., Blackwell, M. S., . . . McGrath, S. (2017). Phosphate stable oxygen isotope variability within a temperate agricultural soil. *Geoderma, 285*, 64-75. doi:10.1016/j.geoderma.2016.09.020

Granger, S. J., Yang, Y. G., Pfahler, V., Hodgson, C., Smith, A. C., Le Cocq, K., . . . Howden, N. J. K. (2018). The stable oxygen isotope ratio of resin extractable phosphate derived from fresh cattle faeces. *Rapid Communications in Mass Spectrometry, 32*(9), 703-710. doi:10.1002/rcm.8092

Green, C. H., Arnold, J. G., Williams, J. R., Haney, R., & Harmel, R. D. (2007). Soil and water assessment tool hydrologic and water quality evaluation of poultry litter application to small-scale subwatersheds in Texas. *Transactions of the ASABE, 50*(4), 1199-1209.

Gruau, G., Legeas, M., Riou, C., Gallacier, E., Martineau, F., & Henin, O. (2005). The oxygen isotope composition of dissolved anthropogenic phosphates: a new tool for eutrophication research. *Water Research, 39*, 232.

Haggard, B. E., Vadas, P. A., Smith, D. R., DeLaune, P. B., & Moore, P. A. (2005). Effect of poultry litter to water ratios on extractable phosphorus content and its relation to runoff phosphorus concentrations. *Biosystems Engineering, 92*(3), 409-417. doi:10.1016/j.biosystemseng.2005.07.007

Hanrahan, B. R., King, K. W., Williams, M. R., Duncan, E. W., Pease, L. A., & LaBarge, G. A. (2019). Nutrient balances influence hydrologic losses of nitrogen and phosphorus across agricultural fields in northwestern Ohio. *Nutrient Cycling in Agroecosystems, 113*(3), 231-245. doi:10.1007/s10705-019-09981-4

Harmel, R. D., Haney, R. L., & Smith, D. R. (2011). Effects of Annual Turkey Litter Application on Surface Soil Quality of a Texas Blackland Vertisol. *Soil Science, 176*(5), 227-236. doi:10.1097/SS.0b013e318214fab4

Harmel, R. D., Haney, R. L., Smith, D. R., White, M., & King, K. W. (2014). USDA-ARS Riesel Watersheds, Riesel, Texas, USA: Water quality research database. *Water Resources Research, 50*(10), 8374-8382. doi:10.1002/2013wr015191

Harmel, R. D., Harmel, B., & Patterson, M. C. (2008). On-Farm Agro-Economic Effects of Fertilizing Cropland with Poultry Litter. *Journal of Applied Poultry Research, 17*(4), 545-555. doi:10.3382/japr.2008-00039

Harmel, R. D., King, K. W., Haggard, B. E., Wren, D. G., & Sheridan, J. M. (2006). Practical guidance for discharge and water quality data collection on small watersheds. *Transactions of the ASABE, 49*(4), 937-948.

Harmel, R. D., Richardson, C. W., King, K. W., & Allen, P. M. (2006). Runoff and soil loss relationships for the Texas Blackland Prairies ecoregion. *Journal of Hydrology, 331*(3-4), 471-483. doi:10.1016/j.jhydrol.2006.05.033

Harmel, R. D., Smith, D. R., Haney, R. L., & Dozier, M. (2009). Nitrogen and phosphorus runoff from cropland and pasture fields fertilized with poultry litter. *Journal of Soil and Water Conservation, 64*(6), 400-412. doi:10.2489/jswc.64.6.400

Harmel, R. D., Torbert, H. A., Haggard, B. E., Haney, R., & Dozier, M. (2004). Water quality impacts of converting to a poultry litter fertilization strategy. *J Environ Qual, 33*(6), 2229-2242. doi:10.2134/jeq2004.2229

Hedley, M. J., Stewart, J. W. B., & Chauhan, B. S. (1982). CHANGES IN INORGANIC AND ORGANIC SOIL-PHOSPHORUS FRACTIONS INDUCED BY CULTIVATION PRACTICES AND BY LABORATORY INCUBATIONS. *Soil Science Society of America Journal, 46*(5), 970-976. doi:10.2136/sssaj1982.03615995004600050017x

Ho, J. C., Michalak, A. M., & Pahlevan, N. (2019). Widespread global increase in intense lake phytoplankton blooms since the 1980s. *Nature, 574*(7780), 667-+. doi:10.1038/s41586-019-1648-7

Holford, I. C. R. (1997). Soil phosphorus: Its measurement, and its uptake by plants. *Australian Journal of Soil Research, 35*(2), 227-239. doi:10.1071/s96047

Hoover, N. L., Law, J. Y., Long, L. A. M., Kanwar, R. S., & Soupir, M. L. (2019). Long-term impact of poultry manure on crop yield, soil and water quality, and crop revenue. *Journal of Environmental Management, 252*, 11. doi:10.1016/j.jenvman.2019.109582

Jaisi, D. P., & Blake, R. E. (2010). Tracing sources and cycling of phosphorus in Peru Margin sediments using oxygen isotopes in authigenic and detrital phosphates. *Geochimica et Cosmochimica Acta, 74*(11), 3199-3212. doi:https://doi.org/10.1016/j.gca.2010.02.030

Jarvie, H. P., Johnson, L. T., Sharpley, A. N., Smith, D. R., Baker, D. B., Bruulsema, T. W., & Confesor, R. (2017). Increased Soluble Phosphorus Loads to Lake Erie: Unintended Consequences of Conservation Practices? *J Environ Qual, 46*(1), 123-132. doi:10.2134/jeq2016.07.0248

Jiang, Z. H., Zhang, H., Jaisi, D. P., Blake, R. E., Zheng, A. R., Chen, M., . . . Chen, Z. G. (2017). The effect of sample treatments on the oxygen isotopic composition of phosphate pools in soils. *Chemical Geology, 474*, 9-16. doi:10.1016/j.chemgeo.2017.10.017

Joshi, S. R., Li, X. N., & Jaisi, D. P. (2016). Transformation of Phosphorus Pools in an Agricultural Soil: An Application of Oxygen-18 Labeling in Phosphate. *Soil Science Society of America Journal, 80*(1), 69-78. doi:10.2136/sssaj2015.06.0219

Kashem, M. A., Akinremi, O. O., & Racz, G. J. (2004). Phosphorus fractions in soil amended with organic and inorganic phosphorus sources. *Canadian Journal of Soil Science, 84*(1), 83-90. doi:10.4141/s03-018

Kebreab, E., & Vitti, D. (2010). PHOSPHORUS AND CALCIUM UTILIZATION AND REQUIREMENTS IN FARM ANIMALS General Introduction. In D. Vitti & E. Kebreab (Eds.), *Phosphorus and Calcium Utilization and Requirements in Farm Animals* (pp. 1-7). Wallingford: Cabi Publishing-C a B Int.

Kendall, C., & McDonell, J. J. (1998). *Isotopes Tracers in Catchment Hydrology*.

King, K. W., Williams, M. R., Dick, W. A., & LaBarge, G. A. (2016). Decreasing Phosphorus Loss in Tile-Drained Landscapes Using Flue Gas Desulfurization Gypsum. *J Environ Qual, 45*(5), 1722-1730. doi:10.2134/jeq2016.04.0132

Kingery, W. L., Wood, C. W., Delaney, D. P., Williams, J. C., & Mullins, G. L. (1994). IMPACT OF LONG-TERM LAND APPLICATION OF BROILER LITTER ON ENVIRONMENTALLY RELATED SOIL PROPERTIES. *J Environ Qual, 23*(1), 139-147. doi:10.2134/jeq1994.00472425002300010022x

Kleinman, P. J. A., Fanelli, R. M., Hirsch, R. M., Buda, A. R., Easton, Z. M., Wainger, L. A., . . . Shenk, G. W. (2019). Phosphorus and the Chesapeake Bay: Lingering Issues and Emerging Concerns for Agriculture. *J Environ Qual, 48*(5), 1191-1203. doi:10.2134/jeq2019.03.0112

Kleinman, P. J. A., & Sharpley, A. N. (2003). Effect of broadcast manure on runoff phosphorus concentrations over successive rainfall events. *J Environ Qual, 32*(3), 1072-1081. doi:10.2134/jeq2003.1072

Kleinman, P. J. A., Sharpley, A. N., Wolf, A. M., Beegle, D. B., Elliott, H. A., Weld, J. L., & Brandt, R. (2006). Developing an environmental manure test for the phosphorus index. *Communications in Soil Science and Plant Analysis, 37*(15-20), 2137-2155. doi:10.1080/00103620600817242

Kok, B., & Varner, J. E. (1967). EXTRATERRESTIAL LIFE DETECTION BASED ON OXYGEN ISOTOPE EXCHANGE REACTIONS. *Science, 155*(3766), 1110-+. doi:10.1126/science.155.3766.1110

Kolodny, Y., Luz, B., & Navon, O. (1983). Oxygen isotope variations in phosphate of biogenic apatites, I. Fish bone apatite- rechecking the rules of the game. *Earth Planet. Sci. Lett., 64*, 398.

Kornexl, B. E., Gehre, M., Hofling, R., & Werner, A. (1999). On-line δ18O measurement of organic and inorganic substances. *Rapid Communications in Mass Spectrometry, 13*, 1685.

Kusmer, A. S., Goyette, J. O., MacDonald, G. K., Bennett, E. M., Maranger, R., & Withers, P. J. A. (2019). Watershed Buffering of Legacy Phosphorus Pressure at a Regional Scale: A Comparison Across Space and Time. *Ecosystems, 22*(1), 91-109. doi:10.1007/s10021-018-0255-z

Larsen, S., Middelboe, V., & Johansen, H. S. (1989). THE FATE OF O-18 LABELED PHOSPHATE IN SOIL PLANT-SYSTEMS. *Plant and Soil, 117*(1), 143-145. doi:10.1007/bf02206267

Liang, Y., & Blake, R. E. (2006a). Oxygen isotope composition of phosphate in organic compounds: Isotope effects of extraction methods. *Org. Geochem., 37*, 1263.

Liang, Y., & Blake, R. E. (2006b). Oxygen isotope signature of Pi regeneration from organic compounds by phosphomonoesterases and photooxidation. *Geochim. Cosmochim. Acta, 70*, 3957.

Lin, Y. R., Watts, D. B., van Santen, E., & Cao, G. Q. (2018). Influence of Poultry Litter on Crop Productivity under Different Field Conditions: A Meta-Analysis. *Agronomy Journal, 110*(3), 807-818. doi:10.2134/agronj2017.09.0513

Logsdon, S., Clay, D., Moore, D., & Tsegaye, T. (2008). Measuring Nutrient Removal, Calculating Nutrient Budgets. In *Soil Science: Step-by-Step Field Analysis* (pp. 159-182): Soil Science Society of America.

Lohani, S., Baffaut, C., Thompson, A. L., & Sadler, E. J. (2020). Soil Vulnerability Index assessment as a tool to explain annual constituent loads in a nested watershed. *Journal of Soil and Water Conservation, 75*(1), 42-52. doi:10.2489/jswc.75.1.42

Longinelli, A., Bartelloni, M., & Cortecci, G. (1976). The isotopic cycle of oceanic phosphate, I. *Earth Planet. Sci. Lett., 32*, 389.

Longinelli, A., & Nuti, S. (1968). Oxygen isotopic composition of phosphorites from marine deposits. *Earth Planet. Sci. Lett., 5*, 13.

Longinelli, A., & Nuti, S. (1973). Revised phosphate-water isotopic temperature scale. *Earth Planet. Sci. Lett., 19*, 373.

Maccoux, M. J., Dove, A., Backus, S. M., & Dolan, D. M. (2016). Total and soluble reactive phosphorus loadings to Lake Erie A detailed accounting by year, basin, country, and tributary. *Journal of Great Lakes Research, 42*(6), 1151-1165. doi:10.1016/j.jgh.2016.08.005

Marriott, C. A., Hudson, G., Hamilton, D., Neilson, R., Boag, B., Handley, L. L., . . . Robinson, D. (1997). Spatial variability of soil total C and N and their stable isotopes in an upland Scottish grassland. *Plant and Soil, 196*(1), 151-162. doi:10.1023/a:1004288610550

McLaughlin, K., Cade-Menun, B. J., & Paytan, A. (2006). The oxygen isotopic composition of phosphate in Elkhorn Slough, California: A tracer for phosphate sources. *Estuarine, Coastal Shelf Sci., 70*, 499.

McLaughlin, K., Chavez, F. P., Pennington, J. T., & Paytan, A. (2006). A time series investigation of the oxygen isotopic composition of dissolved inorganic phosphate in Monterey Bay. *Limnol. Oceanogr., 111*, G03003.

McLaughlin, K., Kendall, C., Silva, S., Young, M., & Paytan, A. (2006). Phosphate oxygen isotope ratios as a tracer for sources and cycling of phosphate in North San Francisco Bay, California. *J. Geophys. Res.: Biogeosci., 111*, G03003.

McLaughlin, K., & Paytan, A. (2007). The oceanic phosphorus cycle. *Chem. Rev., 107*, 563.

McLaughlin, K., Paytan, A., Kendall, C., & Silva, S. (2006). Oxygen isotopes of phosphatic compounds- Application for marine particulate matter, sediments and soils. *Mar. Chem., 98*, 148.

McLaughlin, K., Silva, S., Kendall, C., Stuart-Williams, H., & Paytan, A. (2004). A precise method for the analysis of δ18O of dissolved inorganic phosphate in seawater. *Limnol. Oceanogr.: Methods, 2*, 202.

Mehlich, A. (1984). MEHLICH-3 SOIL TEST EXTRACTANT - A MODIFICATION OF MEHLICH-2 EXTRACTANT. *Communications in Soil Science and Plant Analysis, 15*(12), 1409-1416. doi:10.1080/00103628409367568

Messiga, A. J., Ziadi, N., Belanger, G., & Morel, C. (2014). Relationship between Soil Phosphorus and Phosphorus Budget in Grass Sward with Varying Nitrogen Applications. *Soil Science Society of America Journal, 78*(4), 1481-1488. doi:10.2136/sssaj2013.05.0200

NASS. (2001). *Chicken and Eggs*. Retrieved from Washington, D.C.: https://downloads.usda.library.cornell.edu/usda-esmis/files/fb494842n/2v23vv71v/zp38wf016/ChicEggs-01-30-2001.pdf

NASS. (2020). *Chickens and Eggs* (ISSN: 1948-9064). Retrieved from Washington, D.C.: https://downloads.usda.library.cornell.edu/usda-esmis/files/fb494842n/4b29bp888/0p096q47w/ckeg0120.pdf

Negassa, W., & Leinweber, P. (2009). How does the Hedley sequential phosphorus fractionation reflect impacts of land use and management on soil phosphorus: A review. *Journal of Plant Nutrition and Soil Science, 172*(3), 305-325. doi:10.1002/jpln.200800223

NOAA. (2017). Experimental Lake Erie Harmful Algal Bloom Bulletin [Press release]. Retrieved from https://www.glerl.noaa.gov/res/HABs_and_Hypoxia/lakeErieHABArchive/HAB20171107_2017035_LE.pdf

Okafor, J. (2014). *Investigating pedogenic carbonate ormation by measuring the stable isotope composition of water in vertisols.* (Master of Science), University of Texas, University of Texas.

Osmond, D., Sharpley, A., Bolster, C., Cabrera, M., Feagley, S., Lee, B., . . . Zhang, H. (2012). Comparing Phosphorus Indices from Twelve Southern U.S. States against Monitored Phosphorus Loads from Six Prior Southern Studies. *J Environ Qual, 41*(6), 1741-1749. doi:10.2134/jeq2012.0013

Paytan, A., Kolodny, Y., Neori, A., & Luz, B. (2002). Rapid biologically mediated oxygen isotope exchange between water and phosphate. *Global Biogeochem. Cycles, 16*, 1013.

Paytan, A., & McLaughlin, K. (2011). *Tracing the Sources and Biogeochemical Cycling of Phosphorus in Aquatic Systems Using Isotopes of Oxygen in Phosphate*. Berlin: Springer-Verlag Berlin.

Pease, L. A., King, K. W., Williams, M. R., LaBarge, G. A., Duncan, E. W., & Fausey, N. R. (2018). Phosphorus export from artificially drained fields across the Eastern Corn Belt. *Journal of Great Lakes Research, 44*(1), 43-53. doi:10.1016/j.jglr.2017.11.009

Penn, C. J., Bryant, R. B., Needelman, B., & Kleinman, P. (2007). Spatial distribution of soil phosphorus across selected new york dairy farm pastures and hay fields. *Soil Science, 172*(10), 797-810. doi:10.1097/SS.0b013e3180d0a3c0

Peukert, S., Bol, R., Roberts, W., Macleod, C. J. A., Murray, P. J., Dixon, E. R., & Brazier, R. E. (2012). Understanding spatial variability of soil properties: a key step in establishing field-to farm-scale agro-ecosystem experiments. *Rapid Communications in Mass Spectrometry, 26*(20), 2413-2421. doi:10.1002/rcm.6336

Pistocchi, C., Tamburini, F., Gruau, G., Ferhi, A., Trevisan, D., & Dorioz, J. M. (2017). Tracing the sources and cycling of phosphorus in river sediments using oxygen isotopes: Methodological adaptations and first results from a case study in France. *Water Research, 111*, 346-356. doi:10.1016/j.watres.2016.12.038

Pote, D. H., Daniel, T. C., Sharpley, A. N., Moore, P. A., Edwards, D. R., & Nichols, D. J. (1996). Relating extractable soil phosphorus to phosphorus losses in runoff. *Soil Science Society of America Journal, 60*(3), 855-859. doi:10.2136/sssaj1996.03615995006000030025x

Pote, D. H., Kingery, W. L., Aiken, G. E., Han, F. X., Moore, P. A., & Buddington, K. (2003). Water-quality effects of incorporating poultry litter into perennial grassland soils. *J Environ Qual, 32*(6), 2392-2398. doi:10.2134/jeq2003.2392

Powers, S. M., Bruulsema, T. W., Burt, T. P., Chan, N. I., Elser, J. J., Haygarth, P. M., . . . Zhang, F. (2016). Long-term accumulation and transport of anthropogenic phosphorus in three river basins. *Nature Geoscience, 9*, 353. doi:10.1038/ngeo2693 https://www.nature.com/articles/ngeo2693#supplementary-information

Qin, Z., & Shober, A. (2018). The Challenges of Managing Legacy Phosphorus Losses from Manure-Impacted Agricultural Soils. *Current Pollution Reports, 4*(4), 265-276. doi:10.1007/s40726-018-0100-1

R Core Team. (2017). R: A language and enivronment or statistical computing. Vienna, Austria: R Foundation for Statistical Computing. Retrieved from https://www.R-project.org/

Reid, K., & Schneider, K. D. (2019). Phosphorus accumulation in Canadian agricultural soils over 30 yr. *Canadian Journal of Soil Science, 99*(4), 520-532. doi:10.1139/cjss-2019-0023

Richards, R. P., Baker, D. B., & Crumrine, J. P. (2009). Improved water quality in Ohio tributaries to Lake Erie: A consequence of conservation practices. *Journal of Soil and Water Conservation, 64*(3), 200-211. doi:10.2489/jswc.64.3.200

Ruane, E. M., Treacy, M., McNamara, K., & Humphreys, J. (2014). Farm-gate phosphorus balances and soil phosphorus concentrations on intensive dairy farms in the south-west of Ireland. *Irish Journal of Agricultural and Food Research, 53*(2), 105-119.

Scavia, D., Kalcic, M., Muenich, R. L., Aloysius, N., Arnold, J., Boles, C., . . . Yen, H. (2016). *Informing Lake Erie agriculture nutrient management via scenario evaluation*. Retrieved from http://pubs.er.usgs.gov/publication/70170956

Sharpley, A., Jarvie, H. P., Buda, A., May, L., Spears, B., & Kleinman, P. (2013). Phosphorus Legacy: Overcoming the Effects of Past Management Practices to Mitigate Future Water Quality Impairment. *J Environ Qual, 42*(5), 1308-1326. doi:10.2134/jeq2013.03.0098

Sharpley, A. N. (1995). DEPENDENCE OF RUNOFF PHOSPHORUS ON EXTRACTABLE SOIL-PHOSPHORUS. *J Environ Qual, 24*(5), 920-926. doi:10.2134/jeq1995.00472425002400050020x

Simpson, R. J., Stefanski, A., Marshall, D. J., Moore, A. D., & Richardson, A. E. (2015). Management of soil phosphorus fertility determines the phosphorus budget of a temperate grazing system and is the key to improving phosphorus efficiency. *Agriculture Ecosystems & Environment, 212,* 263-277. doi:10.1016/j.agee.2015.06.026

Sims, J. T. (1998). Phosphorus soil testing: Innovations for water quality protection. *Communications in Soil Science and Plant Analysis, 29*(11-14), 1471-1489. doi:10.1080/00103629809370044

Sims, J. T., Edwards, A. C., Schoumans, O. F., & Simard, R. R. (2000). Integrating soil phosphorus testing into environmentally based agricultural management practices. *J Environ Qual, 29*(1), 60-71. doi:10.2134/jeq2000.00472425002900010008x

Smith, D. R., Wilson, R. S., King, K. W., Zwonitzer, M., McGrath, J. M., Harmel, R. D., . . . Johnson, L. T. (2018). Lake Erie, phosphorus, and microcystin: Is it really the farmer's fault? *Journal of Soil and Water Conservation, 73*(1), 48-57. doi:10.2489/jswc.73.1.48

Sparks, D. L. (1996). *Methods of soil analysis. Part 3, Part 3*. Madison, Wis.: Soil Science Society of America : American Society of Agronomy.

SSSA. (2018). Eutrophication. Retrieved from https://www.soils.org/discover-soils/soils-in-the-city/green-infrastructure/important-terms/eutrophication

Stott, D. E., Karlen, D. L., Cambardella, C. A., & Harmel, R. D. (2013). A Soil Quality and Metabolic Activity Assessment after Fifty-Seven Years of Agricultural Management. *Soil Science Society of America Journal, 77*(3), 903-913. doi:10.2136/sssaj2012.0355

Stratful, I., Scrimshaw, M. D., & Lester, J. N. (2001). Conditions influencing the precipitation of magnesium ammonium phosphate. *Water Research, 35*(17), 4191-4199. doi:https://doi.org/10.1016/S0043-1354(01)00143-9

Tamburini, F., Bernasconi, S. M., Angert, A., Weiner, T., & Frossard, E. (2010). A method for the analysis of the delta O-18 of inorganic phosphate extracted from soils with HCl. *European Journal of Soil Science, 61*(6), 1025-1032. doi:10.1111/j.1365-2389.2010.01290.x

Tamburini, F., Pfahler, V., Bunemann, E. K., Guelland, K., Bernasconi, S. M., & Frossard, E. (2012). Oxygen Isotopes Unravel the Role of Microorganisms in Phosphate Cycling in Soils. *Environmental Science & Technology, 46*(11), 5956-5962. doi:10.1021/es300311h

Tamburini, F., Pfahler, V., Bünemann, E. K., Guelland, K., Bernasconi, S. M., & Frossard, E. (2012). Oxygen Isotopes Unravel the Role of Microorganisms in Phosphate Cycling in Soils. *Environmental Science & Technology, 46*(11), 5956-5962. doi:10.1021/es300311h

Tamburini, F., Pfahler, V., Sperber, C. v., Frossard, E., & Bernasconi, S. M. (2014). Oxygen isotopes for unraveling phosphorus transformations in the soil-plant system: a review.(Report). *Soil Science Society of America Journal, 78*(1), 38. doi:10.2136/sssaj2013.05.0186dgs

Tonderski, K., Andersson, L., Lindström, G., St Cyr, R., Schönberg, R., & Taubald, H. (2017). Assessing the use of δ18O in phosphate as a tracer for catchment phosphorus sources. *Science of The Total Environment, 607-608*, 1-10. doi:https://doi.org/10.1016/j.scitotenv.2017.06.167

USDA. (2017). Houston Black Series. National Cooperative Soil Survey, USA Retrieved 4/4/2020 https://soilseries.sc.egov.usda.gov/OSD_Docs/H/HOUSTON_BLACK.html

USDA Agricultural Research Service Grassland, S. a. W. R. L. (2020). Riesel Hydrologic Data. Retrieved from https://www.ars.usda.gov/plains-area/temple-tx/grassland-soil-and-water-research-laboratory/docs/hydrologic-data/

Vadas, P. A., Harmel, R. D., & Kleinman, P. J. A. (2007). Transformations of soil and manure phosphorus after surface application of manure to field plots. *Nutrient Cycling in Agroecosystems, 77*(1), 83-99. doi:10.1007/s10705-006-9047-5

Waldrip, H. M., Pagliari, P. H., He, Z. Q., Harmel, R. D., Cole, N. A., & Zhang, M. C. (2015). Legacy Phosphorus in Calcareous Soils: Effects of Long-Term Poultry Litter Application. *Soil Science Society of America Journal, 79*(6), 1601-1614. doi:10.2136/sssaj2015.03.0090

Wang, X., Harmel, R. D., Williams, J. R., & Harman, W. L. (2006). Evaluation of epic for assessing crop yield, runoff, sediment and nutrient losses from watersheds with poultry litter fertilization. *Transactions of the ASABE, 49*(1), 47-59.

Weiner, T., Mazeh, S., Tamburini, F., Frossard, E., Bernasconi, S. M., Chiti, T., & Angert, A. (2011). A method for analyzing the delta O-18 of resin-extractable soil inorganic phosphate. *Rapid Communications in Mass Spectrometry, 25*(5), 624-628. doi:10.1002/rcm.4899

WHOI. (2018). National Office for Harmful Algal Blooms at Woods Hole Oceanographic Institution. *PSP World Distribution.* Retrieved from https://www.whoi.edu/redtide /regions/world-distribution

Williams, M. R., King, K. W., Macrae, M. L., Ford, W., Van Esbroeck, C., Brunke, R. I., . . . Schiff, S. L. (2015). Uncertainty in nutrient loads from tile-drained landscapes: Effect of sampling frequency, calculation algorithm, and compositing strategy. *Journal of Hydrology, 530*, 306-316. doi:10.1016/j.jhydrol.2015.09.060

Williams, M. R., King, K. W., & Penn, C. J. (2018). Integrating Temporal Inequality into Conservation Planning to Improve Practice Design and Efficacy. *Journal of the American Water Resources Association, 54*(5), 1039-1054. doi:10.1111/1752-1688.12662

Yan, W., Li, P. Q., & Meng, F. H. (2018). Magnesium Ammonium Phosphate Crystallization: A Possible Way for Recovery of Phosphorus from Wastewater. *IOP Conf. Series: Materials Science and Engineering*(392). doi:doi:10.1088/1757-899X/392/3/032032

Young, M. B., McLaughlin, K., Kendall, C., Stringfellow, W., Rollog, M., Elsbury, K., . . . Paytan, A. (2009). Characterizing the Oxygen Isotopic Composition of Phosphate Sources to Aquatic Ecosystems. *Environmental Science & Technology, 43*(14), 5190-5196. doi:10.1021/es900337q

Zohar, I., Shaviv, A., Klass, T., Roberts, K., & Paytan, A. (2010). Method for the Analysis of Oxygen Isotopic Composition of Soil Phosphate Fractions. *Environmental Science & Technology, 44*(19), 7583-7588. doi:10.1021/es100707f

Zohar, I., Shaviv, A., Young, M., Kendall, C., Silva, S., & Paytan, A. (2010). Phosphorus dynamics in soils irrigated with reclaimed waste water or fresh water - A study using oxygen isotopic composition of phosphate. *Geoderma, 159*(1-2), 109-121. doi:10.1016/j.geoderma.2010.07.002

Zopp, Z. P., Ruark, M. D., Thompson, A. M., Stuntebeck, T. D., Cooley, E., Radatz, A., & Radatz, T. (2019). Effects of Manure and Tillage on Edge-of-Field Phosphorus Loss in Seasonally Frozen Landscapes. *J Environ Qual, 48*(4), 966-977. doi:10.2134/jeq2019.01.0011